Technische Universität München
Physik Department
Institut für Theoretische Physik
T39
Univ.-Prof. Dr. W. Weise

TECHNISCHE UNIVERSITÄT MÜNCHEN

Thermodynamics of the Chiral Condensate

Dipl.-Phys. Thomas M. Schwarz

Vollständiger Abdruck der von der Fakultät für Physik der Technischen Universität München zur Erlangung des akademischen Grades eines

Doktors der Naturwissenschaften (Dr. rer. nat.)

genehmigten Dissertation.

Vorsitzender:	Univ.-Prof. Dr. St. Paul
Prüfer der Dissertation:	
	1. Univ.-Prof. Dr. W. Weise
	2. Univ.-Prof. Dr. P. Ring

Die Dissertation wurde am 15.1.2003 bei der Technischen Universität München eingereicht und durch die Fakultät für Physik am 23.1.2003 angenommen.

Thermodynamics of the Chiral Condensate

To Lisa and Nicole

To my Family

TECHNISCHE
UNIVERSITÄT
MÜNCHEN

Thermodynamics of the chiral condensate

We study the temperature and density dependence of the scalar quark condensate $\langle\bar{q}q\rangle$ using effective field theory methods. Nucleons interact via perturbative chiral pion exchange and scalar plus vector four-point interactions. The latter are treated in relativistic mean field approximation giving rise to an effective nucleon mass M^* and an effective chemical potential μ^*. Contributions from pion fluctuations at two-loop level are included in the self consistency equations for M^* and μ^*. The strengths of the contact interactions are adjusted to the empirical nuclear matter saturation point and compressibility κ. From this we predict an effective nucleon mass of $M^*(\rho_0) \simeq 0.8M$. At a temperature $T \simeq 16.6\,\mathrm{MeV}$ a liquid-gas phase transition is observed.
In a further step we include three-loop contributions from 2π-exchange at finite density but $T = 0$. The dependence of the equation of state $P(T, \mu, m_\pi)$ on the pion mass allows to calculate deviations from the leading linear decrease in density of the quark condensate. We find that these are small below normal nuclear matter density.

Thermodynamik des chiralen Kondensats

Wir untersuchen die Temperatur- und Dichteabhhängigkeit des skalaren Quark-Kondensats $\langle\bar{q}q\rangle$ mit Hilfe von Methoden der effektiven Feldtheorie. Nukleonen wechselwirken durch chiralen Pionaustausch sowie über skalare und vektorielle Vier-Punkt-Kopplungen. Letztere werden in Mean-Field-Näherung behandelt. Dies führt zu einer effektiven Nukleonenmasse M^* und einem effektiven chemischen Potential μ^*. Beiträge des Einpionaustausches werden in die Selbstkonsistenz-Gleichungen für M^* und μ^* eingebunden. Die Stärke der Kontaktwechselwirkungen wird so eingestellt, dass der empirische Sättigungspunkt und die Kompressibilität von Kernmaterie reproduziert werden. Dies führt zu Voraussagen für die effektive Nukleonenmasse von $M^*(\rho_0) \simeq 0.8M$. Bei einer Temperatur von $T \simeq 16.6\,\mathrm{MeV}$ beobachten wir den Flüssigkeits-Gas-Phasenübergang der Kernmaterie.
Desweiteren behandeln wir die Beiträge des 2π-Austauschs in Drei-Schleifen-Näherung bei endlicher Dichte und $T = 0$. Die Abhängigkeit der Zustandsgleichung $P(T, \mu, m_\pi)$ von der Pionmasse erlaubt die Berechnung der Abweichungen von der führenden linearen Abnahme des chiralen Kondensats als Funktion der Dichte. Wir finden, dass diese Beiträge unterhalb normaler Kerndichte klein sind.

Contents

1 Introduction **5**

2 Theory of strong interactions **11**
2.1 Quantum Chromodynamics 11
2.2 Chiral Symmetry 14
2.3 Symmetry Breaking Patterns 15
2.4 Partially Conserved Axial Current 17
2.5 The Chiral Condensate 18
2.6 Chiral Effective Lagrangian 18
2.6.1 Meson Sector: Non-linear Sigma Model 19
2.6.2 Including Baryons 20
2.7 Gell-Mann-Oakes-Renner Relation 21
2.8 Pion-Nucleon Sigma Term 22
2.9 Goldberger-Treiman Relation 23

3 Field Theory at Finite Temperature and Density **25**
3.1 The Grand Canonical Ensemble 26
3.1.1 Free Fermions 26
3.1.2 Non-interacting Bosons 27
3.2 Chiral Condensate at Finite Temperature and Density 27
3.2.1 Hellmann-Feynman Theorem 28
3.2.2 Free and Interacting Pion Gas at Finite Temperature 30
3.2.3 Nucleons: Low Density Approximation 32

4 Nuclear Matter **35**
4.1 The Walecka Model 37
4.1.1 Mean Field Approximation 39
4.1.2 Self-consistency Equations 40

4.1.3 Contact Interactions . . . 42
4.1.4 Thermodynamic Quantities and Relations . . . 43
4.2 Numerical Results . . . 45
4.2.1 Liquid-Gas Phase Transition . . . 47
4.2.2 Parameter Dependence of the Nuclear Matter Saturation Point . . . 50
4.2.3 The Compressibility of Nuclear Matter . . . 52
4.2.4 Energy and Entropy Densities . . . 53
4.2.5 The Chiral Condensate (I) . . . 55
4.2.6 The Phase Diagram of Nuclear Matter . . . 57
4.3 Additional Parameter: Improved Results . . . 58
4.3.1 New Parameter Sets . . . 60
4.3.2 Effective Nucleon Mass . . . 64
4.3.3 Liquid-Gas Transition with Improved Interaction . . . 66
4.3.4 The Chiral Condensate (II) . . . 68
4.4 Pionic Fluctuations . . . 69
4.4.1 Thermal Pions and Pion Exchange . . . 70
4.4.2 The Chiral Condensate (III) . . . 74
4.5 Two-Pion Exchange Terms . . . 79
4.5.1 The Chiral Condensate (IV) . . . 85
4.5.2 Justification to Use the Approximation . . . 87

5 Summary and Conclusions 93

A Mathematical Details 99
A.1 Feynman Rules . . . 99
A.1.1 Vertex and Propagators . . . 100
A.1.2 Traces . . . 100
A.2 SU(N) . . . 101
A.2.1 Pauli Matrices . . . 101
A.2.2 Gell-Mann Matrices . . . 102
A.3 Conventions . . . 102
A.3.1 γ-Matrices . . . 103
A.4 Distribution functions . . . 104
A.4.1 Bose-Einstein Distribution Function . . . 104
A.4.2 Fermi-Dirac Distribution Function . . . 105
A.5 Formula Collection and Matsubara frequencies . . . 107
A.5.1 Direct Summation Of Matsubara Frequencies . . . 107
A.6 Contact Interaction Lagrangian . . . 108

B The Ideal Gas Pressure **111**
B.1 Derivation of P_{FG} 111
B.2 Derivatives of P_{FG} 117

C Pion Exchange Diagrams **119**
C.1 The 1π-exchange Fock Term 119
C.1.1 Calculation of $P_{1\pi}$ 120
C.2 Two Pion Exchange 128

References **131**

Acknowledgements - Danksagung **137**

Chapter 1

Introduction

The generally accepted theory of strong interactions is quantum chromodynamics (QCD), a gauge theory of colored quarks and gluons. The running quark-gluon coupling constant is small at short distances (*asymptotic freedom*) and increases at long distances, leading to the formation of color singlet bound states. *Confinement* [1, 2] expresses the absence of free quarks and gluons in asymptotic states, only colorless hadrons appear in final states.
QCD with light quarks has an approximate chiral symmetry, exact in the limit of vanishing quark masses ($m_q = 0$). This symmetry is spontaneously broken at low energies. The order parameter of spontaneously broken chiral symmetry is the quark condensate $\langle \bar{q}q \rangle$. From its dependence on temperature and density one can construct the phase diagram of QCD. The corresponding phase transition line separates regions with finite $\langle \bar{q}q \rangle$ (hadronic matter) from those where $\langle \bar{q}q \rangle = 0$. There are indications from lattice calculations that chiral symmetry is restored above a critical temperature $T_c = (173 \pm 8)\,\mathrm{MeV}$. Above T_c the condensate $\langle \bar{q}q \rangle$ is found to vanish. The confinement-deconfinement transition related to the liberation of colored degrees of freedom seems to occur in the same temperature range. The corresponding deconfined phase is referred to as the quark-gluon plasma.

In the discussion of nuclear matter the chiral condensate is also of importance. Nuclear matter denotes an infinite and homogeneous isospin-symmetric many-nucleon system, i.e. matter consisting of equally many protons and neutrons, being subject only to the strong interaction. For a study of nuclei and nuclear matter at low energies, quarks and gluons are not the proper "effective" degrees of freedom because color is confined on the relevant length scales. Low-energy QCD is in fact realized as an effective field theory of weakly interacting Goldstone bosons (pions) coupled to heavy nucleons.

The aim of this work ist to study the temperature and density dependence of $\langle\bar{q}q\rangle$ using effective field theory methods. This dependence derives from the quark mass dependence of the grand canonical partition function or equivalently the total pressure of the interacting hadronic system. Due to the GOLDSTONE boson nature of the pion this quark mass dependence can be converted directly into an m_π^2-dependence by using the GELL-MANN−OAKES−RENNER relation.
Explicit pion degrees of freedom therefore play a prominent role in the discussion of chiral symmetry restoration trends at low temperatures and densities. A suitable starting point in thermodynamics is the total pressure $P(T,\mu)$ written as a function of the natural variables of the hadronic system, chemical potential μ and temperature T.
At low energy it can be written as the sum of contributions from interacting nucleons at finite temperature and density on the one hand and free and interacting pions in the heat bath on the other hand:

$$P(T,\rho) = P_N(T,\rho) + P_\pi(T).$$

The part $P_N(0,\rho)$ corresponds to cold nuclear matter. At the nuclear matter saturation density $\rho_0 \simeq 0.17\,\mathrm{fm}^{-3} = 2p_f^3/(3\pi^2)$ the FERMI momentum $p_f = 268\,\mathrm{MeV}$ and the pion mass $m_\pi = 138\,\mathrm{MeV}$ are comparable scales $p_f \simeq 2m_\pi$. This is a further argument in favor of including pions as explicit degrees of freedom in describing nuclear many-body dynamics.
Our dynamical calculation of nuclear matter includes 1- and 2-pion exchange as well as four-nucleon interactions. The related coupling strengths are adjusted such that they reproduce the known properties of nuclear matter. We already mentioned the saturation density ρ_0, furthermore the binding energy per nucleon $B = 16\,\mathrm{MeV}$ and the nuclear matter (in-)compressibility $\kappa = (250 \pm 10)\,\mathrm{MeV}$ are known. This adjustment renders our equation of state more realistic.
Our main interest lies in the form of the chiral condensate $\langle\bar{q}q\rangle$ which we obtain from the pion mass dependence of our realistic equation of state. In contrast to earlier work we do not just use FERMIgas estimates of $\langle\bar{q}q\rangle$ but properly treat nuclear matter as a self-bound FERMI liquid.

The present work is organised as follows:

• We start in chapter 2 by summarising important aspects of the theory of strong interactions where our main focus will be on symmetries as well as symmetry breaking patterns in Quantum Chromodynamics.
Then we construct the effective chiral Lagrangian of low-energy QCD to leading order. Its explicit degrees of freedom are GOLDSTONE bosons (pions) and nucleons with interactions dictated by chiral symmetry.

• The appropriate framework when dealing with relativistic many-particle systems is the grand canonical ensemble. Chapter 3 will be about basic concepts of field theory at finite temperature and density.
In this general context we rediscover the low density theorem. It states that to leading order in density the chiral condensate drops linearly with a slope determined by the so-called pion-nucleon sigma term $\sigma_N \simeq 45\,\mathrm{MeV}$. This quantity $\sigma_N = m_q \partial M/\partial m_q$ gives the portion of the nucleon mass coming from the finite up- and down-quark mass.
At low temperatures the T-dependence of the chiral condensate is determined exclusively by the dynamics of the thermal pion gas. We discuss the quantitative influence of free and interacting pions on $\langle \bar{q}q \rangle(T)$.

• We will reach the main part of this work in chapter 4 where we first recall the relativistic WALECKA model. In this approach nucleons are treated as DIRAC quasi-particles, moving in self-consistently generated scalar and vector mean-fields. With regard to the implementation of 1- and 2-pion exchange effects later it is advantageous to eliminate the scalar and vector mean-fields by the effective nucleon mass and nucleon chemical potential respectively. This guarantees a clearly arranged and well-structured thermodynamic treatment.

• After presenting results for nuclear matter at $T = 0$ from the 2-parameter WALECKA model we encounter some well-known shortcomings. These are the by far too large value of the nuclear matter compressibility and the rather low effective nucleon mass at saturation density $M^*(\rho_0) \simeq 0.54M$. We improve this model by adding a cubic (or quartic) term in the scalar mean-field of the form $\sim (M - M^*)^{3(,4)}$ to the grand canonical partition function. This term introduces a new parameter with which we can simultaneously fit all three nuclear matter properties ρ_0, B and κ. At the same time the effective nucleon mass increases to a more realistic value of $M^*(\rho_0) \simeq 0.8M$.
A welcome side effect is the lowering of the critical temperature of the liquid-gas phase transition to $T_c^{\mathrm{LG}} \simeq 16.5\,\mathrm{MeV}$. This value of T_c^{LG} is in perfect

agreement with a recent analysis of limiting temperatures in heavy ion collisions [3].
In the next step we go beyond the mean-field description and include the one-pion exchange FOCK term. We evaluate the contribution of the 1π-exchange FOCK diagram to the partition function fully relativistically. In this general form one accounts for various scattering processes of thermal pions (and thermal antinucleons) with nucleons.
The 1π-exchange corrections are included in the self-consistent determination of the effective nucleon mass and chemical potential, or equivalently the scalar and vector mean-fields.
It turns out that a non-relativistic approximation, in which effects from thermal pions and antinucleons are neglected, works well in the temperature and density regime of interest. This opens the possibility to treat 2π-exchange corrections in the same approximation reliably. To be more specific: by 2π-exchange we mean iterated 1π-exchange HARTREE and FOCK diagram, where PAULI blocking is automatically taken care of.
In particular, we will give a "master formula" for the temperature and density dependence of the chiral condensate.

• Having at hand a dynamical description of nuclear matter which includes systematically pion exchange contributions and at the same time fulfills the empirical constraints at the saturation point one can focus on the temperature and density dependence of $\langle \bar{q}q \rangle$. This is done by taking the pressure's derivative with respect to the pion mass.

• Finally we summarise our results, draw conclusions and give an outlook to possible future work in chapter 5.

Chapter 2

Theory of strong interactions

In this chapter we briefly summarise the basic features of Quantum Chromodynamics with its local $SU(3)_c$ gauge and chiral symmetries. The latter symmetry is of great importance in the discussion of low energy hadronic physics.

2.1 Quantum Chromodynamics

The generally accepted gauge theory [4, 5] of the strong interactions is quantum chromodynamics[1] (QCD) [6, 7, 8]. It is a theory of colored quarks and gluons initiated by Gell-Mann [9], Zweig [10] and others [1, 2, 11, 12] in the 1960s and 70s.

Quarks are spin-1/2 fermions carrying electric charge in fractions of the proton charge. They come in six different flavors: *up*, *down*, *strange*, *charm*, *bottom* and *top*, see Table 2.1. In order to be able to construct the observed hadrons without violating the Pauli exclusion principle, quarks are assigned an additional degree of freedom named color [11, 12]. Only color-neutral objects exist in nature. There are two ways to group quarks in order to obtain such "white" particles: We already mentioned hadrons which consist of three quarks ($q_R q_G q_B$) whose red, green and blue colors combine to white. Mesons are paired quark-antiquark systems ($q\bar{q}$) where color+anti-color=neutral.
The necessity for this hidden quantum number is most easily illustrated by looking at the fermionic $\Delta^{++} = |uuu\rangle$-resonance having $J^P = 3/2^+$. Obviously

Charge	I	II	III
+2/3	u	c	t
-1/3	d	s	b

Table 2.1: Quark flavors, families and electric charge.

[1] *the Greek word $\chi\rho\tilde{\omega}\mu\alpha$ (chroma) means color*

the wave-function of this system is symmetric under exchange of quarks (all u's are identical). Also the spins of all three quarks need to be parallel in order to yield $J = 3/2$. The color degree of freedom allows to construct an anti-symmetric wave-function for this state.
An observable where the hidden color degree of freedom becomes visible is the ratio of cross sections

$$R = \frac{\sigma(e^+e^- \to \text{hadrons})}{\sigma(e^+e^- \to \mu^+\mu^-)} \tag{2.1}$$

which - at large centre of mass energies $s \to \infty$ - is given by the sum of all the squared quark charges seen by the electromagnetic field at that energy

$$\lim_{s\to\infty} R = N_c \sum_{i=flavor} Q_i^2 = N_c \left[\left(\frac{2}{3}\right)^2 + \left(\frac{1}{3}\right)^2 + \left(\frac{1}{3}\right)^2 \right] = 2\frac{N_c}{3}, . \tag{2.2}$$

The observed ratio R implies that there are three different colors which inspired naming this internal quantum number: $N_c = 3$, i.e. QCD is based on local $SU(3)$ ($\to$ section A.2) color gauge invariance.
Interactions between quarks are mediated by massless spin-1 bosons called gluons. They carry color themselves and thus interact amongst each other making the theory non-Abelian.
QCD, as a non-Abelian gauge field theory, exhibits some distinct properties like a decreasing force at short distances, or very high momentum transfers. This phenomenom is called asymptotic freedom because it implies that the nucleon's constituents behave like weakly interacting point particles at high energies and momentum transfer. On the other hand the interaction between quarks has to be very strong at long distance, or small momentum transfer, as to explain the nonobservation of isolated quarks - this feature is called confinement.
All experimental searches for free quarks since 1977 have had negative results [13]. This is explained by the concept of confinement of color charges: quarks are assigned the colors *red*, *green* and *blue* (antiquarks carry the corresponding anti-colors). Nature only allows color-singlet ("white") particle combinations. There are two basic ways to combine colors and anti-colors to achieve this. 3-quark particles (qqq) are fermions called baryons whereas quark-antiquark particles ($\bar{q}q$) are bosons called mesons.

The quark fields in the 3 flavor case are

$$\psi(x) = \begin{pmatrix} u(x) \\ d(x) \\ s(x) \end{pmatrix} \tag{2.3}$$

Only u, d and s have current quark masses below 1 GeV, the c, b and t quarks are heavy, their typical values are listed in Table 2.2. Treating the heavier ones as infinitely heavy is a good approximation at low energy and makes them inactive, they are "frozen" degrees of freedom.

q	m_q
up	1.5-4.5 MeV
down	5-8.5 MeV
strange	80-155 MeV
charm	1-1.4 GeV
bottom	4-4.5 GeV
top	169.2-179.4 GeV

Table 2.2: Current quark masses m_q taken from [13].

where u, d, s are DIRAC field operators that exists in $N_c = 3$ colors. Thus $\psi(x)$ has 36 components. The QCD Lagrangian density has the form

$$\mathcal{L}_{QCD} = \bar{\psi}(x)\left[i\gamma_\mu D^\mu - M\right]\psi(x) - \frac{1}{4}G^a_{\mu\nu}(x)G^{\mu\nu}_a(x) \tag{2.4}$$

where the first part involves the mass matrix

$$M = \begin{pmatrix} m_u & 0 & 0 \\ 0 & m_d & 0 \\ 0 & 0 & m_s \end{pmatrix}. \tag{2.5}$$

Quarks obey the DIRAC equation

$$(i\not{D} - M)\psi(x) = 0. \tag{2.6}$$

Local $SU(3)$ color gauge invariance requires $\mathcal{L}_{QCD}$ to be invariant under arbitrary transformations

$$U = \exp\left(-\frac{i}{2}\lambda_a\Theta_a(x)\right) \tag{2.7}$$

in color space. This requires the introduction of the covariant derivative

$$D_\mu(x) = \partial_\mu - ig_s\frac{\lambda_a}{2}A^a_\mu(x) \tag{2.8}$$

involving eight LORENTZ-vector fields A^a_μ - the gluon fields. Their transformation properties are defined such that the covariant derivative of the quark field, namely $D_\mu(x)\psi(x)$, transforms in exactly the same way as $\psi(x)$ itself. Then $\bar{\psi}(x)i\gamma_\mu D^\mu(x)\psi(x)$ is gauge invariant.
$G_{\mu\nu}(x)$ is the non-Abelian gluon field tensor

$$G^a_{\mu\nu}(x) = \partial_\mu A^a_\nu(x) - \partial_\nu A^a_\mu(x) + g_s f_{abc}A^b_\mu(x)A^c_\nu(x) \tag{2.9}$$

where λ_a are the generators and f_{abc} the group structure constants of flavor-$SU(3)$, see Appendix A.2.2.

2.2 Chiral Symmetry

In this work we will be concerned with nuclear matter. As protons and neutrons contain mainly *up* and *down* quarks it will be sufficient for us to consider QCD with 2 flavors. The quark masses in (2.5) are among the parameters in the QCD Lagrangian (2.4). Compared with the nucleon mass of

$$M_0 = 939\,\mathrm{MeV} \tag{2.10}$$

the current quark masses $m_{u,d}$ as given in Table 2.2 are smaller than 1%. Therefore it is a good starting point to consider the (chiral) limit of massless quarks $m_u = m_d = 0$ as a first approximation. In the case of free massless quarks the DIRAC equation simplifies to

$$i\partial\!\!\!/\psi(x) = 0 \tag{2.11}$$

and its solution is given by

$$\psi(x) = const \cdot \begin{pmatrix} \chi \\ h\,\chi \end{pmatrix} e^{-ipx} \tag{2.12}$$

where h is the helicity - the projection of spin onto the direction of momentum

$$h = \sigma \cdot \frac{\vec{p}}{|\vec{p}|} \tag{2.13}$$

The helicity is an invariant in the case of massless particles (that travel at the speed of light $\beta = v/c = 1$), in which case it is also called chirality. If the particle had a rest mass it would travel at lower speed $\beta < 1$ and one could always find a reference frame in which the particle is overtaken - changing its direction of motion and therefore its helicity.
The chirality operator $\gamma_5 = i\gamma^0\gamma^1\gamma^2\gamma^3$ fulfills $(\gamma_5)^2 = 1$ and therefore has the eigenvalues ± 1:

$$\gamma_5\psi(x) = \pm\psi(x). \tag{2.14}$$

For massless fermions the DIRAC equation has two solutions, states with positive and negative chirality. We can introduce right- and left-handed quarks $(H = R, L)$

$$\psi_{R,L} = \frac{1}{2}(1 \pm \gamma_5)\psi =: \psi_H \tag{2.15}$$

which allow the separation of $\bar{\psi}(x)\not{D}\psi(x)$

$$\bar{\psi}(x)\not{D}\psi(x) = \bar{\psi}_L(x)\not{D}\psi_L(x) + \bar{\psi}_R(x)\not{D}\psi_R(x) \tag{2.16}$$

into these R- and L-fields. $\mathcal{L}_{QCD}$ in (2.4) with two flavors and $M = 0$ is invariant under the following global transformations

$$\psi_H \to H\psi_H = e^{i\Theta^i_H \tau_i/2}\psi_H \tag{2.17}$$

This invariance is called chiral $SU(2)_R \times SU(2)_L$ symmetry. The NOETHER theorem [14] tells us that for each continuous symmetry of the Lagrangian there exists an associated conserved current. (2.17) implies 6 conserved currents

$$J^\mu_{H,i}(x) = \bar{\psi}_H(x)\gamma^\mu \frac{\tau_i}{2}\psi_H(x)\,, \quad \partial_\mu J^\mu_{H,i} = 0. \tag{2.18}$$

from which we can combine the isovector and axial currents

$$V^\mu_i(x) = J^\mu_{R,i}(x) + J^\mu_{L,i}(x) = \bar{\psi}(x)\gamma^\mu \frac{\tau_i}{2}\psi(x) \quad ; \qquad \partial_\mu V^\mu_i(x) = 0 \tag{2.19}$$

$$A^\mu_i(x) = J^\mu_{R,i}(x) - J^\mu_{L,i}(x) = \bar{\psi}(x)\gamma^\mu\gamma_5 \frac{\tau_i}{2}\psi(x) \quad ; \qquad \partial_\mu A^\mu_i(x) = 0 \tag{2.20}$$

where the τ_i are the PAULI matrices in (A.14) and Θ is an arbitrary 3-component rotation angle in isospin space. The associated conserved charges

$$Q^V_i = \int \mathrm{d}^3x\, V^0_i(x), \qquad Q^A_i = \int \mathrm{d}^3x\, A^0_i(x) \tag{2.21}$$

generate the LIE algebra $SU(2)_L \times SU(2)_R$ with commutation relations

$$\begin{aligned} \left[Q^V_i, Q^V_j\right] &= i f_{ijk} Q^V_k \\ \left[Q^V_i, Q^A_j\right] &= i f_{ijk} Q^A_k \\ \left[Q^A_i, Q^A_j\right] &= i f_{ijk} Q^V_k \end{aligned} \tag{2.22}$$

where the structure constants $f_{ijk} = \epsilon_{ijk}$ are just the components of the totally antisymmetric tensor.
The chiral symmetry will be of great importance in our discussion of the chiral condensate in chapter 4.

2.3 Symmetry Breaking Patterns

So far the considerations about symmetries were always related to the Lagrangian density. But what about the ground state of the system? In principle there are two possibilities: either the resulting ground state does share the full symmetry of the Lagrangian (WIGNER-WEYL realisation) or not (NAMBU-GOLDSTONE realisation). In the case of QCD the former would indicate perfect symmetry between vector and axial current. If the ground state were

chirally symmetric, both vector and axial charge operators would annihilate the vacuum:

$$Q_i^V|0\rangle = Q_i^A|0\rangle = 0. \tag{2.23}$$

Due to the different parity properties of Q_i^V and Q_i^A the particle spectra are $SU(2)_L \times SU(2)_R$ multiplets, i.e. the hadron spectrum would consist of pairs of particles with equal mass but opposite parity. However, no such parity doublets are observed in the low-energy hadron spectrum. Therefore chiral symmetry must be realised in the NAMBU-GOLDSTONE way[2]: the Lagrangian density is chirally invariant but not the vacuum state:

$$Q_i^V|0\rangle = 0, \qquad Q_i^A|0\rangle \neq 0. \tag{2.24}$$

This situation is subject to the GOLDSTONE theorem [17]:

> If the LAGRANGE density has a continuous symmetry represented by the group G_1 with N_{G_1} generators whereas the ground state is invariant under the subgroup G_2 with $N_{G_2} < N_{G_1}$ generators then the breaking of this (exact) symmetry implies the existence of $N_{G_1} - N_{G_2}$ massless states (degenerate with the vacuum), called GOLDSTONE bosons.

In addition there is evidence from lattice QCD calculations that chiral symmetry is spontaneously broken [16] down to the flavor group $SU(2)_V$:

$$SU(2)_R \times SU(2)_L \rightarrow SU(2)_V. \tag{2.25}$$

The group $SU(N)$ has $N^2 - 1$ generators, see section A.2. In our case there are three GOLDSTONE bosons , the pions (π^0, π^+, π^-)[3].
But why are the pions *not* massless? We had just emphasized that this is only the case for an exact symmetry. In the last section we learned about the chiral symmetry which is exact only for massless quarks $M = 0$.
Apart from the symmetry breaking pattern discussed above there is a second kind of symmetry breaking called *explicit*. It comes about due to the mass term in the Lagrangian density.

[2] *if quarks are confined, then chiral symmetry must be spontaneously broken [15, 16]*
[3] *for* $SU(3)_R \times SU(3)_L$ *there are 8* GOLDSTONE *bosons* $(\pi^0, \pi^+, \pi^-, \bar{K}^0, K^0, K^+, K^-, \eta)$

2.4 Partially Conserved Axial Current

In the two previous sections we learned that the chiral $SU(2)_R \times SU(2)_L$ symmetry is spontaneously broken down to $SU(2)_V$. The GOLDSTONE theorem tells us that in the chiral limit ($m_u = m_d = 0$) - where the symmetry is exact - this leads to three massless bosons, the pions. Let their state vectors $|\pi_j(p)\rangle$ be normalized

$$\langle \pi_j(p)|\pi_k(p')\rangle = 2E_p\delta_{jk}(2\pi)^3\delta^3(\vec{p}-\vec{p}')\,, \quad p^\mu = (E_p, \vec{p}). \tag{2.26}$$

The theorem also implies non-vanishing transition matrix elements of the axial current which connect $|\pi_j(p)\rangle$ with the vacuum:

$$\langle 0|A_i^\mu(x)|\pi_j(p)\rangle = if_\pi p^\mu \delta_{ij} e^{-ipx}. \tag{2.27}$$

This matrix element describes the charged pion decay $\pi^+ \to \mu^+ + \nu_\mu$. The constant

$$f_\pi = (92.4 \pm 0.3)\,\text{MeV} \tag{2.28}$$

is the physical pion decay constant. Chiral symmetry is broken explicitly in nature by the small but finite quark masses in

$$\mathcal{L}_{mass} \equiv \mathcal{L}_M = -\bar{\psi}M\psi\,; \quad M = \text{diag}(m_u, m_d) \tag{2.29}$$

shifting the pion mass from zero to the observed value and changing the divergence of the axial current (2.20) which is obtained from the matrix element

$$\langle 0|\partial_\mu A_i^\mu(x)|\pi_j(p)\rangle = f_\pi p^2 \delta_{ij} e^{-ipx} = f_\pi m_\pi^2 \delta_{ij} e^{-ipx} \tag{2.30}$$

and the relation for the pion field $\langle 0|\pi_i(x)|\pi_j(p)\rangle = \delta_{ij}e^{-ipx}$ to be

$$\partial_\mu A_i^\mu(x) = f_\pi m_\pi^2 \pi_i(x). \tag{2.31}$$

This relation is commonly known as the PCAC[4] relation. As discussed above we see that in the chiral limit with vanishing pion mass ($m_{u,d} = 0 \to m_\pi = 0$, see (2.58)) the axial current is conserved.

[4] *partially conserved axial current*

2.5 The Chiral Condensate

The chiral quark condensate plays an important role in the spontaneous chiral symmetry breaking (SχSB). Its precise definition is

$$\begin{aligned} \langle 0|\bar{\psi}\psi|0\rangle &= -i\,\mathbf{Tr}\lim_{y\to x_+} S_F(x,y) \\ \text{where } S_F(x,y) &= -i\langle 0|\mathcal{T}\psi(x)\bar{\psi}(y)|0\rangle \end{aligned} \tag{2.32}$$

is the full quark propagator. SχSB is accompanied by a rearrangement of the vacuum which is populated by a condensate of quark-antiquark pairs. The scalar-isoscalar quark density $\bar{\psi}(x)\psi(x)$ has a non-vanishing expectation value:

$$\langle 0|\bar{\psi}\psi|0\rangle \equiv \langle\bar{\psi}\psi\rangle = \langle\bar{q}_i q_i\rangle = \langle\bar{u}u\rangle + \langle\bar{d}d\rangle. \tag{2.33}$$

SχSB leads to a non-trivial vacuum. The scalar quark density

$$\bar{\psi}\psi = \bar{\psi}_R\psi_L + \bar{\psi}_L\psi_R \tag{2.34}$$

mixes right- and left-handed quark fields, recall (2.15). A nonvanishing vacuum expectation value therefore breaks chiral symmetry explicitly.
The condensate $\langle\bar{\psi}\psi\rangle$ is a measure for the strength of SχSB in the way that $\langle\bar{\psi}\psi\rangle = 0$ resembles the phase with exact chiral symmetry whereas $\langle\bar{\psi}\psi\rangle \neq 0$ represents the phase with broken symmetry. Thus it plays the role of an order parameter in the theory of the phase transition.

2.6 Chiral Effective Lagrangian

An effective low energy theory of QCD must be constructed such that chiral symmetry and its spontaneous and explicit breaking are implemented. We will now construct the prototype of such a chiral effective Lagrangian $\mathcal{L}_{\mathit{eff}}$. The effective degrees of freedom in QCD at low energies are no longer the elementary quarks and gluons, but composite hadrons, primarily the Goldstone boson(s). The basic idea of an effective field theory is to treat light particles as active and heavy particles as frozen degrees of freedom, the latter being reduced to nearly static sources.
SχSB leads to a characteristic gap in the hadron spectrum

$$\Delta \sim 4\pi f_\pi \sim 1\,\text{GeV}. \tag{2.35}$$

The energy scale introduced by Δ seperates between light and heavy particles.

2.6.1 Meson Sector: Non-linear Sigma Model

We will now construct $\mathcal{L}_{\mathit{eff}}$ in the meson sector with $N_f = 2$. A convenient representation for the pseudoscalar GOLDSTONE bosons is a unitary 2×2 matrix field $U(x) \,\epsilon\, SU(2)$ with $U^\dagger U = 1$ and $\det U = 1$.

$$U(x) = \sqrt{1 - \frac{\vec{\pi}^2(x)}{2f_\pi^2}} + i\frac{\vec{\tau} \cdot \vec{\pi}(x)}{f_\pi} \tag{2.36}$$

Under chiral transformations, see (2.17), the matrix U transforms as

$$U \to U' = RUL^\dagger\,; \quad R, L \,\epsilon\, SU(2)_{R,L}. \tag{2.37}$$

Consequently the pion field $\vec{\pi}(x)$ transforms non-linearly. In general the Lagrangian $\mathcal{L}_{\mathit{eff}}$ is a function of $U(x)$ and its derivatives

$$\mathcal{L}_{QCD} \to \mathcal{L}_{\mathit{eff}} = \mathcal{L}_{\mathit{eff}}(U, \partial_\mu U). \tag{2.38}$$

$\mathcal{L}_{\mathit{eff}}$ is expanded in terms of powers of these derivatives

$$\mathcal{L}_{\mathit{eff}} = \mathcal{L}_2 + \mathcal{L}_4 + \mathcal{L}_6 + ... \tag{2.39}$$

where the index gives the number of derivatives $\partial_\mu U$. LORENTZ invariance implies that the number of derivatives must be even. The leading term

$$\mathcal{L}_2 = \frac{f_\pi^2}{4}\mathbf{tr}\left[\partial^\mu U^\dagger \partial_\mu U\right] \tag{2.40}$$

is known as the non-linear sigma model. Expanding just this term, after adding the leading symmetry breaking term such that $\mathcal{L}_2$ is still even in the GOLDSTONE boson fields,

$$\mathcal{L}_2 = \frac{f_\pi^2}{4}\,\mathbf{tr}\left[\partial^\mu U^\dagger \partial_\mu U\right] + \frac{B}{2} f_\pi^2\,\mathbf{tr}\left[M(U + U^\dagger)\right] \tag{2.41}$$

in the isotriplet pion field $\vec{\pi}$ from (2.36) yields

$$\mathcal{L}_2 = \frac{1}{2}\partial_\mu \vec{\pi} \partial^\mu \vec{\pi} + 2m_q B\left(f_\pi^2 - \frac{1}{2}\vec{\pi}^2\right) \tag{2.42}$$

where we used $m_q = m_u = m_d$. The parameter B in this equation turns out to be the quark condensate $\langle 0|\bar{q}q|0\rangle$. This leads to the GELL-MANN-OAKES-RENNER relation, see section 2.7.

2.6.2 Including Baryons

If we now want to construct the effective Lagrangian for systems of mesons *and* baryons we have to replace the pure mesonic Lagrangian $\mathcal{L}_{\mathit{eff}}$ in (2.38) by

$$\mathcal{L}_{\mathit{eff}} = \mathcal{L}_{\mathit{eff}}(U, \partial_\mu U, \Psi_B, ...). \tag{2.43}$$

We will denote the additional terms which include the baryon fields Ψ_B as $\mathcal{L}^B_{\mathit{eff}}$ and expand them again in powers of derivatives:

$$\mathcal{L}^B_{\mathit{eff}} = \mathcal{L}^{(1)}_{\Phi B} + \mathcal{L}^{(2)}_{\Phi B} + \dots . \tag{2.44}$$

The leading term $\mathcal{L}^{(1)}_{\Phi B}$ will be of primary interest. We start from the free baryon Lagrangian

$$\mathcal{L}_B = \mathbf{Tr}\left[\bar{\Psi}_B \left(i\gamma_\mu \partial^\mu - M_0\right) \Psi_B\right] \tag{2.45}$$

in which we will replace ∂^μ by a chiral covariant derivative ($\rightarrow \mathcal{L}'_B$, see (2.53)). This introduces vector current interactions and axial vector couplings between the baryons and mesons.
We will first derive these interaction terms from the linear sigma model where massless fermions have YUKAWA couplings with a composite scalar field σ and a pseudoscalar, isovector field $\vec{\phi}$

$$\mathcal{L}_F = \bar{\psi}\left[i\partial\!\!\!/ - g(\sigma - i\gamma_5 \vec{\tau}\cdot\vec{\phi})\right]\psi = i\bar{\psi}\partial\!\!\!/\psi - g\left[\bar{\psi}_L \Sigma^\dagger \psi_R + \bar{\psi}_R \Sigma \psi_L\right] \tag{2.46}$$

where $\Sigma \equiv \sigma + i\vec{\tau}\cdot\vec{\phi}$ transforms like $\Sigma \rightarrow R\Sigma L^\dagger$ under chiral $SU(2)_R \times SU(2)_L$.

We decompose σ into its vacuum expectation value $\langle\sigma\rangle$ and fluctuations, identify the fermion mass $M_0 = g\langle\sigma\rangle \rightarrow g f_\pi$ with the nucleon mass and set $\Sigma = \langle\sigma\rangle U$ with U in (2.36), making contact with the chiral field of the non-linear sigma model discussed in the previous section. Then $\mathcal{L}_F$ becomes

$$\mathcal{L}_F = \bar{\psi}_R i\partial\!\!\!/\psi_R + \bar{\psi}_L i\partial\!\!\!/\psi_L - M_0\left(\bar{\psi}_L U^\dagger \psi_R + \bar{\psi}_R U \psi_L\right) \tag{2.47}$$

The following redefinition of their fields

$$\Psi_R \equiv \xi^\dagger \psi_R, \quad \Psi_L \equiv \xi \psi_L, \quad U = \xi\xi, \quad \xi = \exp(i\vec{\tau}\cdot\vec{\pi}/2f_\pi) \tag{2.48}$$

will *dress* our baryons, i.e. turning them into quasi-particles surrounded by a meson cloud. In terms of these dressed fields $\Psi = \Psi_R + \Psi_L$ (2.47) reads

$$\mathcal{L}_F = \bar{\Psi}\left(i\gamma_\mu D^\mu - M_0 + \gamma_\mu\gamma_5 a^\mu\right)\Psi \tag{2.49}$$

with the chiral covariant derivative

$$D^\mu = \partial^\mu - iv^\mu \tag{2.50}$$

mentioned above and the vector and axial vector quantities which we also expand to second order in the pion fields

$$v^\mu = \frac{i}{2}\left(\xi^\dagger\partial^\mu\xi + \xi\partial^\mu\xi^\dagger\right) \quad \rightarrow \quad -\frac{1}{4f_\pi^2}\vec{\tau}\cdot(\vec{\pi}\times\partial^\mu\vec{\pi}) \tag{2.51}$$

$$a^\mu = \frac{i}{2}\left(\xi^\dagger\partial^\mu\xi - \xi\partial^\mu\xi^\dagger\right) \quad \rightarrow \quad -\frac{1}{2f_\pi}\vec{\tau}\cdot\partial^\mu\vec{\pi} \tag{2.52}$$

The Yukawa couplings of the bare fermions have turned into vector and pseudovector couplings of the dressed fermions. Identifying the dressed fermions with our baryons $\Psi \equiv \Psi_B = (p, n)$ we can write the leading order term of the chiral meson-baryon effective Lagrangian as

$$\mathcal{L}^{(1)}_{\Phi B} = \bar{\Psi}_B\left(i\not{D} - M_0 + g_A\gamma_\mu\gamma_5 a^\mu\right)\Psi_B = \mathcal{L}'_B + \mathcal{L}_{\pi N} \tag{2.53}$$

where $\mathcal{L}'_B = \mathcal{L}_B(\partial^\mu \rightarrow D^\mu)$, see (2.45), and

$$\mathcal{L}_{\pi N} = -\frac{g_A}{2f_\pi}\bar{\Psi}\gamma_\mu\gamma_5\vec{\tau}\partial^\mu\vec{\pi}\Psi \tag{2.54}$$

with the value for g_A given in (2.64).

2.7 Gell-Mann-Oakes-Renner Relation

We have seen that the vanishing quark masses in the chiral limit lead to zero pion mass and that the order parameter for spontaneous chiral symmetry breaking is the quark condensate $\langle\bar{q}q\rangle$.
There exists a relation between fundamental quantities of QCD like the quark mass m_q, the chiral condensate $\langle\bar{q}q\rangle$ and experimentally measured hadron properties like the pion mass m_π and its decay constant f_π in (2.28).
In order to obtain it we compare the mass term of the QCD Lagrangian $-m_q\bar{q}q$ with that of the effective theory in (2.42) above. Taking the vacuum expectation values leads to

$$-m_q\langle\bar{q}q\rangle = 2m_q B f_\pi^2. \tag{2.55}$$

The last term in (2.42) can be identified as the pion mass term

$$-m_q B\vec{\pi}^2 = -\frac{1}{2}m_\pi^2\vec{\pi}^2 \tag{2.56}$$

allowing identification of the proportionality constant

$$B = -\frac{\langle \bar{q}q \rangle}{2f_\pi^2}. \tag{2.57}$$

Inserting B back into (2.55) yields

$$m_\pi^2 f_\pi^2 = -m_q \langle \bar{q}q \rangle, \tag{2.58}$$

the GELL-MANN-OAKES-RENNER (GOR) relation [18]. It also holds for the case of three flavors. For two flavors we have

$$m_\pi^2 = -\frac{1}{2f_\pi^2}(m_u + m_d)\langle \bar{u}u + \bar{d}d \rangle + \mathcal{O}(m_q^2). \tag{2.59}$$

The GOR relation is not exact. There are quadratic corrections. Recent precise $\pi\pi$-data indicate that the term linear in m_q is responsible for at least 95% of $m_\pi^2 f_\pi^2$ [19].

2.8 Pion-Nucleon Sigma Term

We will now define the pion-nucleon sigma term and state the value which we use for it in our calculations. It can be deduced from low-energy πN scattering data

$$\Sigma = f_\pi^2 \bar{D}^+(0, 2m_\pi^2) = \sigma(2m_\pi^2) + \Delta_R \tag{2.60}$$

where the bar on the isoscalar invariant scattering amplitude[5] $D^+(\nu, t)$ indicates that the pseudovector BORN term was removed. Δ_R is small ($< 2\,\mathrm{MeV}$). The so-called CHENG-DASHEN point ($\nu = 0, t = 2m_\pi^2$) lies outside the physical πN scattering region. Therefore the experimental data must be extrapolated to obtain Σ. The most reliable extrapolations are based on dispersion relation calculations first carried out by [20] and later improved by [21].
The sigma-nucleon term parametrises the explicit chiral symmetry breaking in QCD and measures the nucleon mass shift away from the chiral limit $m_q = m_{u,d} = 0$ - and therefore the contribution of the quark mass to the nucleon mass M:

$$\sigma_N = \sigma(0) = \sigma(2m_\pi^2) - \Delta_\sigma = \frac{\langle N | m_q(\bar{u}u + \bar{d}d) | N \rangle}{2M} = m_q \frac{\partial M}{\partial m_q} \tag{2.61}$$

[5] *f_π is the pion decay constant, ν the crossing energy variable and t the 4-momentum transfer*

where $|N\rangle$ denotes the state of a nucleon. The shift of the scalar form factor of the nucleon from $t = 0$ to $t = 2m_\pi^2$ is $\Delta_\sigma = \sigma(2m_\pi^2) - \sigma(0) = 15.2\,\text{MeV}$. In other words σ_N gives the portion of the nucleon mass arising from explicit chiral symmetry breaking in QCD. We will work with the value from [21]

$$\sigma_N = (45 \pm 8)\,\text{MeV} \tag{2.62}$$

Because of the complexity of the extrapolation the involved value of σ_N is still under discussion. In comparison to more recent determinations it might be too small [22, 23].

2.9 GOLDBERGER-TREIMAN Relation

The GOLDBERGER-TREIMAN relation [24] is a chiral low energy theorem

$$g_{\pi N} = g_A \frac{M_0}{f_\pi} + O(m_q) = 12.88 \tag{2.63}$$

which connects the pion nucleon coupling constant [25] with the axial vector coupling constant of the nucleon. This can be used to find the value

$$g_A = 1.267 \tag{2.64}$$

by inserting $M_0 = 939\,\text{MeV}$ and f_π from (2.28).

Chapter 3

Field Theory at Finite Temperature and Density

The chiral condensate $\langle\bar{q}q\rangle$ serves as an order parameter of spontaneous chiral symmetry breaking. We have established the connection between the QCD ground state and the quark condensate in the previous chapter. The chiral condensate changes the structure of the vacuum, populating it with correlated quark-antiquark pairs.
The asymptotic freedom of QCD leads to restoration of chiral symmetry at high temperatures. The low temperature behaviour of $\langle\bar{q}q\rangle(T)$ is determined by GOLDSTONE bosons. In order to be able to study the chiral phase transition, i.e. the condensate's dependence upon temperature and baryon density, we need to perform our calculations in a suitable framework. Equilibrium statistical mechanics offers three types of ensembles: microcanonical (isolated system; E, N and V fixed), canonical (system in contact with a heat bath; T, N and V fixed) and grand canonical (particles and energy exchangeable with a reservoir; T, μ and V fixed). The selection of a certain ensemble is arbitrary and without loss of generality since a LAPLACE transformation allows to pass over to either of the other ensembles.
In relativistic quantum systems where particles can be created and annihilated the grand canonical ensemble is the proper choice. There $\beta = 1/T$ and μ can be thought of as LAGRANGE multipliers which determine the mean energy and particle number respectively. The suitable framework for us is *thermal field theory* where an imaginary time formalism is introduced to connect quantum field theory to statistical mechanics in a grand canonical ensemble [26, 27].

3.1 The Grand Canonical Ensemble

Starting with the grand canonical partition function

$$\mathcal{Z} = \mathbf{Tr}\, \exp\left[-\beta(H - \mu N)\right] \tag{3.1}$$

we will determine our equation of state (EOS) - the pressure

$$P = \frac{T}{V} \ln \mathcal{Z} \tag{3.2}$$

which is directly related to the thermodynamic potential

$$\Omega = -P. \tag{3.3}$$

From P all other thermodynamic properties can be calculated as we will show in the upcoming sections.
Unfortunately it is in general not possible to obtain the pressure in closed form. Usually one starts from a special case where the pressure of an idealised system is calculated exactly and adds the corrections perturbatively.

3.1.1 Free Fermions

The explicit calculation of the pressure of an ideal fermion gas from the Dirac Lagrangian in absence of interactions

$$\mathcal{L}_{\text{Dirac}} = \bar{\psi}(i\partial\!\!\!/ - M)\psi \tag{3.4}$$

with the result

$$P = \frac{2}{3\pi^2} \int_M^\infty \mathrm{d}E \left(E^2 - M^2\right)^{3/2} \left[f_E^+ + f_E^-\right] \tag{3.5}$$

is to be found in Appendix B. We used the abbreviation $f_E^\pm = f(E \pm \mu)$ for the Fermi distribution function $f(x) = (e^{x/T} + 1)^{-1}$.

3.1.2 Non-interacting Bosons

Consider the Lagrangian of a free (pseudo) scalar boson field such as the pion:

$$\mathcal{L} = \frac{1}{2}\partial_\mu \pi \partial^\mu \pi - \frac{1}{2} m_\pi^2 \pi^2. \tag{3.6}$$

A similar calculation as that in the fermionic case above, see e.g. [26], yields

$$\ln \mathcal{Z} = -V \int_0^\infty \frac{\mathrm{d}^3 p}{(2\pi)^3} \ln\left(1 - e^{-\beta E}\right) \tag{3.7}$$

where $E^2 = \vec{p}^2 + m_\pi^2$. The thermodynamical relation (3.2) yields the corresponding pressure of a pion gas

$$P(T) = \frac{T}{V} \ln \mathcal{Z} = \frac{1}{6\pi^2} \int_{m_\pi}^\infty \mathrm{d}E \frac{\left(E^2 - m_\pi^2\right)^{3/2}}{e^{\beta E} - 1} \tag{3.8}$$

In the case of a conserved charge this result is modified to

$$P(T,\mu) = \frac{1}{6\pi^2} \int_{m_\pi}^\infty \mathrm{d}E \left(E^2 - m_\pi^2\right)^{3/2} \left[b(E+\mu) + b(E-\mu)\right] \tag{3.9}$$

where μ is the chemical potential and b is the Bose distribution function $b(x) = (e^{x/T} - 1)^{-1}$.

3.2 Chiral Condensate at Finite Temperature and Density

We have already mentioned chiral restoration under extreme conditions and we learned about the order parameter of chiral symmetry. Therefore we will study the dependence of this order parameter - the chiral quark condensate $\langle \bar{q} q \rangle$ - on finite temperature T and baryon density ρ in this section.
We will start with a useful theorem from quantum mechanics, the Hellmann-Feynman theorem from which we will be able to derive the master formula for the chiral condensate. This will easily be generalised to finite T and then separated into a nucleon and a pion sector. The first will lead us to the low density theorem. For the latter we will discuss the contributions of 1- and 2-loop diagrams of the free and interacting pion gas.

3.2.1 Hellmann-Feynman Theorem

For a given Hamiltonian $H(\lambda)$, which depends on a parameter λ that can be changed adiabatically, with eigenstates

$$H(\lambda)|\psi_\lambda\rangle = E(\lambda)|\psi_\lambda\rangle \tag{3.10}$$

the Hellmann-Feynman theorem [28, 29] states that the change of energy E with respect to λ does not depend upon the change of the normalised states $|\psi_\lambda\rangle$

$$\frac{\mathrm{d}E(\lambda)}{\mathrm{d}\lambda} = \left\langle \psi_\lambda \left| \frac{\partial H(\lambda)}{\partial \lambda} \right| \psi_\lambda \right\rangle. \tag{3.11}$$

Let us first consider the zero temperature case ($T = 0$). In the Hamiltonian density

$$\mathcal{H}_{QCD}(m_q) = \mathcal{H}_0 + m_q(\bar{u}u + \bar{d}d), \tag{3.12}$$

where $\mathcal{H}_0$ represents massless QCD, the quark mass plays the role of such a parameter λ. We will only consider two flavors $m_{u,d}$ with equal mass m_q. Now let $|\psi\rangle$ be an eigenstate (e.g. the vacuum $|0\rangle$, a free nucleon $|N\rangle$ or nuclear matter at density ρ):

$$H_{QCD}|\psi\rangle = E(m_q)|\psi\rangle; \qquad H_{QCD} = \int \mathrm{d}^3x\, \mathcal{H}_{QCD}(x). \tag{3.13}$$

Then it follows

$$\frac{\mathrm{d}E(m_q)}{\mathrm{d}m_q} = \int \mathrm{d}^3x \left\langle \psi \left| \frac{\partial \mathcal{H}_{QCD}(m_q)}{\partial m_q} \right| \psi \right\rangle = V \left\langle \psi \left| \bar{u}u + \bar{d}d \right| \psi \right\rangle, \tag{3.14}$$

or in terms of the energy density $\epsilon = E/V$

$$\frac{\mathrm{d}\epsilon(m_q)}{\mathrm{d}m_q} = \left\langle \psi \left| \bar{u}u + \bar{d}d \right| \psi \right\rangle. \tag{3.15}$$

Only differences in energy can be measured, therefore we subtract the vacuum expectation value from (3.15)

$$\begin{aligned} &\frac{\mathrm{d}\epsilon(m_q)}{\mathrm{d}m_q} - \frac{\mathrm{d}\epsilon_0(m_q)}{\mathrm{d}m_q} = \left\langle \psi \left| \bar{u}u + \bar{d}d \right| \psi \right\rangle - \left\langle 0 \left| \bar{u}u + \bar{d}d \right| 0 \right\rangle \\ \Leftrightarrow\ &\frac{\left\langle \psi \left| \bar{u}u + \bar{d}d \right| \psi \right\rangle}{\left\langle 0 \left| \bar{u}u + \bar{d}d \right| 0 \right\rangle} =: \frac{\langle \bar{q}q \rangle(\rho)}{\langle \bar{q}q \rangle_0} = 1 + \frac{1}{\langle \bar{q}q \rangle_0} \frac{\mathrm{d}}{\mathrm{d}m_q}(\epsilon - \epsilon_0). \end{aligned} \tag{3.16}$$

The change in the quark condensate is given by the change of the energy density with varying quark mass. As most models for hadronic systems are formulated in terms of hadron masses rather than the quark mass we will replace $\mathrm{d}/\mathrm{d}m_q$. Consider a system with nucleons and pions with masses M and m_π which themselves depend upon the quark mass

$$\frac{\mathrm{d}}{\mathrm{d}m_q} = \frac{\partial m_\pi^2}{\partial m_q}\frac{\partial}{\partial m_\pi^2} + \frac{\partial M}{\partial m_q}\frac{\partial}{\partial M} + \ldots \quad . \tag{3.17}$$

In principle there are further implicit m_q-dependences denoted by the dots. Inserting (3.17) into (3.16) and using the GOR relation (2.58) and its derivative

$$\frac{\partial m_\pi^2}{\partial m_q} = -\frac{\langle\bar{q}q\rangle_0}{f_\pi^2} \tag{3.18}$$

as well as the definition of the pion-nucleon sigma term (2.61), $\partial M/\partial m_q = \sigma_N/m_q$, we can write

$$\begin{aligned}
\frac{\langle\bar{q}q\rangle(\rho)}{\langle\bar{q}q\rangle_0} &= 1 + \frac{1}{\langle\bar{q}q\rangle_0}\left[\frac{\partial m_\pi^2}{\partial m_q}\frac{\partial}{\partial m_\pi^2} + \frac{\partial M}{\partial m_q}\frac{\partial}{\partial M}\right](\epsilon - \epsilon_0) \\
&= 1 - \frac{1}{f_\pi^2}\frac{\partial(\epsilon-\epsilon_0)}{\partial m_\pi^2} + \frac{\sigma_N}{\langle\bar{q}q\rangle_0 m_q}\frac{\partial(\epsilon-\epsilon_0)}{\partial M} \\
&\overset{(2.58)}{=} 1 - \frac{1}{f_\pi^2}\left[\frac{\partial}{\partial m_\pi^2} + \frac{\sigma_N}{m_\pi^2}\frac{\partial}{\partial M}\right](\epsilon - \epsilon_0),
\end{aligned} \tag{3.19}$$

which can easily be generalised to finite temperature T by replacing the energy density with the thermodynamic potential Ω of the grand canonical ensemble which is directly related to the pressure of the system via $\Omega = -P$. Therefore the master formula in calculating the chiral condensate for a system of pions and nucleons takes on the form

$$\boxed{\frac{\langle\bar{q}q\rangle(\rho,T)}{\langle\bar{q}q\rangle_0} = 1 + \frac{1}{f_\pi^2}\left(\frac{\partial P}{\partial m_\pi^2} + \frac{\sigma_N}{m_\pi^2}\frac{\partial P}{\partial M}\right).} \tag{3.20}$$

This is a special case of the general relation

$$\frac{\langle\bar{q}q\rangle(\rho,T)}{\langle\bar{q}q\rangle_0} = 1 + \frac{1}{f_\pi^2}\frac{\mathrm{d}P}{\mathrm{d}m_\pi^2}, \tag{3.21}$$

expressed in terms of the total derivative of the pressure with respect to m_π^2. The first term in brackets of eq. (3.20) is closely related to pions, the second to nucleons. We will start with the first:

3.2.2 Free and Interacting Pion Gas at Finite Temperature

Let us now concentrate on the low temperature dependence of the chiral condensate which we first study at zero baryon density. Heavy hadrons are suppressed by their BOLTZMANN factor $\exp(-E/T)$. The leading behaviour of the chiral condensate at temperatures $T \leq 100\,\mathrm{MeV}$ comes from the light pions. The first calculations concerning the T-dependence of the quark condensate were carried out in [30]. Later in [31] the thermodynamics of a pion gas was calculated up to three loops in chiral perturbation theory. More recent calculations can be found in [32, 33]. The starting point is the leading order effective chiral $\pi\pi$ Lagrangian which we get by inserting B from (2.57) into (2.42):

$$\begin{aligned} \mathcal{L}_2 = \mathcal{L}^{(2)}_{\pi\pi} &= \frac{f_\pi^2}{4}\mathrm{tr}\left[\partial_\mu U \partial^\mu U^\dagger + m_\pi^2\left(U + U^\dagger\right)\right], \\ U &= \sqrt{1 - f_\pi^{-2}\vec{\pi}^2} + i f_\pi^{-1}\vec{\tau}\cdot\vec{\pi}. \end{aligned} \tag{3.22}$$

We have used that $B\,\mathbf{tr}\,M = B \cdot 2m_q = m_\pi^2 = \frac{1}{2}\mathbf{tr}\,m_\pi^2$. Our results hold for any parametrization of U. Expanding $\mathcal{L}^{(2)}_{\pi\pi}$ to fourth order in $\vec{\pi}$ one finds

$$\begin{aligned} \mathcal{L}^{(2)}_{\pi\pi} &= \frac{1}{2}\partial_\mu\vec{\pi}\cdot\partial^\mu\vec{\pi} + \frac{1}{6f_\pi^2}\left[(\vec{\pi}\cdot\partial_\mu\vec{\pi})(\vec{\pi}\cdot\partial^\mu\vec{\pi}) - (\vec{\pi}\cdot\vec{\pi})(\partial_\mu\vec{\pi}\cdot\partial^\mu\vec{\pi})\right] \\ &+ m_\pi^2\left[f_\pi^2 - \frac{1}{2}\vec{\pi}\cdot\vec{\pi} + \frac{1}{24f_\pi^2}(\vec{\pi}\cdot\vec{\pi})^2\right] + O(\vec{\pi}^6) \end{aligned} \tag{3.23}$$

From $\mathcal{L}^{(2)}_{\pi\pi}$ one can derive the following pressure

$$P_\pi(T) = \frac{T^4}{2\pi^2}\left[h_5(y) - 3\alpha h_3^2(y)\right] \tag{3.24}$$

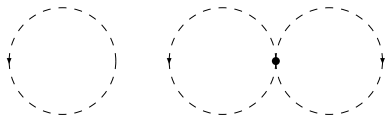

where

$$y = \frac{m_\pi}{T},\ \alpha = \left(\frac{m_\pi}{4\pi f_\pi}\right)^2 \quad \text{and} \quad h_n(y) = \int_y^\infty \mathrm{d}x\,\frac{(x^2 - y^2)^{n/2-1}}{\exp(x) - 1}. \tag{3.25}$$

We already encountered the first term in (3.24)

$$\frac{T^4}{2\pi^2}h_5(y) = 3\cdot\frac{1}{6\pi^2}\int_{m_\pi^2}^\infty \mathrm{d}E\frac{(E^2 - m_\pi^2)^{3/2}}{e^{E/T} - 1} \tag{3.26}$$

in our discussion of bosons in (3.8). The additional factor of "3" here comes from the three different pions $(\pi^0, \pi^\pm)$.
The contribution to the chiral condensate is easily obtained from $P_\pi(T)$

$$\frac{\langle\bar{q}q\rangle(T)}{\langle\bar{q}q\rangle(0)} = 1 - 12\alpha y^{-2} h_3(y) \left\{1 + 2\alpha \left[y^{-2} h_3(y) - h_1(y) + \bar{c}\right]\right\}. \qquad (3.27)$$

with the low energy constant $\bar{c} \simeq 3$ which accounts for quadratic quark mass corrections in the GOR relation etc. [33].
It is only temperature dependent. The "1" in the bracket belongs to the free piece, the rest is the interacting 2-loop part. These contributions are shown in Fig. 3.1.

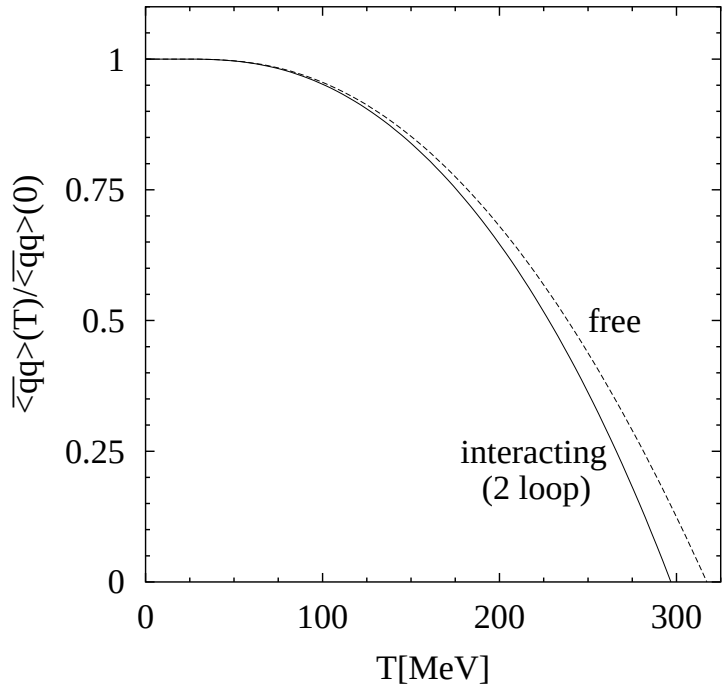

Figure 3.1: Contributions of free (dashed) and interacting (solid) thermal pion gas to the chiral condensate as given in (3.27)

Finally

$$s_\pi = \frac{\mathrm{d}P_\pi(T)}{\mathrm{d}T} = \frac{4}{T} P_\pi(T) + \frac{3Tm_\pi^2}{\pi^2} h_3(y) \left(\frac{1}{2} - \alpha h_1(y)\right), \qquad (3.28)$$

is the corresponding contribution to the entropy density.

3.2.3 Nucleons: Low Density Approximation

Consider a FERMI gas of free nucleons at $T = 0$ and baryon density

$$\rho = 4 \int_{p<p_F} \frac{\mathrm{d}^3 p}{(2\pi)^3} = \frac{2p_F^3}{3\pi^2}, \qquad p_F ...\text{FERMI momentum} \tag{3.29}$$

assuming the same number of protons and neutrons where the degeneracy factor of 4 is for spin and isospin.
The scalar density is defined like $n_s = -\partial P/\partial M$, therefore we can rewrite the last term in (3.20) as follows

$$\frac{\langle \bar{q}q \rangle_\rho}{\langle \bar{q}q \rangle_0} = 1 - \frac{\sigma_N}{m_\pi^2 f_\pi^2} n_s \tag{3.30}$$

At small baryon density the difference between ρ and the scalar density n_s can be neglected, so that in this limit it is applicable to work with

$$\frac{\langle \bar{q}q \rangle_\rho}{\langle \bar{q}q \rangle_0} \simeq 1 - \frac{\sigma_N}{m_\pi^2 f_\pi^2} \rho. \tag{3.31}$$

This is known as the low density approximation (LDA). More on the consequences involved can be found e.g. in [34] and the references therein.

Chapter 4

Nuclear Matter

We mentioned the importance of chiral symmetry ($\rightarrow$ 2.2) in the study of low energy hadron physics, in particular the nuclear matter problem. After introducing the basic features of this symmetry in chapter 2 we emphasised at the beginning of chapter 3 the key role played by its order parameter - the chiral quark condensate $\langle\bar{q}q\rangle$. At high temperature and/or baryon density chiral symmetry is restored which results in a vanishing quark condensate $\langle\bar{q}q\rangle = 0$. In the chiral symmetric phase hadrons are unstable, quarks are quasi-free and (almost) massless. This phase is named quark-gluon plasma. The chiral phase transition between hadronic or nuclear matter ($\langle\bar{q}q\rangle \neq 0$) to the plasma phase ($\langle\bar{q}q\rangle = 0$) is interesting to study for several reasons: due to the big bang theory the universe started out from a singularity, an extremely hot and dense state. The system expanded and cooled down with decreasing density, thus the early universe must have gone through this phase transition ($\rightarrow$ formation of nucleons). Another situation where the chirally symmetric phase may be realised is the extremely compressed matter in compact (neutron) stars. Therefore knowledge about such matter may allow to improve our understanding of dense stars. Anyhow the study of the chiral condensate allows to construct a phase diagram of nuclear matter. Sooner or later a lot of related questions might be answered by the currently performed heavy ion collision experiments.
Whereas the knowledge about typical baryon densities at which such a phase transition occurs is rather poor, the critical temperature above which chiral symmetry is restored is

$$T_c = (173 \pm 8)\,\mathrm{MeV} \tag{4.1}$$

known from lattice calculations. This value corresponds to the two-flavor result from [35].

Before going into details we want to clarify the notion of nuclear matter: an infinite homogeneous system of equally many protons and neutrons being subject only to the strong interaction.
It is not an easy task to obtain empirical information about its properties since equilibrated nuclear matter does not exist in the laboratory and astrophysics measurements are rather indirect and therefore subject to large uncertainties. However, we will see that some of its properties can be deduced more or less directly from the study of nuclei. A nucleus consists of Z protons and N neutrons. Because the mass of a nucleus is mainly given by the sum of the masses of these components one defines the mass number $A = Z + N$.
There are two sources that can be used to draw helpful qualitative conclusions: First the phenomenological BETHE-WEIZSÄCKER mass formula [36, 37, 38] whose parametrisation is dependent upon A and Z. And second: the FOURIER transform of the nuclear form factor which yields the charge distribution of a nucleus. Such form factors have been measured for a wide range of nuclei at various electron accelerator facilities during the last four decades with high precision. The results can be summarised as follows [39]:

- If nuclei are approximated as spheres with homogeneous charge distribution, the radius of this sphere is

$$R \simeq 1.2\,\mathrm{fm} \cdot A^{1/3}. \tag{4.2}$$

- The term in the BETHE-WEIZSÄCKER mass formula which dominates the binding energy is the volume term ($\sim A$):

$$B = \frac{|E|}{A} \simeq 16\,\mathrm{MeV}. \tag{4.3}$$

The fact that B is a constant as function of nuclear mass number is called saturation.
- The nuclear charge distribution can be approximated by a FERMI function with two parameters $\rho(r) = \rho_0/[1 + e^{(r-c)/a}]$. As a consequence of the saturation (nearly) all nuclei have the same density in their centre:

$$\rho_0 \simeq 0.17\,\mathrm{fm}^{-3} \simeq 0.0013\,\mathrm{GeV}^3. \tag{4.4}$$

The third property of nuclear matter we will come across is unfortunately not known so well. It is the nuclear matter compressibility κ. It can be obtained by extrapolation of isoscalar giant monopole resonances. A range which

covers results of non-relativistic [40] as well as relativistic [41] analysis is

$$\kappa = (230 \pm 50)\,\mathrm{MeV} \tag{4.5}$$

More about it can be found in section 4.2.3.
Non-relativistic models are able to describe nuclear matter quite well, e.g. in [42] where advanced many-body techniques and an adjustable three-body force are used. In [43, 44] an alternative approach is used where the energy per particle of isospin-symmetric nuclear matter is calculated in the three-loop approximation of chiral perturbation theory. Both approaches differ in the treatment of effective short-range interactions. Nevertheless with only one adjustable parameter a good nuclear matter equation of state can be obtained.

The relativistic approach to the nuclear many-body problem was initiated by WALECKA and his coworkers [45]. Such relativistic mean field models were refined for applications to nuclear structure by inclusion of additional non-linear terms, e.g. as in [46]. A recent overview over mean-field models of nuclear structure can be found in [47].
The starting point of our model will also be the treatment of the nucleons as DIRAC quasi-particles moving in self-consistently generated scalar and vector mean fields. An extensive discussion of the relativistic mean-field approach can be found in [48, 49].

4.1 The WALECKA Model

At the beginning of the introduction to this chapter we explained why effective nuclear field theory is the tool chosen in describing nuclear matter. Using effective field theory one has to decide about the following questions:

- Which particle species to be included?
- What precise form of the Lagrangian should be used?

The model Lagrangian used in scalar-vector mean field theory is

$$\begin{aligned}\mathcal{L}_{\mathrm{W}} &= \bar{\psi}\left[i\gamma_\mu\partial^\mu - M + g_\sigma\sigma - g_\omega\gamma_\mu\omega^\mu\right]\psi + \frac{1}{2}\left(\partial_\mu\sigma\partial^\mu\sigma - m_\sigma^2\sigma^2\right) \\ &\quad -\frac{1}{4}\mathrm{F}^{\mu\nu}\mathrm{F}_{\mu\nu} + \frac{1}{2}m_\omega^2\omega^\mu\omega_\mu\,; \quad F_{\mu\nu} = \partial_\mu\omega_\nu - \partial_\nu\omega_\nu.\end{aligned} \tag{4.6}$$

This Lagrangian includes the YUKAWA couplings of the baryon field ψ of mass M to σ, a neutral scalar boson field, and ω, a neutral vector boson field.

The exchange of σ is thought to simulate dynamics of 2-pion exchange. Their masses are m_σ and m_ω respectively. The long-range part of the nuclear force comes from 1-pion exchange. However, in isospin symmetric matter (equal numbers of protons and neutrons: $N_p = N_n$) it averages to zero in the mean-field approximation. The same holds for rho meson exchange.
The particular choice of Lagrangian (4.6) is motivated by considering the interaction of two heavy nonrelativistic nucleons. The corresponding instantaneous and spin-independent potential in coordinate space can then be written as the sum of two YUKAWA interactions:

$$V(r) = \frac{g_\omega^2\, e^{-m_\omega r}}{4\pi r} - \frac{g_\sigma^2\, e^{-m_\sigma r}}{4\pi r}. \tag{4.7}$$

For $g_\omega > g_\sigma$ this potential is repulsive at short distances and with $m_\omega > m_\sigma$ it will be attractive at large distances, thus resembling the main features of the nucleon-nucleon force which are responsible for binding and saturation properties of nuclear matter.

With the parameters from [26]

$$\begin{aligned} m_\omega &= 783\,\text{MeV} \qquad & m_\sigma &= 550\,\text{MeV} \\ g_\omega^2/4\pi &= 14.37 \qquad & g_\sigma^2/4\pi &= 9.33 \end{aligned} \tag{4.8}$$

the potential takes the form as shown in Fig.4.1.

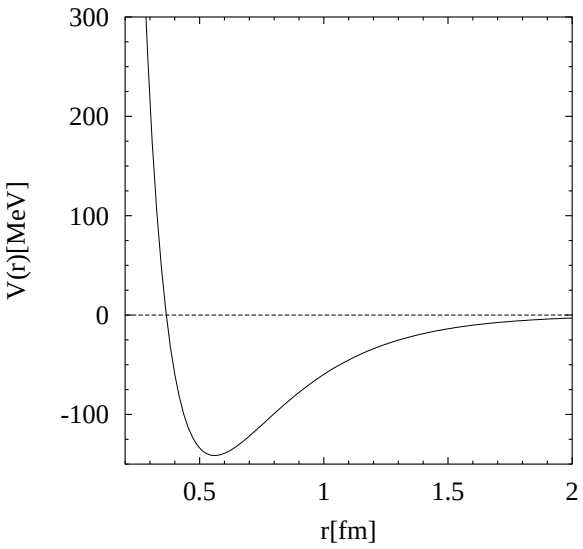

Figure 4.1: Model potential (4.7) of the nucleon-nucleon interaction with the parameters from (4.8).

The partition function at finite density is

$$\begin{aligned} \mathcal{Z} \;&=\; \int \left[\mathrm{d}\bar{\psi}_\mathrm{p}\right] [\mathrm{d}\psi_\mathrm{p}] \left[\mathrm{d}\bar{\psi}_\mathrm{n}\right] [\mathrm{d}\psi_\mathrm{n}] [\mathrm{d}\sigma] [\mathrm{d}\omega_\mu] \cdot \\ &\cdot\; \exp\left(\int_0^\beta \mathrm{d}\tau \int \mathrm{d}^3x \left[\mathcal{L}_W + \mu_p \psi_p^+ \psi_p + \mu_n \psi_n^+ \psi_n\right]\right) \end{aligned} \tag{4.9}$$

with chemical potentials μ_p and μ_n for protons and neutrons, where we have $\mu = \mu_n = \mu_p$ for isospin symmetric matter and

$$\mathcal{L}_W \;\rightarrow\; \mathcal{L}_W + \mu_p \psi_p^+ \psi_p + \mu_n \psi_n^+ \psi_n = \mathcal{L}_W + \mu \psi^+ \psi = \mathcal{L}_W + \mu \bar{\psi} \gamma_0 \psi \tag{4.10}$$

from which all properties of this system can be derived.

4.1.1 Mean Field Approximation

The nucleons act as sources in the boson field equations derived from (4.6). The fields σ and ω_0 can have nonzero expectation values, so they are expressed as their ensemble average (bar) plus the fluctuations about it:

$$\begin{aligned} \sigma &= \bar{\sigma} + \delta\sigma \\ \omega_\mu &= \delta_{\mu 0}\bar{\omega}_0 + \delta\omega_\mu \quad (\bar{\omega}_i = 0 \text{ due to rotational symmetry}) \end{aligned} \tag{4.11}$$

In mean field approximation (MFA) the fluctuating part will be neglected, so that $\delta\sigma, \delta\omega_\mu \to 0$. The nucleons move independently in the mean fields $\bar{\sigma}$ and $\bar{\omega}_0$ which are generated self-consistently.
We have $\sigma \to \bar{\sigma}$ and $\omega_\mu \to \bar{\omega}_0$. Therefore the integrand (4.10) of the exponential in the partition function (4.9) is approximated by

$$\begin{aligned} \mathcal{L}_W &= \bar{\psi}\left(i\partial\!\!\!/ - M + g_\sigma\bar{\sigma} - g_\omega\bar{\omega}_0\right)\psi + \mu\bar{\psi}\gamma_0\psi - \frac{1}{2}m_\sigma^2\bar{\sigma}^2 + \frac{1}{2}m_\omega^2\bar{\omega}_0^2 = \\ &= \bar{\psi}\left(i\partial\!\!\!/ - M^* + \mu^*\gamma_0\right)\psi - \frac{1}{2}m_\sigma^2\bar{\sigma}^2 + \frac{1}{2}m_\omega^2\bar{\omega}_0^2 =: \mathcal{L}^* + \mathcal{L}(\bar{\sigma}, \bar{\omega}_0) \end{aligned} \tag{4.12}$$

where $\mathcal{L}^* = \mathcal{L}^*(\bar{\psi}, \psi) = \bar{\psi}\left(i\partial\!\!\!/ - M^* + \mu^*\gamma_0\right)\psi$. The remaining calculation of $\mathcal{Z}$ can be performed explicitly because the functional integral is just a product of Gaussian integrals. It is straightforward to obtain the pressure from $P = T/V \ln \mathcal{Z}$ where

$$\mathcal{Z} = \int \left[\mathrm{d}\psi^\dagger\right][\mathrm{d}\psi] \cdot e^{\mathcal{S}} \quad \text{and} \quad \mathcal{S} = \int_0^\beta \mathrm{d}\tau \int \mathrm{d}^3x\, \mathcal{L}_W \tag{4.13}$$

and $\psi^\dagger$ is the field conjugate to ψ. With (4.12) we find for the pressure

$$\begin{aligned} P &= \frac{T}{V}\ln \int \left[\mathrm{d}\psi^\dagger\right][\mathrm{d}\psi] \cdot \exp\left\{\int_0^\beta \mathrm{d}\tau \int \mathrm{d}^3x\, \mathcal{L}^*(\bar{\psi}, \psi) + \mathcal{L}(\bar{\sigma}, \bar{\omega}_0)\right\} \\ &= \frac{T}{V}\ln\left[\exp\left\{\beta V \mathcal{L}(\bar{\sigma}, \bar{\omega}_0)\right\} \cdot \int \left[\mathrm{d}\psi^\dagger\right][\mathrm{d}\psi] \cdot \exp\left\{\int_0^\beta \mathrm{d}\tau \int \mathrm{d}^3x\, \mathcal{L}^*(\bar{\psi}, \psi)\right\}\right] \\ &= \mathcal{L}(\bar{\sigma}, \bar{\omega}_0) + \frac{T}{V}\ln \int \left[\mathrm{d}\psi^\dagger\right][\mathrm{d}\psi] \cdot \exp\left\{\int_0^\beta \mathrm{d}\tau \int \mathrm{d}^3x\, \mathcal{L}^*(\bar{\psi}, \psi)\right\}. \end{aligned} \tag{4.14}$$

The reader who has seen Appendix B will recognise that we already encountered the last term in (4.14) there, with the replacements

$$M \to M^*, \quad \mu \to \mu^* \tag{4.15}$$

into (B.18). This led to the result for a free FERMI gas which can be found in (B.30). In our case - because of (4.15) - we deal with nucleons as quasi particles of effective mass M^* and effective chemical potential μ^*. Then

$$\begin{aligned} P &= \frac{2}{3\pi^2}\int_{M^*}^{\infty} \mathrm{d}E \left(E^2 - M^{*2}\right)^{3/2} \left[f_E^- + f_E^+\right] + \frac{1}{2}m_\omega^2\bar{\omega}_0^2 - \frac{1}{2}m_\sigma^2\bar{\sigma}^2 \\ &= P_{FG}(T,\mu^*,M^*) + \frac{1}{2}m_\omega^2\bar{\omega}_0^2 - \frac{1}{2}m_\sigma^2\bar{\sigma}^2 \end{aligned} \tag{4.16}$$

is our expression for the pressure derived from (4.12). The first term on the right-hand side is the pressure of a free FERMI gas of quasiparticles (quasi-nucleons) with effective mass M^* and shifted chemical potential μ^*. The last two terms represent the vector and scalar fields in mean field approximation.

4.1.2 Self-consistency Equations

From (4.12) we can read off the relations for the nucleon effective mass and shifted chemical potential:

$$\boxed{\begin{aligned} M^* &= M - g_\sigma\bar{\sigma} && (4.17)\\ \mu^* &= \mu - g_\omega\bar{\omega}_0 && (4.18) \end{aligned}}$$

These are used to eliminate $\bar{\sigma}$ and $\bar{\omega}_0$. The following derivatives

$$\frac{\partial M^*}{\partial M} = \frac{\partial \mu^*}{\partial \mu} = 1 \tag{4.19}$$

$$\frac{\partial M^*}{\partial \bar{\sigma}} = -g_\sigma \quad ; \qquad \frac{\partial \mu^*}{\partial \bar{\omega}_0} = -g_\omega \tag{4.20}$$

taken from these self-consistency equations will be useful in our next step: the determination of $\bar{\sigma}$ and $\bar{\omega}_0$. The equilibrium configuration for these varying mean fields are obtained when the thermodynamic potential is extremal. This is equivalent to having an extremum in $P \Leftrightarrow \partial P/\partial\bar{\sigma} = \partial P/\partial\bar{\omega}_0 = 0$:

$$\left.\begin{aligned} \frac{\partial P}{\partial \bar{\sigma}} = \frac{\partial P_{FG}}{\partial M^*}\frac{\partial M^*}{\partial \bar{\sigma}} - m_\sigma^2\bar{\sigma} = 0 &\overset{(4.20)}{\Longrightarrow} \bar{\sigma} = -\frac{g_\sigma}{m_\sigma^2}\frac{\partial P_{FG}}{\partial M^*} \\ n_s = -\frac{\partial P}{\partial M} = -\frac{\partial P_{FG}}{\partial M^*}\frac{\partial M^*}{\partial M} &\overset{(4.19)}{=} -\frac{\partial P_{FG}}{\partial M^*} \end{aligned}\right\} \quad \bar{\sigma} = \frac{g_\sigma}{m_\sigma^2}n_s \tag{4.21}$$

and analogous

$$\left.\begin{aligned} \frac{\partial P}{\partial \bar{\omega}_0} = \frac{\partial P_{FG}}{\partial \mu^*}\frac{\partial \mu^*}{\partial \bar{\omega}_0} + m_\omega^2 \bar{\omega}_0 = 0 &\overset{(4.20)}{\Longrightarrow} \bar{\omega}_0 = \frac{g_\omega}{m_\omega^2}\frac{\partial P_{FG}}{\partial \mu^*} \\ \rho = \frac{\partial P}{\partial \mu} = \frac{\partial P_{FG}}{\partial \mu^*}\frac{\partial \mu^*}{\partial \mu} &\overset{(4.19)}{=} \frac{\partial P_{FG}}{\partial \mu^*} \end{aligned}\right\} \quad \bar{\omega}_0 = \frac{g_\omega}{m_\omega^2}\rho. \tag{4.22}$$

The pressure (4.16) can be written with these results for the mean fields as

$$P \;=\; P_{FG} + \frac{1}{2}\frac{g_\omega^2}{m_\omega^2}\rho^2 - \frac{1}{2}\frac{g_\sigma^2}{m_\sigma^2}n_s^2 =: P_{FG} + \frac{1}{2}G_{\mathrm{v}}\rho^2 - \frac{1}{2}G_{\mathrm{s}}n_s^2. \tag{4.23}$$

Combining (4.17) with (4.21) the scalar density is expressed in terms of the difference between the free nucleon mass M and the effective mass M^*:

$$g_\sigma \bar{\sigma} = G_{\mathrm{s}} n_{\mathrm{s}} \;\Leftrightarrow\; \bar{\sigma} = \frac{g_\sigma}{m_\sigma^2} n_s = \left(M - M^*\right)/g_\sigma \quad \Rightarrow \quad n_s = \frac{M - M^*}{G_{\mathrm{s}}} \tag{4.24}$$

An analogous relation holds for the baryon density and the (effective) chemical potential, thus we can rewrite (4.23) as:

$$P \;=\; P_{FG}(T, \mu^*, M^*) + \frac{\left(\mu - \mu^*\right)^2}{2G_{\mathrm{v}}} - \frac{\left(M - M^*\right)^2}{2G_{\mathrm{s}}}. \tag{4.25}$$

We have introduced the two parameters

$$G_{\mathrm{s}} = \frac{g_\sigma^2}{m_\sigma^2} \quad \text{and} \quad G_{\mathrm{v}} = \frac{g_\omega^2}{m_\omega^2} \tag{4.26}$$

mentioned in [26] which we will use from now on. They are fixed by reproducing the saturation density (4.4) and energy per nucleon (4.3). We will later see that in order to be able to receive the correct value for the compressibility κ we will have to introduce an additional third- or fourth-order term with coupling strengths $G_{\mathrm{n}}\,(n = 3, 4)$. This can be achieved, restricting ourselves to the nucleon, omega and sigma fields, by adding a cubic or quartic term

$$\lambda_3 \bar{\sigma}^3 \quad \text{or} \quad \lambda_4 \bar{\sigma}^4. \tag{4.27}$$

In the nonrelativistic case these terms correspond to a three- or four-body force.

4.1.3 Contact Interactions

In the mean field approximation, the WALECKA model is equivalent to a model with corresponding contact interactions. Let us start with the following Lagrangian with contact interactions:

$$\mathcal{L}_{ci} = \mathcal{L}^{\mu}_{Dirac} - \frac{G_{\mathrm{s}}}{2}\left(\bar{\psi}\psi\right)^2 + \frac{G_{\mathrm{v}}}{2}\left(\bar{\psi}\gamma_\mu\psi\right)^2 \tag{4.28}$$

where $\mathcal{L}^{\mu}_{Dirac}$ from (B.6) describes noninteracting DIRAC particles and the last two terms represent scalar and vector four-nucleon interactions. Under the transformation

$$\begin{aligned} \bar{\psi}\psi &\rightarrow \bar{\psi}\psi - \langle\bar{\psi}\psi\rangle = \bar{\psi}\psi - n_s \\ \bar{\psi}\gamma_\mu\psi &\rightarrow \bar{\psi}\gamma_\mu\psi - \langle\psi^\dagger\psi\rangle\delta_{\mu 0} = \bar{\psi}\gamma_\mu\psi - \rho\delta_{\mu 0} \end{aligned} \tag{4.29}$$

$\mathcal{L}_{ci}$ behaves like

$$\begin{aligned} \mathcal{L}_{ci} &= \mathcal{L}^{\mu}_{Dirac} - \frac{G_s}{2}\left[\left(\bar{\psi}\psi\right)^2 - 2\bar{\psi}\psi\langle\bar{\psi}\psi\rangle + \langle\bar{\psi}\psi\rangle^2\right] \\ &\quad + \frac{G_v}{2}\left[\left(\bar{\psi}\gamma_\mu\psi\right)^2 - 2\bar{\psi}\gamma_\mu\psi\langle\psi^\dagger\psi\rangle + \langle\psi^\dagger\psi\rangle^2\right] = \\ &= \mathcal{L}^{\mu}_{Dirac} + G_s\langle\bar{\psi}\psi\rangle\bar{\psi}\psi - \frac{1}{2}G_s\langle\bar{\psi}\psi\rangle^2 - G_v\langle\psi^\dagger\psi\rangle\psi^\dagger\psi + \frac{1}{2}G_v\langle\psi^\dagger\psi\rangle^2 \end{aligned} \tag{4.30}$$

where we neglected quadratic fluctuations. If we now identify the following forms for the scalar and baryon density

$$n_s = \langle\bar{\psi}\psi\rangle \overset{(4.21)}{=} \frac{m_\sigma^2}{g_\sigma}\bar{\sigma} \tag{4.31}$$

$$\rho = \langle\bar{\psi}\gamma_0\psi\rangle = \langle\psi^\dagger\psi\rangle \overset{(4.22)}{=} \frac{m_\omega^2}{g_\omega}\bar{\omega}_0 \tag{4.32}$$

and insert them back into equation (4.30) this becomes

$$\begin{aligned} \mathcal{L}_{ci} &= \bar{\psi}\left(i\partial\!\!\!/ - M + \mu\gamma_0\right)\psi + \bar{\psi}G_{\mathrm{s}}n_s\psi - \bar{\psi}\gamma_0 G_{\mathrm{v}}\rho\psi + \frac{1}{2}G_{\mathrm{v}}\rho^2 - \frac{1}{2}G_{\mathrm{s}}n_s^2 \\ &\overset{(4.26)}{=} \bar{\psi}\left(i\partial\!\!\!/ - M^* + \mu^*\gamma_0\right)\psi - \frac{1}{2}m_\sigma^2\bar{\sigma}^2 + \frac{1}{2}m_\omega^2\bar{\omega}_0^2 \equiv \mathcal{L}_W \end{aligned} \tag{4.33}$$

which is our Lagrangian (4.12) in the WALECKA model. We have thus shown that in mean field approximation (MFA), the WALECKA model with its four parameters $g_\sigma, m_\sigma, g_\omega$ and m_ω is equivalent to a model with contact interactions and only two parameters G_{s} and G_{v}. In the mean field limit, detailed information about "masses" of scalar and vector bosons is thus irrelevant since only the ratios g^2/m^2 of coupling constants and masses matter.

4.1.4 Thermodynamic Quantities and Relations

In section 3.1 we decided to perform our calculations in the grand canonical ensemble. As mentioned there we can get all other interesting information from the pressure P. The scalar and baryon densities are calculated from

$$n_s = -\frac{\partial P}{\partial M}, \qquad \rho = \frac{\partial P}{\partial \mu}, \tag{4.34}$$

the entropy density is defined as

$$s = \frac{\partial P}{\partial T}. \tag{4.35}$$

The energy density can be calculated from the Gibbs-Helmholtz relation

$$\epsilon = \mu\rho + Ts - P \tag{4.36}$$

and finally the slope of P at normal nuclear matter density ρ_0 and $T = 0$

$$\kappa = 9 \left.\frac{\partial P}{\partial \rho}\right|_{\rho=\rho_0} \tag{4.37}$$

yields the (in-)compressibility[1].
Before we come to the summary of our results performed in the calculational framework introduced in the previous sections we will briefly give an overview as to how one computes the various thermodynamical quantities. We have already pointed out the importance of the equation of state, namely the pressure $P = P(T, \mu, \mu^*, M, M^*)$, from which we derive these quantities. Let us first write down its total differential and then identify the thermodynamic relations using (4.34f):

$$\begin{aligned} \mathrm{dP} &= \frac{\partial P}{\partial T}\mathrm{dT} + \frac{\partial \mathrm{P}}{\partial \mu}\mathrm{d}\mu + \frac{\partial \mathrm{P}}{\partial \mu^*}\mathrm{d}\mu^* + \frac{\partial \mathrm{P}}{\partial \mathrm{M}}\mathrm{dM} + \frac{\partial \mathrm{P}}{\partial \mathrm{M}^*}\mathrm{dM}^* \\ &= s\mathrm{dT} + \rho\mathrm{d}\mu - \mathrm{n_s dM} \end{aligned} \tag{4.38}$$

which allows reading off the self-consistency equations as extremal conditions

$$\frac{\partial P}{\partial \mu^*} = \frac{\partial P}{\partial M^*} = 0 \tag{4.39}$$

of the total pressure with respect to the auxiliary variables μ^* and M^*.
We will now describe the strategy we use in calculating a complete set of thermodynamic quantities, this list of steps does not have to be altered substantially when we later discuss changes by adding pion exchange terms to our equation of state, see section 4.4.

[1] *both names are used throughout the literature, we will talk of compressibility*

- The fixed variables in the grand canonical ensemble are V, T and μ. In the macrosopic limit $V \to \infty$, we need to choose T and μ^*.
- Then we solve the self-consistent mass equation (4.17) which comes from $\partial P/\partial M^* = 0$. This is equivalent to finding the roots of
$$F(M^*) = M - M^* + G_\mathrm{s} \cdot n_\mathrm{s} \tag{4.40}$$
- In the previous step we implicitly calculated the scalar density
$$n_\mathrm{s} = -\frac{\partial P}{\partial M} \overset{(4.21)}{=} -\frac{\partial P_{FG}}{\partial M^*}\,, \text{ see (B.32)} \tag{4.41}$$
- We get the baryon density from (4.34):
$$\rho = \frac{\partial P}{\partial \mu} \overset{(4.22)}{=} \frac{\partial P_{FG}}{\partial \mu^*}\,, \text{ see (B.33)} \tag{4.42}$$
- As stated in (4.35) the entropy density is
$$s = \frac{\partial P}{\partial T} \tag{4.43}$$
- Of course we are interested in the pressure P of the system itself:
$$P \overset{(4.23)}{=} P_{FG} + \frac{1}{2} G_\mathrm{v} \rho^2 - \frac{1}{2} G_\mathrm{s} n_\mathrm{s}^2 \tag{4.44}$$
with $P_{FG}(T, \mu^*, M^*)$ from (B.30).
- The second self-consistency equation
$$\frac{\partial P}{\partial \mu^*} = 0 \tag{4.45}$$
allows calculation of the baryon chemical potential μ.
- μ is needed to calculate the energy density from the Gibbs-Helmholtz relation $\epsilon = \mu\rho + Ts - P$ (4.46)
- The compressibility κ is defined as
$$\kappa = 9 \cdot \frac{\partial P}{\partial \rho}\Big|_{\rho=\rho_0} \tag{4.47}$$
where ρ_0 is the normal nuclear matter density in (4.4).

Finally calculating the chiral condensate from our master formula in (3.20),

$$\boxed{\frac{\langle \bar{q}q \rangle(\rho, T)}{\langle \bar{q}q \rangle_0} = 1 + \frac{1}{f_\pi^2}\left(\frac{\partial P}{\partial m_\pi^2} + \frac{\sigma_N}{m_\pi^2}\frac{\partial P}{\partial M}\right),} \tag{4.48}$$

we end up with a complete set of quantities

$$\boxed{\Longrightarrow T, \mu^*, M^*, n_s, \rho, s, P, \mu, \epsilon, \kappa, \langle \bar{q}q \rangle / \langle \bar{q}q \rangle_0} \tag{4.49}$$

which determine basic properties of nuclear matter and its thermal behaviour.

4.2 Numerical Results

We will now proceed through the steps leading to (4.49) by discussing the corresponding results. Let us start with the mass self-consistency equation.

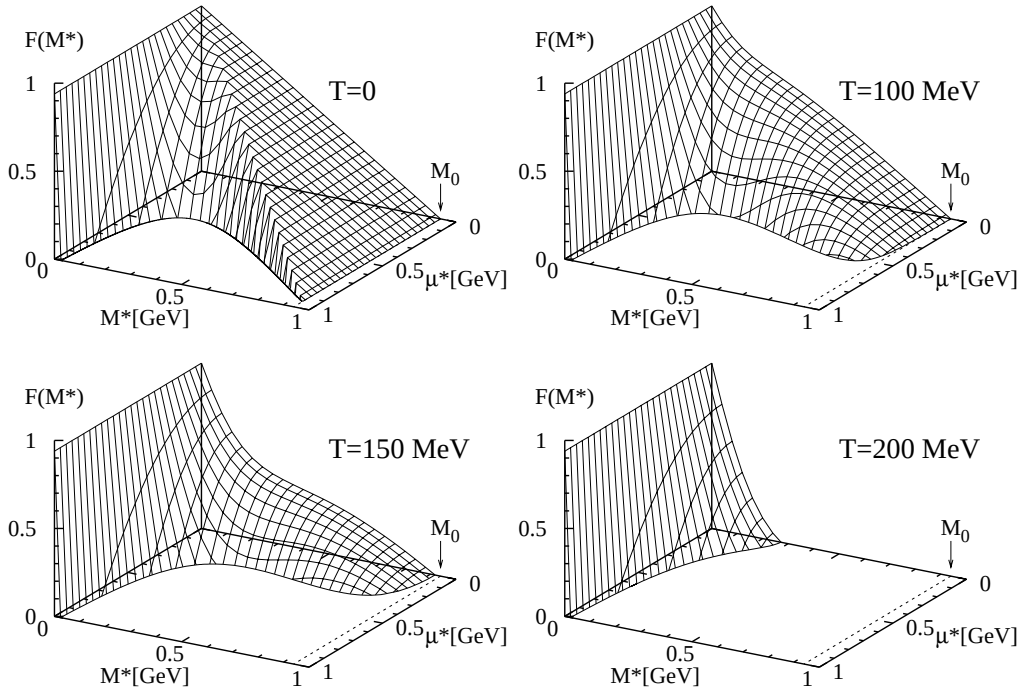

Figure 4.2: The structure of $F = F(T, \mu^*, M^*)$ from (4.40) at temperatures $T =$ 0,100,150,200 MeV. Its zeros are the solutions M^* to (4.17).

The overall structure of the relevant function F of eq.(4.40) is shown in Figure 4.2. It is straightforward to obtain the solutions to the self-consistent mass equation (mass-SCE) by projecting out the $F = 0$-planes. This was done for various temperatures, the results are shown in Fig.4.3. We see that for a certain combination of T and μ^* there can be up to three solutions all of which are physical[2]. For $T = 0$ and $\mu^* = 0.75$ GeV we have marked the three solutions with crosses in the plot.
At this point we emphasize that once one has determined the solutions to the mass-SCE a combination of T, μ^* and such a solution M^* enables us to calculate any of the quantities in (4.49) in arbitrary order. In our next step we will calculate the baryon density ρ as in (4.42).

[2] *this is in contrast to the studies of [50]*

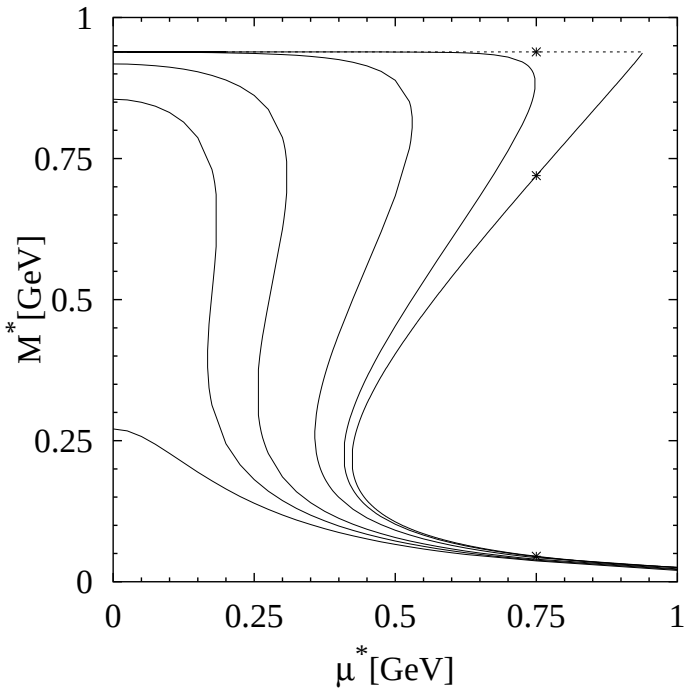

Figure 4.3: Projections of the $F = 0$- planes at temperatures (from right to left) T = 0,50,100,150,175,200 MeV.

It is in no way trivial to obtain a single flat curve from the solutions of the self-consistent equation (SCE) for the mass when plotting M^* as a function of ρ as is our result shown in Fig.4.4. Again we labelled the solutions which correspond to $\mu^* = 0.75\,\mathrm{GeV}$.

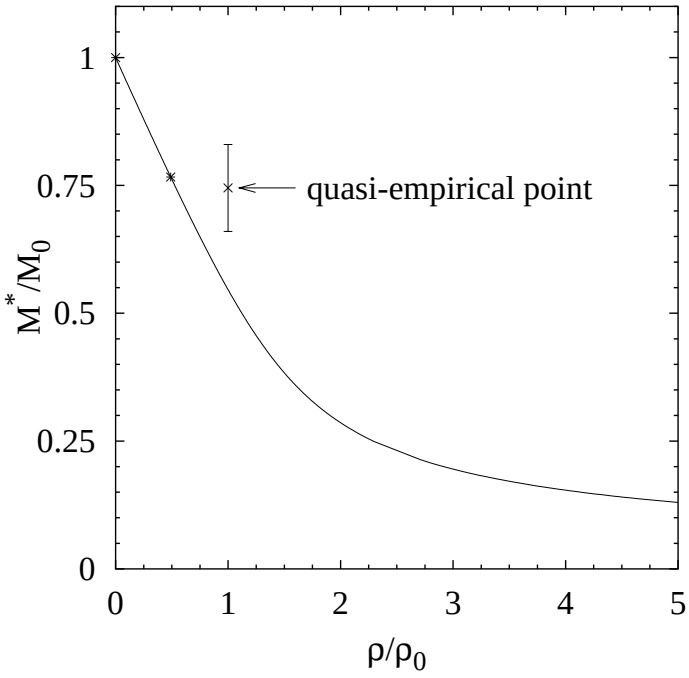

Figure 4.4: The solutions M^*/M_0 of the mass-SCE as a function of normalized baryon density ρ/ρ_0 at temperature $T = 0$ MeV.

There are three points to mention concerning Fig.4.4:

• the solution corresponding to $M^* = M_0$ belongs to $\rho = 0$ because we define our baryon density at $T = 0$ such that it vanishes for $\mu^* > M^*$. Otherwise we would run into a problem with imaginary densities. Remember that in that case we have $\rho_{T=0} = 2p_f^3/(3\pi^2) = 2(\mu^{*2} - M^{*2})^{3/2}/(3\pi^2)$.
• the third solution cannot be seen on the plot as it belongs to the extremely high density $\rho \sim 35\rho_0$, where the model does not apply.
• the point with error bars labelled "quasi-empirical" is the widely accepted value for $M^*/M_0 = 0.75 \pm 0.05$ which we clearly miss with $M^*/M_0 \simeq 0.54$. A detailed discussion about this follows in section 4.3.1. We will see later that this is not the only shortcoming in the Walecka model. In equation (4.54) the compressibility κ comes out nearly a factor of 2 too large. These two problems are related and will be fixed in section 4.3 where we introduce additional couplings and parameters.

4.2.1 Liquid-Gas Phase Transition

With the combinations of T, μ^*, M^* we are capable of calculating the remaining quantities of interest. We start with the equation of state.

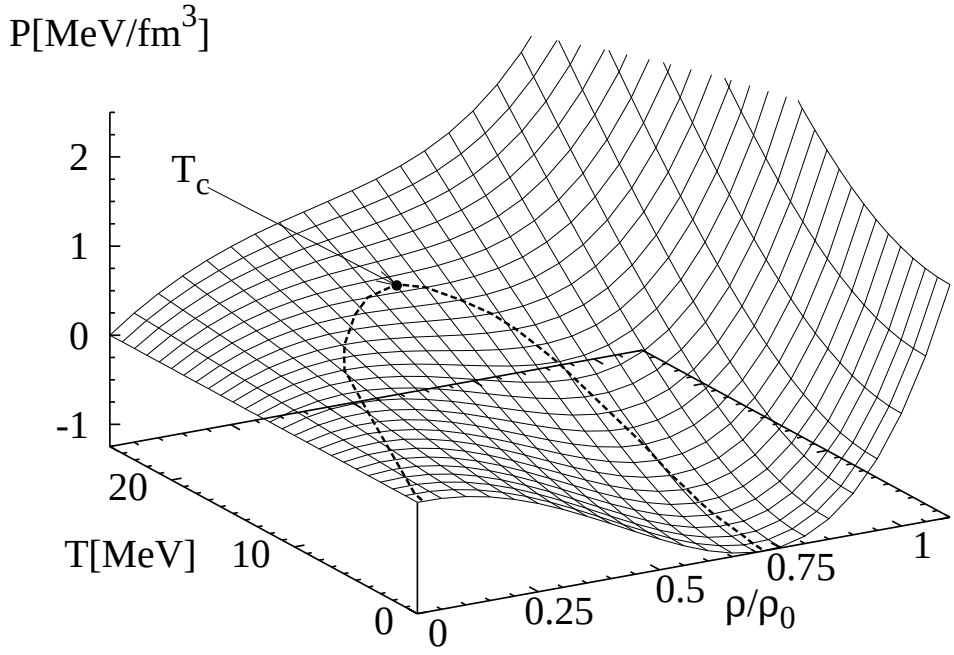

Figure 4.5: Equation of state (4.44): Pressure $P = P(\rho/\rho_0, T)$

We plot the pressure as a function of normalized baryon density and temperature in Fig.4.5. We also show the parabola that one obtains from the maxima and minima of the pressure from the various isotherms in Fig.4.6.

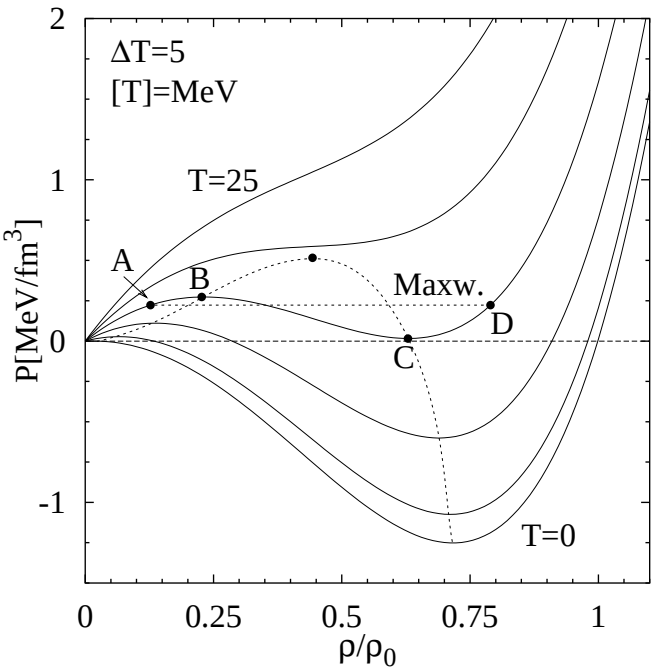

Figure 4.6: The pressure P as a function of normalized baryon density ρ/ρ_0 at T =0,5,10,15,20,25 MeV. The horizontal line labelled A-D represents the MAXWELL construction performed in the P-V-plane as shown in Fig.4.7.

As a further example we have performed the MAXWELL construction at $T = 15\,\mathrm{MeV}$. The horizontal line labelled A-D is obtained from the standard procedure in Fig.4.7:

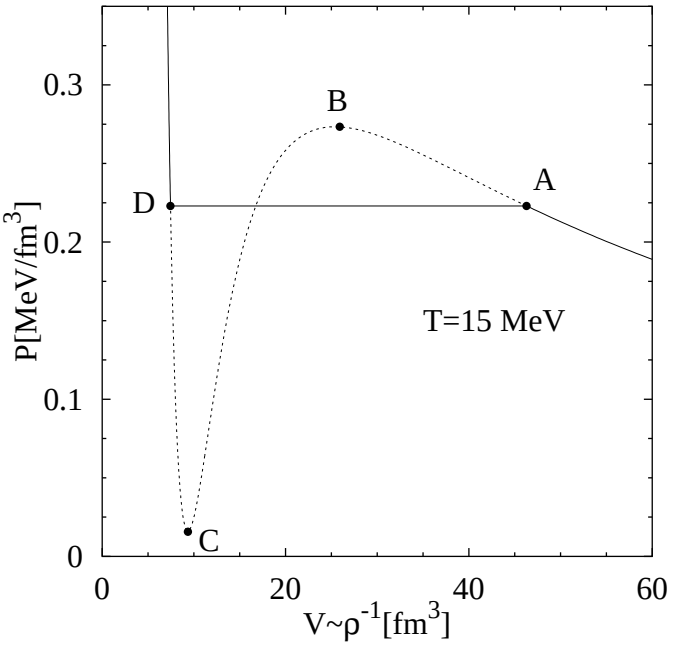

Figure 4.7: The pressure P as a function of volume V at T =15 MeV. The MAXWELL construction is shown. The two areas below and above the horizontal line have same size. The labels A-D are explained in the text.

In the P-V-plane one has to ensure that the two areas above and below the horizontal line become equal in magnitude - as shown. This is equivalent to the condition that A and D represent points of equal chemical potential μ.
Sytems of self-bound fermions in three space dimensions such as the one considered here undergo a liquid-gas phase transition of the VAN DER WAALS type. The binding energy curve at $T = 0$ is presented in Fig.4.8 and displays the characteristic minimum at $\rho = \rho_0$. In this ground state nuclear matter behaves like a FERMI liquid. Increasing the temperature leads to higher kinetic nucleon energy. A mixed phase occurs in which droplets of nucleons coexist with a nucleon gas. This mixed phase disappears at a critical temperature T_c^{LG}. In this model we find its value in the range

$$T_c^{\mathrm{LG}} = 19.5 \pm 0.5\,\mathrm{MeV}. \tag{4.50}$$

Let us return to the horizontal line between A and D which is the MAXWELL construction in Figs. 4.6 and 4.7. Consider moving along the $T = 15$ MeV isotherm. At densities $\rho < \rho_A$ only the gas phase, for $\rho > \rho_D$ only the liquid phase is present. Between A and B this gas phase is metastable, similarly the liquid phase is metastable from C to D. That means that the system can remain in the corresponding phase but it will not survive indefinitely. The curve between B and C is unstable as in this region the stability condition $\partial P/\partial\rho > 0$ is violated.
For $T < T_c^{\mathrm{LG}}$ the phase transition is first order. At the critical temperature T_c^{LG} the points A,B,C and D merge into one, the line of first-order phase transition terminates. Above T_c^{LG} the system is in its gas phase.
Up to now we have not paid much attention to the choice of parameters. Of course the results shown before were obtained with a specific combination of G_{s} and G_{v}. In the following section we explain how we actually determine the parameters used to calculate the numerical results shown up to this point.

4.2.2 Parameter Dependence of the Nuclear Matter Saturation Point

Recall the three fundamental properties of nuclear matter we already encountered: the normal nuclear matter density $\rho_0 \simeq 0.17$ fm^{-3} as in (4.4), the binding energy per nucleon $B = 16$ MeV from (4.3) and the compressibility κ defined in (4.47). A successful description of nuclear matter requires that these properties are reproduced.
We use our two available parameters to fit B and ρ_0. Later we check on the value of κ. In Fig. 4.8 we plotted the values for $\epsilon/\rho - M_0$ with ϵ from (4.46) over normalized baryon density for our best fit where the parameters are

$$G_\mathrm{s} = 353.28\,\mathrm{GeV}^{-2} \quad \text{and} \quad G_\mathrm{v} = 265.05\,\mathrm{GeV}^{-2}. \tag{4.51}$$

Note that this calculation is carried out at $T = 0$.

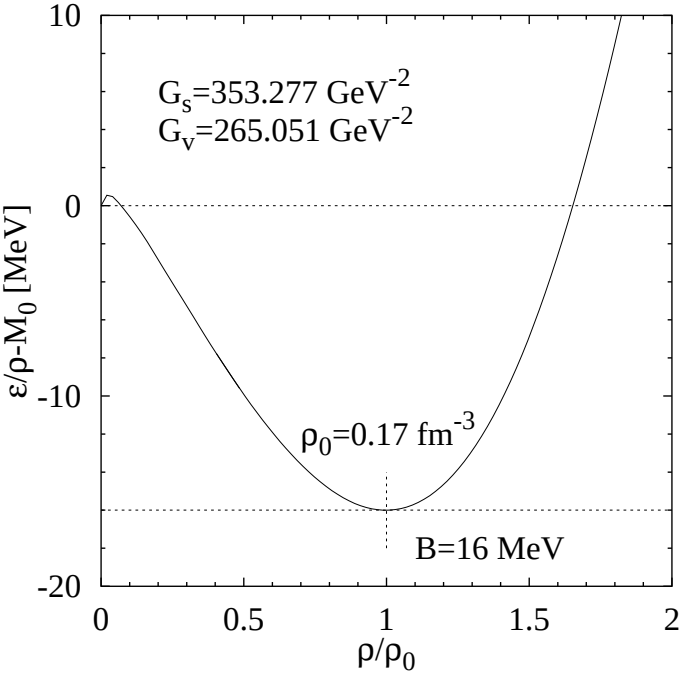

Figure 4.8: Binding energy per nucleon at $T = 0$. The parameters and the values they fit are given in the plot.

Table 4.1: Parameters used to shift the minimum in Fig. 4.8 around. The resulting s- and v-curves are plotted in Fig. 4.9, $[G_{\mathrm{s,v}}] = \mathrm{GeV}^{-2}$.

s-curve		s_1	s_2	s_3	s_4
$(G_\mathrm{v} = 265.051)$	$G_\mathrm{s} =$	340	350	360	370
v-curve		v_1	v_2	v_3	v_4
$(G_\mathrm{s} = 353.277)$	$G_\mathrm{v} =$	250	260	270	280

This parameter set is uniquely determined as can be seen by studying the movement of the minimum in $B(\rho)$ with changing parameters. This trend is understood by looking at Fig. 4.9 and Table 4.1.

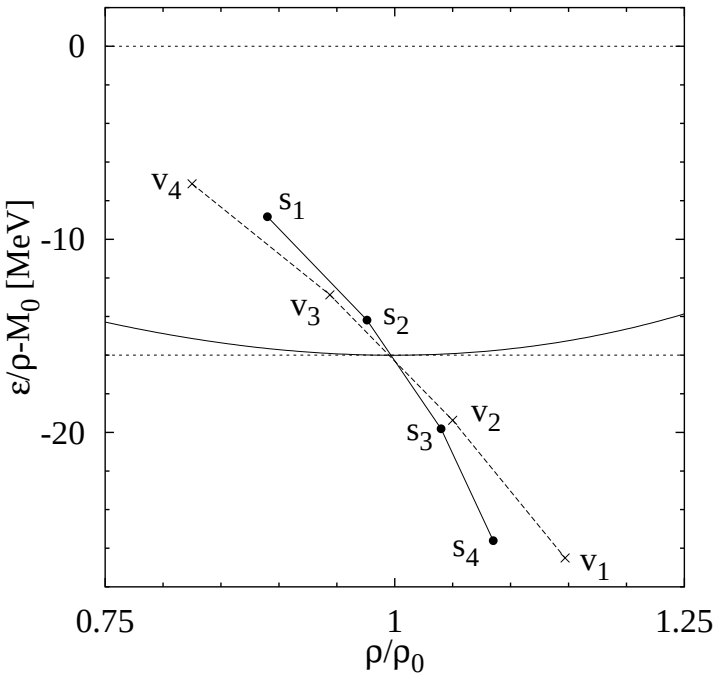

Figure 4.9: The same plot as in Fig. 4.8 where the parameters were varied this time with a focus on the shifting of the minimum. The details about s_i and v_i ($i = 1...4$) can be found in Table 4.1.

The two slightly bent curves shown in Fig. 4.9 represent collections of minima in the energy per nucleon that belong to calculations where only one of the two parameters varied. In the case labelled $s(v)$ the parameter $G_{\rm s}(G_{\rm v})$ is varied whereas $G_{\rm v}(G_{\rm s})$ is held fixed at the value from (4.51) above. Therefore both curves run through the minimum of the solid curve which is the same as the one in Fig. 4.8. The other corresponding values are listed in Table 4.1.

Table 4.2: Relation between parameter values and shifting the minimum. The first column contains the desired shifting direction, the other two give instructions which parameter has to be changed and how.

minimum	G_s	G_v
right	-	decrease
left	-	increase
up	decrease	-
down	increase	-

One can see that when varying the parameters one at a time the minimum does shift up and down as well as from left to right. The shifting seems to be more extreme when we vary $G_{\rm v}$. Nevertheless in that case there is a larger shift from left to right in comparison to that between up and down.
It is easily possible to place the minimum at the desired position when using Table 4.2.

4.2.3 The Compressibility of Nuclear Matter

We have already mentioned the compressibility on several occasions. Unfortunately its value is not known very accurately. In principle it can be extracted from giant monopole resonances[3] found in nuclei heavier than ^{40}Ca [40]. It was first determined to be in the range $\kappa = 210 \pm 30$ MeV [26, 40] but more recent relativistic analysis [41] seems to indicate that κ is more than 20% larger:

$$\kappa \simeq 260 \pm 10\,\mathrm{MeV}. \tag{4.52}$$

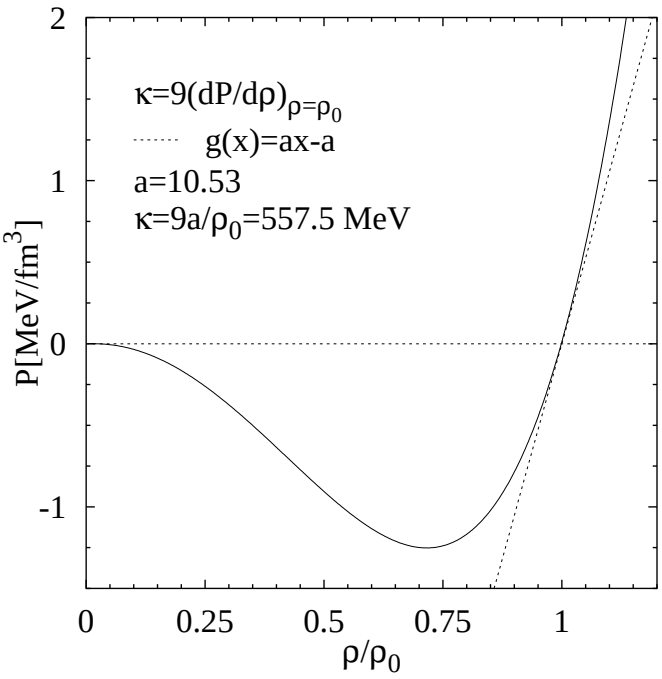

Figure 4.10: The compressibility κ [MeV] obtained from $P(\rho/\rho_0)$.

In order to calculate κ in our model we use equation (4.47) where the slope of the pressure at saturation density plays the key role:

$$\kappa = 9\,\frac{\partial P}{\partial \rho}\bigg|_{\rho=\rho_0} = \frac{9}{\rho_0}\,\frac{\partial P}{\partial(\rho/\rho_0)}\bigg|_{\rho/\rho_0=1}. \tag{4.53}$$

[3] *more precisely: from the energies of isoscalar monopole vibrations in nuclei*

We had already taken a look at the pressure. Therefore Fig. 4.10 is not entirely new. It shows how we fit a straight line $g(x) = a(x-1)$ with $x = \rho/\rho_0$. The slope a is determined at the point $P = g(1) = 0$. It leads to a compressibility

$$\kappa = \frac{9 \cdot a}{\rho_0} \simeq \frac{9 \cdot 10.53\,\mathrm{MeV/fm^3}}{0.17/\mathrm{fm^3}} = 557.5\,\mathrm{MeV} \tag{4.54}$$

which is too large by a factor of about 2. Before tackling this problem in section 4.3 below we will complete to show the results of the quantities on our list in (4.49) that we have not touched so far, as there are the entropy s, the scalar density n_s and the closely related chiral quark condensate $\langle\bar{q}q\rangle$[4].

4.2.4 Energy and Entropy Densities

We already discussed the energy density defined in (4.46) when we calculated the energy per nucleon $\epsilon/\rho - M_0$ with $\epsilon = \mu\rho + Ts - P$.

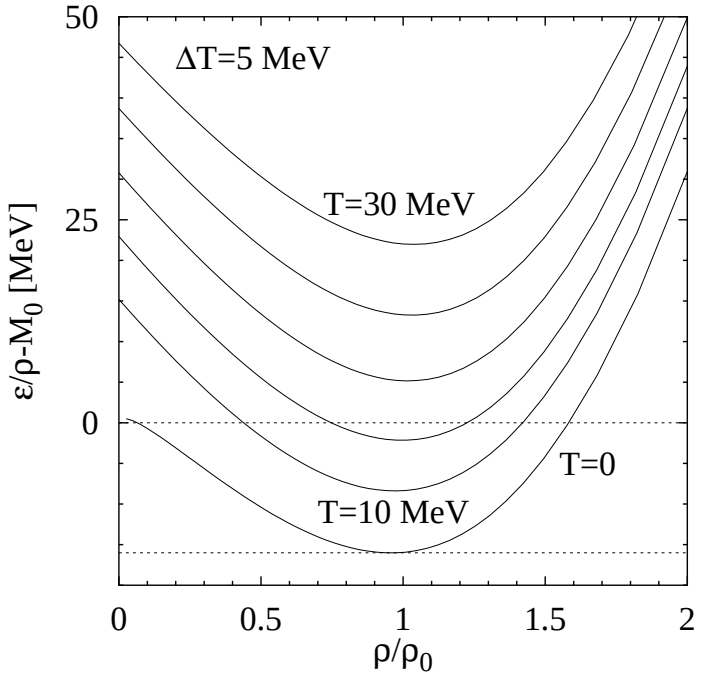

Figure 4.11: $\epsilon/\rho - M_0$ plotted over normalized baryon density for temperatures $T = 0, 10, 15, ..., 30$ MeV.

The latter was only used in the simplified zero temperature limit

$$\epsilon = (\mu^* + G_\mathrm{v}\rho)\rho - P \tag{4.55}$$

where the entropy density does not contribute. In addition to the zero temperature case in Fig. 4.8 we have plotted more isotherms in Fig. 4.11.

[4] *we will use this appreviation for* $\langle\bar{q}q\rangle(\rho,T)/\langle\bar{q}q\rangle(0)$ *throughout this text*

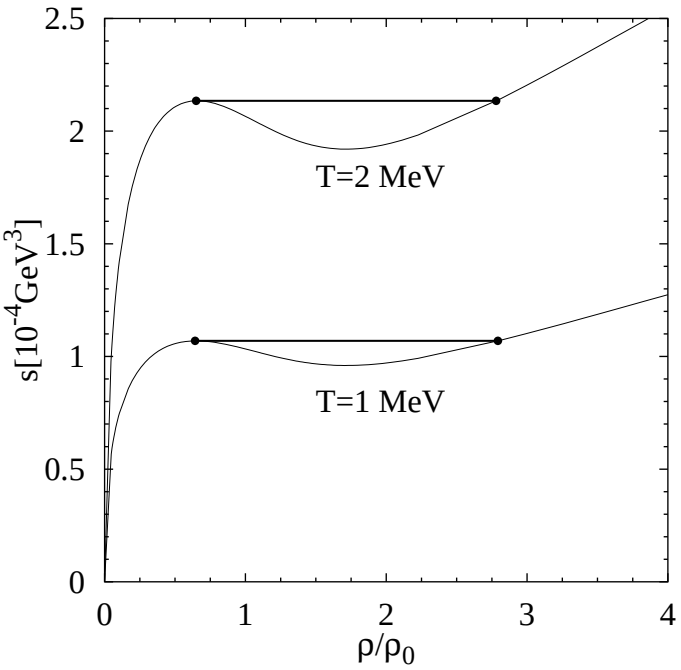

Figure 4.12: Entropy $s = s(\rho/\rho_0)$ at $T = 1, 2\,\text{MeV}$ showing the possibly unphysical regions with decreasing s.

The non-vanishing values close to the y-axis come from the finite value of $\mu(\rho \to 0)$ as $s, P \to 0$ in that limit (the points on the y-axis itself corresponding to $\rho = 0$ are excluded, division by zero).

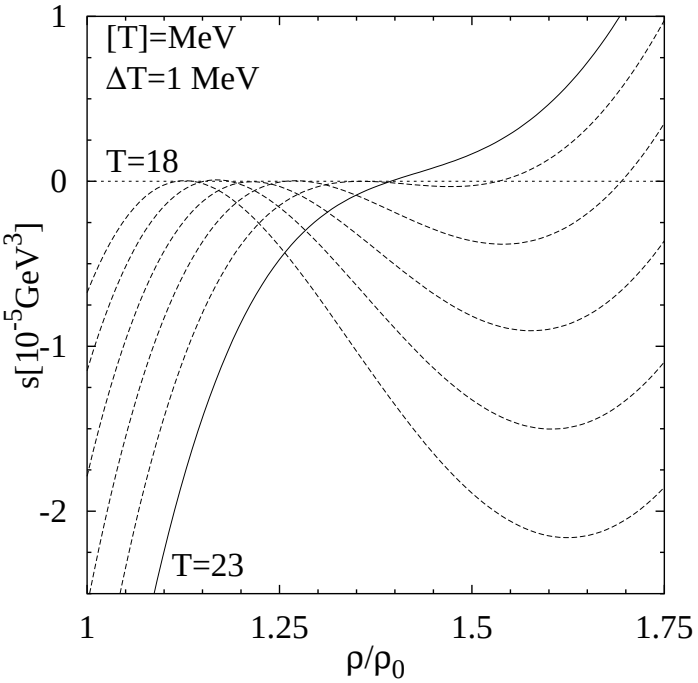

Figure 4.13: Possibly unphysical entropy regions at $T = 18...23$ MeV (read the explanations in the text).

At finite temperature the sT-term contributes to ϵ. We have plotted the entropy density s in Figs. 4.12f. Fig. 4.12 shows the possibly unphysical

regions at $T = 1$ and 2 MeV, higher temperatures are shown in Fig. 4.13, where - in order to be able to compare the different temperatures - the local maxima (and the turning-point for $T = 23$ MeV, solid line) were shifted such that they correspond to $s = 0$.
There is possibly a problem as s decreases in certain density regions. One might think that these regions correspond to the unphysical regions of the MAXWELL constructions, but they differ from those. Also the temperature $T = 22.5 \pm 0.5$ MeV at which this strange behaviour ceases is larger than that of the liquid-gas transition temperature T_c^{LG} in (4.50). After fixing the value of the compressibility later this strange behaviour with decreasing entropy will not be present any more, see Fig. 4.27.

4.2.5 The Chiral Condensate (I)

In this section we will finally cope with our main topic, the chiral quark condensate. It was derived in (3.20). We have neglected thermal pions in the calculation of Fig.4.14, concentrating on the pure WALECKA model for now, therefore the equation used to calculate the condensate reduces to (3.30):

$$\frac{\langle\bar{q}q\rangle(\rho,T)}{\langle\bar{q}q\rangle_0} = 1 + \frac{\sigma_N}{m_\pi^2 f_\pi^2}\frac{\partial P}{\partial M} = 1 - \frac{\sigma_N}{m_\pi^2 f_\pi^2} n_s \tag{4.56}$$

We see that it is closely related to the scalar density n_s. Note that the WALECKA model Lagrangian breaks chiral symmetry explicitly, so that exact "chiral restoration", the dropping of $\langle\bar{q}q\rangle$ to zero at high temperature and density is not an issue. Instead the condensate seems to approach a finite value. The rapid change of the condensate at a characteristic temperature is nevertheless indicating the expected behaviour. Of course we talk about extreme temperatures and densities at which our model should not be valid any more as the hadrons are believed to start to dissolve into quarks and gluons at temperatures $T > 0.2\,\mathrm{GeV}$ and densities far beyond that of normal nuclear matter.
The correction concerning κ will bring the condensate's tail down and the thermal pions considered later will do too. The value that we assign to the chiral phase transition will not reach the (low) value of

$$T_c \simeq 192\,\mathrm{MeV} \tag{4.57}$$

that one can - in principle - read off from the $\rho = 0$-projection of Fig. 4.14. This value has to be compared to the $SU(2)_F$-lattice result which is found to be $T_c = 173 \pm 8$ MeV, see (4.1) and [35]. Our value is slightly too large,

however, it is only indicative since our model is no longer valid near the "real" chiral phase transition.

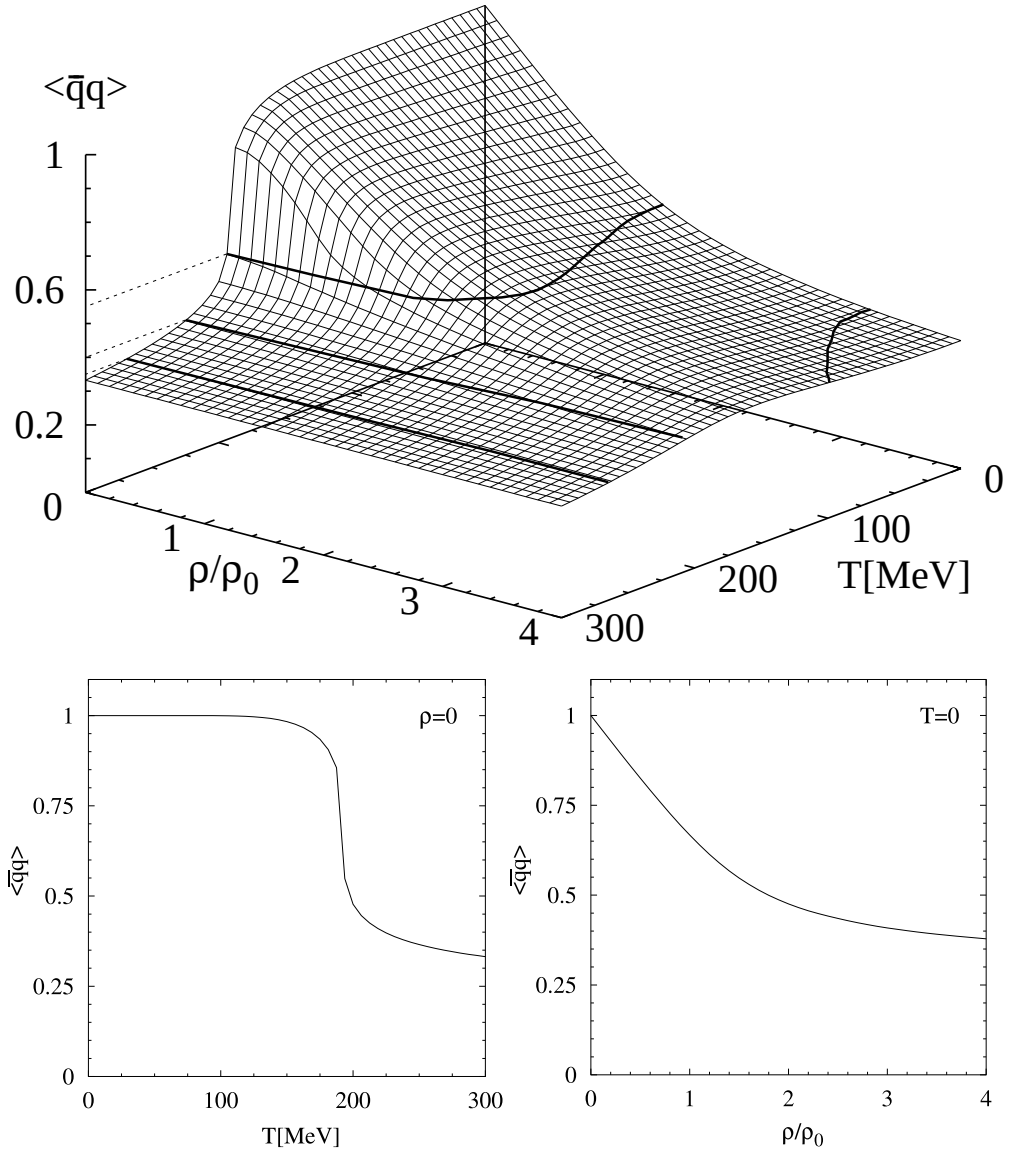

Figure 4.14: The chiral quark condensate in the WALECKA model with the parameters from (4.51), the contour lines with $\langle\bar{q}q\rangle = 0.35, 0.4$ and 0.55 and the projections of $\rho = 0$ and $T = 0$.

For completeness we have plotted the relation between the two densities in Fig. 4.15. We can clearly see that for small densities $\rho < \rho_0$ the linear density approximation in (3.31) is a good one.

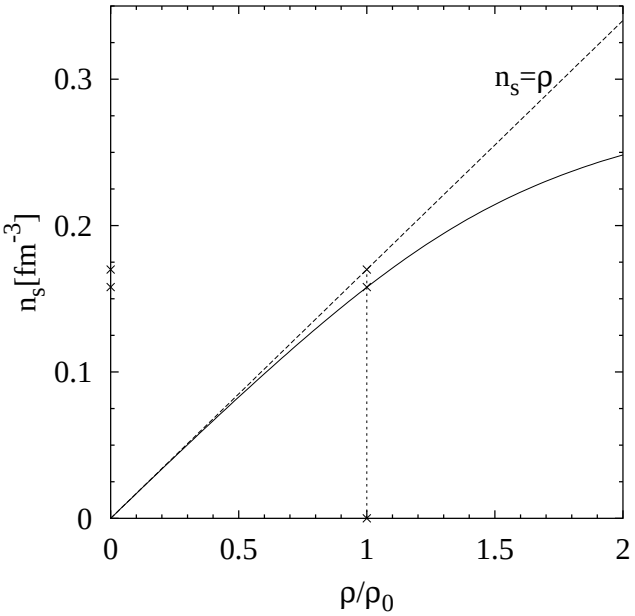

Figure 4.15: Scalar density n_s [fm^{-3}] as a function of ρ/ρ_0 (solid line) with emphasis on normal nuclear matter density (crosses) and $n_s = \rho$ (dashed).

After giving this overview of the results in the WALECKA model we will now improve this calculation in the next section.

4.2.6 The Phase Diagram of Nuclear Matter

In this section we take a look at what the phase diagram of nuclear matter "would look like" in the WALECKA model.

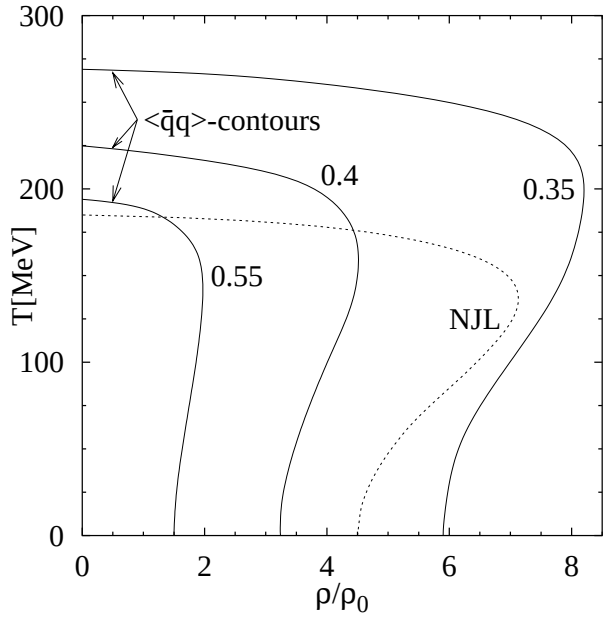

Figure 4.16: The phase diagram of nuclear matter as calculated in the scalar-vector mean field model. For comparison we have also plotted the result of an NJL calculation [51, 52], see text.

In this case the order parameter of the chiral phase transition - the condensate - does not vanish. The rapid dropping of the condensate $\langle\bar{q}q\rangle(\rho,T)/\langle\bar{q}q\rangle_0$ nevertheless indicates a transition of some sort.
It shows the tendency towards chiral restoration and it is interesting to explore qualitatively the resulting phase diagram. Let us consider cutting the diagram in Fig. 4.14 at $\langle\bar{q}q\rangle = 0.35, 0.4, 0.55$ and take a look at these projections. The resulting phase diagram does not differ much qualitatively for the different values as can be seen in Fig. 4.16.
The qualitative behaviour is like that obtained from an $SU(2)_F$ calculation in the NAMBU-JONA-LASINIO (NJL) model [53, 54, 55] and similar calculations [56, 57]. The NJL model is based on an effective Lagrangian of relativistic quarks with effective point-like interactions between them. The gluonic degrees of freedom are frozen. It is a simple model that exhibits spontaneous chiral symmetry breaking.

4.3 Additional Parameter: Improved Results

We had already mentioned the problem of the large compressibility that we found in (4.54) and the corresponding problem of the too small effective nucleon mass. In addition, the value of T_c^{LG} found in (4.50) is slightly too high. It is generally true that its value is monotonically increasing with the compressibility κ. Therefore an improvement in κ will also decrease the value of T_c^{LG}, a welcome effect. We can thus summarise that fixing the value for κ is definitely desired as it will at least improve - if not fix - these problems.

We extend the WALECKA model by adding a higher power of the scalar mean field to the partition function. This brings about a new parameter that allows fitting the value of the compressibility κ as discussed in section 4.2.3, especially (4.52). This new parameter is introduced by adding a term of the form in (4.25). The equation of state of the extended WALECKA model reads:

$$P = P_{\mathrm{FG}} + \frac{1}{2G_v}\left(\mu-\mu^*\right)^2 - \frac{1}{2G_{\mathrm{s}}}\left(M-M^*\right)^2 - \frac{1}{nG_n}\left(M-M^*\right)^n \quad (4.58)$$

Our new coupling parameter is G_n where n can be one of the values $n = 3, 4$. Let us now differentiate P again with respect to M and M^*

$$\frac{\partial P}{\partial M} = -\left(M-M^*\right)/G_{\mathrm{s}} - \left(M-M^*\right)^{n-1}/G_n \quad (4.59)$$

$$\frac{\partial P}{\partial M^*} = \frac{\partial P_{\mathrm{FG}}}{\partial M^*} + \left(M-M^*\right)/G_{\mathrm{s}} + \left(M-M^*\right)^{n-1}/G_n = \frac{\partial P_{\mathrm{FG}}}{\partial M^*} - \frac{\partial P}{\partial M} \quad (4.60)$$

The self-consistency equation for the effective mass reads

$$\frac{\partial P}{\partial M^*} = 0 \quad \Rightarrow \quad \frac{\partial P}{\partial M} = \frac{\partial P_{\rm FG}}{\partial M^*} \tag{4.61}$$

This is equivalent to finding the root of the function

$$\begin{aligned} F(M^*) &= M - M^* + G_{\rm s}\frac{\partial P_{\rm FG}}{\partial M^*} + \frac{G_{\rm s}}{G_n}(M-M^*)^{n-1} \\ &= M - M^* - G_{\rm s}\, n_s + \frac{G_{\rm s}}{G_n}(M-M^*)^{n-1} = 0 \end{aligned} \tag{4.62}$$

where n_s is the scalar density

$$n_s = (M-M^*)/G_{\rm s} + G_n^{-1}\,(M-M^*)^{n-1} = -\frac{\partial P}{\partial M} = -\frac{\partial P_{\rm FG}}{\partial M^*}. \tag{4.63}$$

The second self-consisteny equation for the chemical potential does not differ as we still have

$$\left.\begin{aligned} \frac{\partial P}{\partial \mu} &= \frac{\mu-\mu^*}{G_{\rm v}} \\ \frac{\partial P}{\partial \mu^*} &= \frac{\partial P_{FG}}{\partial \mu^*} - \frac{\partial P}{\partial \mu} = 0 \end{aligned}\right\} \quad \rho = \frac{\mu-\mu^*}{G_{\rm v}} = \frac{\partial P_{FG}}{\partial \mu^*}. \tag{4.64}$$

We have now modified the equation of state of our system in a self-consistent manner without the introduction of an underlying Lagrangian. This is quite straightforward as the relation between the mean σ field and $M - M^*$ has not changed:

$$\mathcal{L}_{O(n)} = \bar\psi\,(i\gamma_\mu\partial^\mu - M^* + \mu^*\gamma_0)\,\psi + \frac{1}{2}m_\omega^2\bar\omega_0^2 - \frac{1}{2}m_\sigma^2\bar\sigma^2 - \frac{1}{2}\lambda_n\bar\sigma^n \tag{4.65}$$

with $G_n = g_\sigma^n/\lambda_n$. We will study the cases $n = 3, 4$. It is just important to note here that this time M^* cannot simply be read off from (4.65) but it is obtained by solving the mass-SCE $\partial P/\partial M^* = 0$. We will refer to the two different extensions of the model as $O(3)$ and $O(4)$.
It is not trivial however to find a corresponding Lagrangian with contact interactions as it was the case in the Walecka model, we have presented the discussion about this in Appendix A.6.

4.3.1 New Parameter Sets

We have now got a new parameter G_n at hand that allows fitting the value of the compressibility κ as discussed in section 4.2.3.

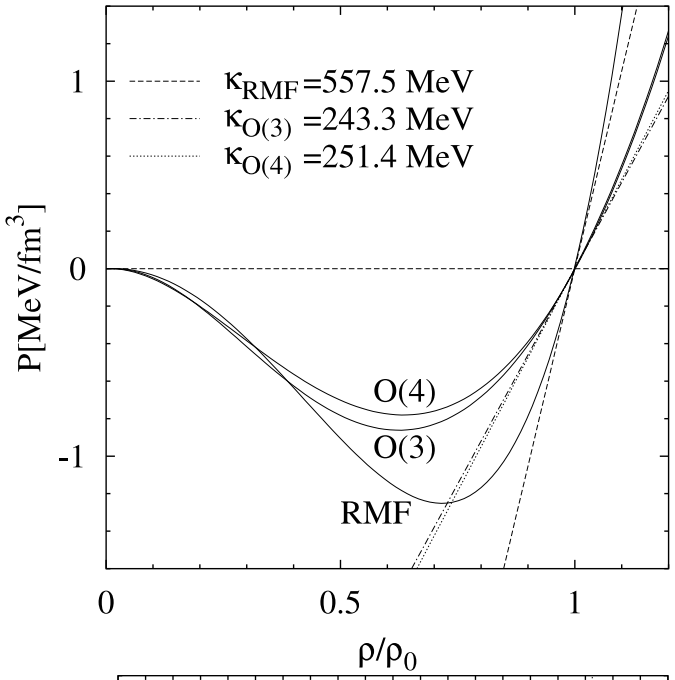

Figure 4.17: Equation of state $P(\rho/\rho_0)$ at $T = 0$ for the three different cases and the corresponding values for κ ($\Rightarrow$ parameters in Table 4.3).

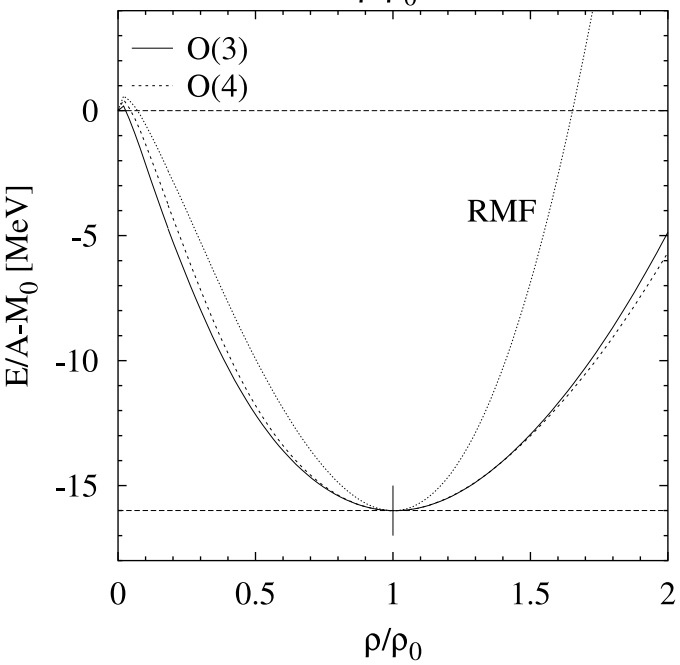

Figure 4.18: G_{s} and G_{v} allow reproduction of the correct binding energy of 16 MeV at saturation density ρ_0 just as before.

The procedure for calculating the quantities in (4.49) now require a readjustment of the parameters such that they shift the saturation density to the right

value and to reproduce the correct binding energy per nucleon. This can be done with only G_s and G_v as described in Table 4.2.

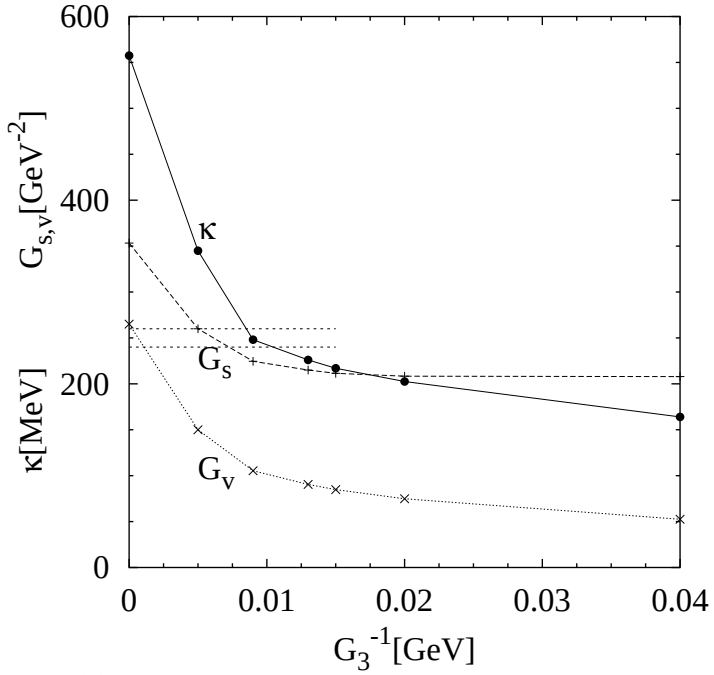

Figure 4.19: Connection between G_3^{-1} and the other parameters as well as κ.

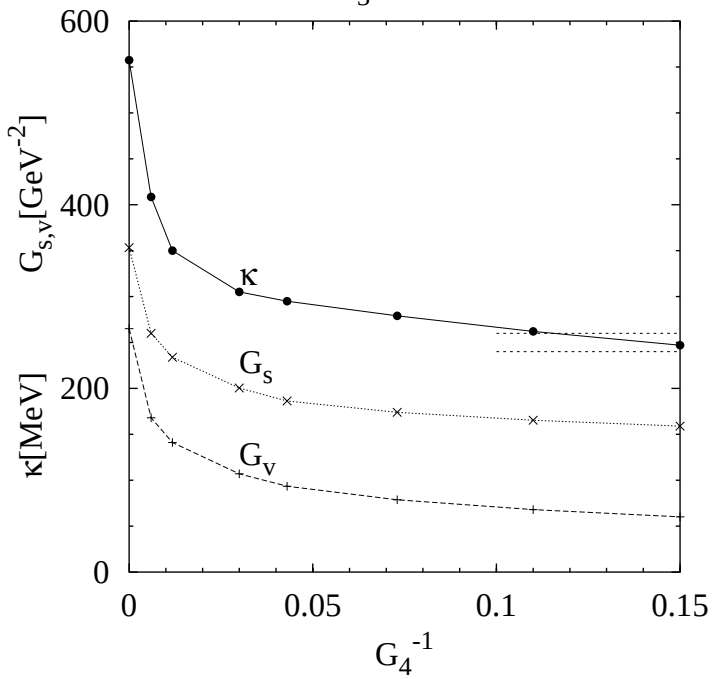

Figure 4.20: Same as in Fig.4.19 for the dimensionless parameter G_4.

The way we proceeded was to assign a certain value to G_n first and to apply this method of adjusting the other two known properties in the second step.

Astonishingly this works just the way it did before, see Figs. 4.17f. Only the value of κ differs accordingly as can be seen in Figs. 4.19f. The parameters used in the three different cases are listed in Table 4.3. It also shows the values that we obtain for $B = |E|/A$, ρ_0 and κ which we can reproduce - in principle - with arbitrary accuracy. As the latter one is not known very accurately we did not put much effort into assigning a special value to it.

Table 4.3: Parameter sets used to calculate the plots in this section, $[G_{\rm s},G_{\rm v}]$=GeV^{-2}, $[G_n]$=GeV^{n-4}, $[E/A,\kappa]$=MeV and $[\rho_0]$=fm^{-3}

set		$G_{\rm s}$	$G_{\rm v}$	n	G_n^{-1}	$\lvert E\rvert/A$	ρ_0	M^*/M_0	κ
1	RMF	353.277	265.051	-	0	16.0004	0.16974	0.546	557.5
2	O(3)	224.506	105.405	3	0.009	15.9964	0.17027	0.787	243.3
3	O(4)	158.905	60.095	4	0.15	16.0005	0.16965	0.853	251.4

The fractions M^*/M_0 are taken at ρ_0, see Fig. 4.22.
From now on we refer to the WALECKA model as discussed in the previous section as relativistic mean field model (RMF).
We have already mentioned that our new approach differs from the old one only by assigning a finite value to G_n. We have not established the connection to the value of the compressibility κ yet. This is done in Figs. 4.19f. We also plotted two parallel horizontal lines that correspond to the extreme values κ could have, see (4.52). In each figure one of our data points lies within this range, these are the data sets we refer to as $O(n), n = 3, 4$.
We decided to show these plots as functions of $1/G_n$ as the parameters $G_{\rm s,v}$ and the values for κ on the y-axis ($G_n^{-1} = 0$) then correspond to our RMF case. This simplifies comparisons and shows that the parameter sets are unique unless G_n^{-1} is increased much further and the curves start to rise again.
With properly readjusted parameters we are now in the position to evaluate all quantities in (4.49).
So far the two realisations $O(n)$ were on a par. We will now discuss their solutions to the mass-SCE. These are plotted in Fig. 4.21 as a function of μ^* just as in Fig. 4.3 from which we have taken the RMF results at $T = 0$ and 150 MeV again for comparison. The corresponding temperatures dependence is plotted for the $O(n)$ cases. In Fig. 4.22 the solutions are shown as a function of baryon density. We encounter again the quasi-empirical point that represents today's knowledge about the effective nucleon mass at saturation density.

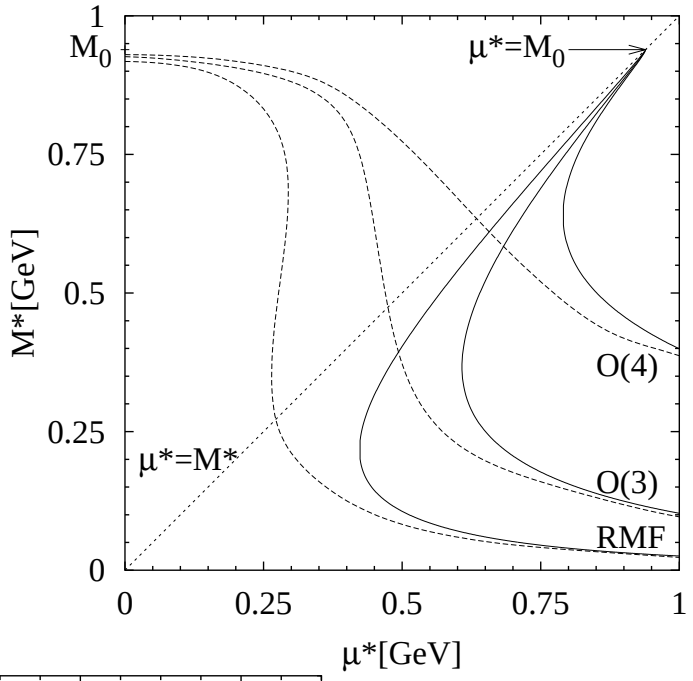

Figure 4.21: The solutions of the mass-SCE in all three cases for $T = 0$ (solid) and $T = 150\,\mathrm{MeV}$ (dashed) as a function of eff. chemical potential μ^*.

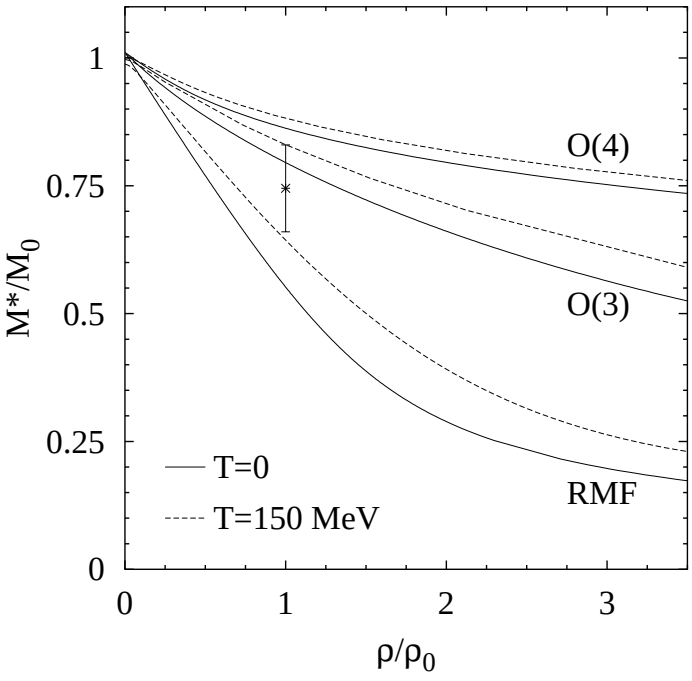

Figure 4.22: The same information as in Fig.4.21, but this time the normalized solutions are plotted versus normalized baryon density ρ/ρ_0.

At this point we want to go a bit more into detail about the various different effective nucleon masses that can be found in the literature.

4.3.2 Effective Nucleon Mass

The authors in [58] defined a nonrelativistic mass M^*_{NR} by the following relation:

$$\frac{M}{M^*_{NR}} = 1 + \frac{M}{p_F}\left.\frac{\partial U(p,p_F)}{\partial p}\right|_{p=p_F} \tag{4.66}$$

where U is the momentum and density dependent nuclear optical potential as defined in [26]

$$U(p,p_F) = \sqrt{p^2 + M^{*2}} + G_{\rm v}\rho - \sqrt{p^2+M^2} \tag{4.67}$$

in terms of "our" effective nucleon mass which is the mass of a DIRAC quasi nucleon $M^* \equiv M^*_D$. Inserting the derivative of U into (4.66) yields the following relation that links the nonrelativistic mass M^*_{NR} - which is obtained by solving a SCHRÖDINGER-type equation - with our DIRAC mass M^*_D

$$\frac{1}{M^*_{NR}} = \frac{1}{M} + \frac{1}{\sqrt{p^2 + M^{*\,2}_D}} - \frac{1}{\sqrt{p^2+M^2}}. \tag{4.68}$$

This relation is plotted in Fig. 4.23 at saturation density ρ_0 where the FERMI momentum[5] is $p_F = 268$ MeV.

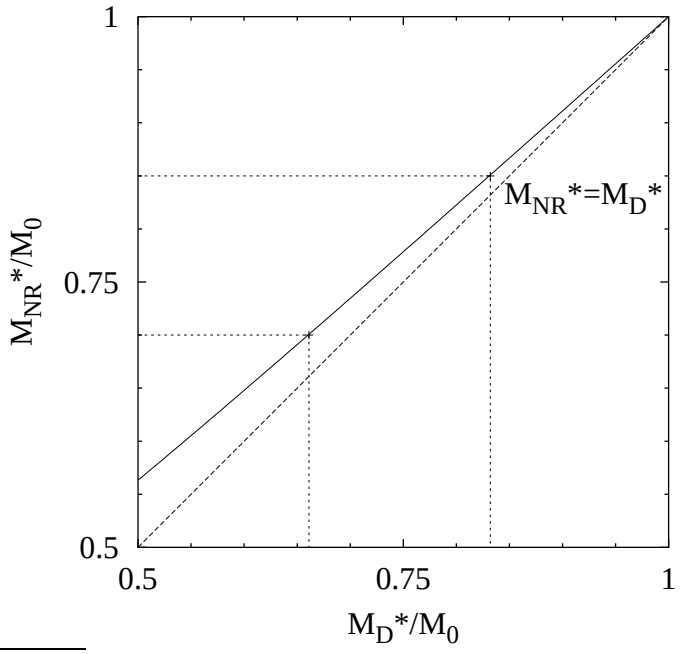

Figure 4.23: Relation between the different effective masses: M^*_D obtained from our model and the nonrelativistic one M^*_{NR} which should be compared to the values obtained from experiments.

[5] *remember that at* $T = 0$ *we have* $\rho = 2p_F^3/(3\pi^2)$.

We can see that the nonrelativistic masses are sligthly higher, the discrepancy is rather small though and can be neglected as the phenomenological values are subject to uncertainties. The nuclear single particle potential (4.67) for the three cases is shown in Fig. 4.24.
The quasi-empirical point in Fig. 4.22 is the empirical effective nucleon mass $M^*_{emp} = (0.7 - 0.85)M$ derived from experimental data in the framework of nonrelativistic shell or optical models [59, 60, 61]. It allows to decide which parameter realisation to favor: $O(3)$. The range for M^*_{emp} is shown in Fig. 4.23 for both effective masses.

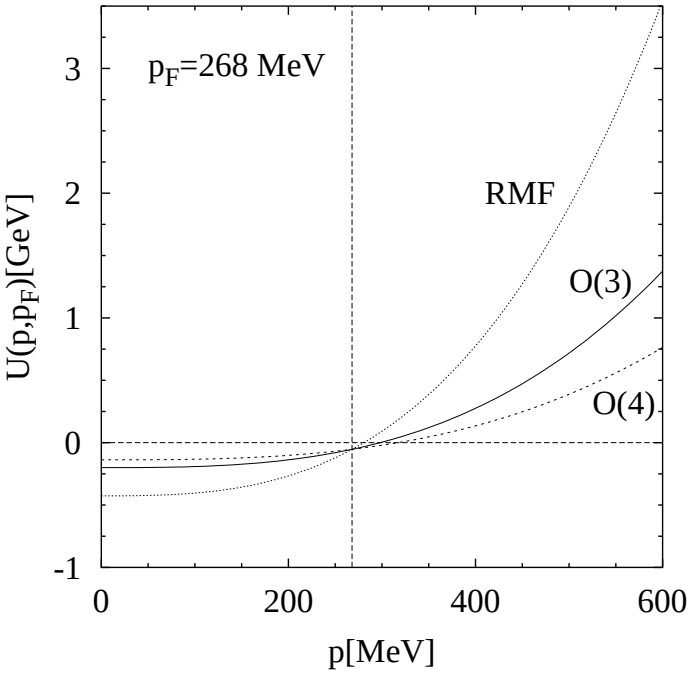

Figure 4.24: Nuclear single particle potential as a function of momentum.

Such potentials are used to interpret proton-nucleus scattering.

4.3.3 Liquid-Gas Transition with Improved Interaction

We have already seen the most interesting quantities in the previous sections: the equation of state $P(\rho/\rho_0)$ at zero temperature in Fig. 4.17, the binding energy per nucleon E/A at saturation density ρ_0 in Fig. 4.18, the relation between our new parameter and the value of the compressibility κ in Fig. 4.19f and the solutions to the mass-SCE in Fig. 4.21.
We also discussed effective nucleon masses and these helped us to decide which version $O(n), n = 3, 4$ for a new parameter we should use. The choice fell for $n = 3$ which is easily understood by looking at Fig. 4.22. Therefore we now study the changes that the new $O(3)$-term implies. The corresponding quantities are summarised in Table 4.3.
We first want to have a look at the equation of state at finite T in Fig. 4.25 and the corresponding change in the value of the liquid-gas phase transition temperature.
We already mentioned that the value of $T_c^{\rm LG}$, see (4.50), is monotonically increasing with the compressibility κ. As we have decreased the value of κ that for $T_c^{\rm LG}$ should have become smaller accordingly. This is indeed the case and the value came down to

$$T_c^{\rm LG} = 16.6 \pm 0.2\,{\rm MeV}, \tag{4.69}$$

see Fig. 4.26. This value is in perfect agreement with a recent analysis of limiting temperatures in heavy ion collisions [3].

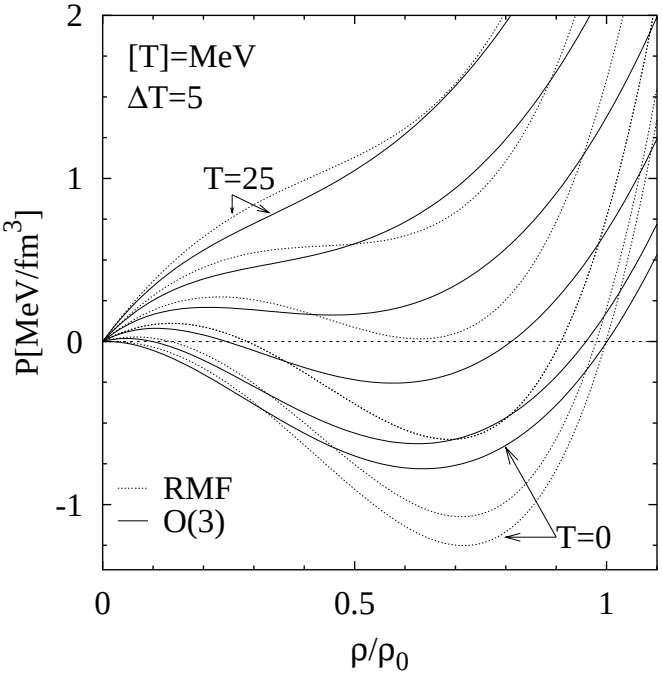

Figure 4.25: Change in the pressure: O(3) (solid) vs. RMF (dotted) at T =5,10,...,25 MeV.

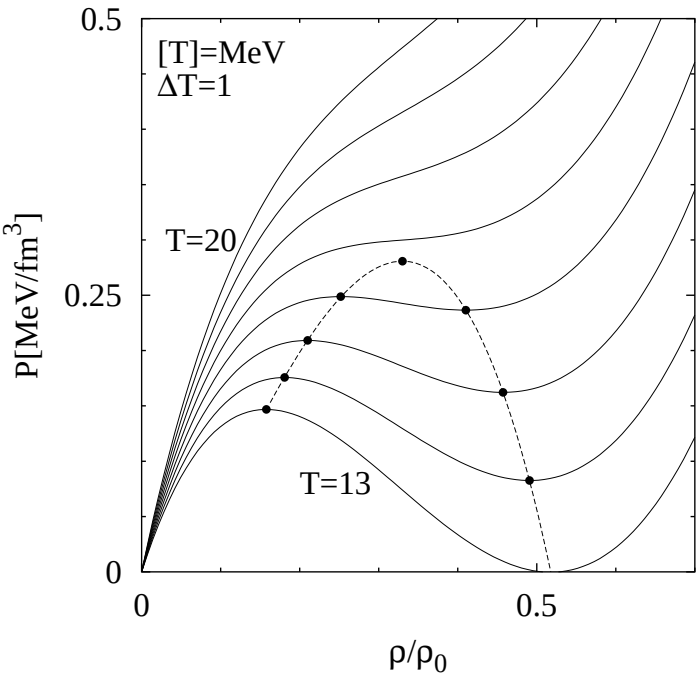

Figure 4.26: The interesting region that allows reading off T_c^{LG} enlarged, T =13, 14,...,20 MeV, see (4.69).

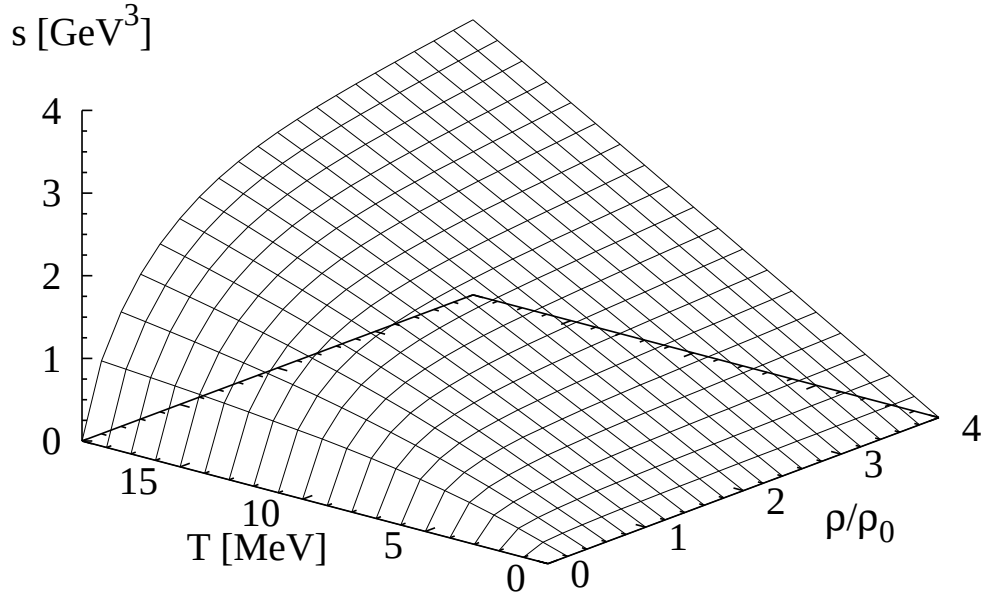

Figure 4.27: The entropy as a function of temperature and baryon density in our case O(3).

We saw in section 4.2.4 that the RMF calculation resulted in ranges with decreasing entropy. Such regions are not present any more after fitting the right value to the compressibility as can be seen in Fig. 4.27 above.

4.3.4 The Chiral Condensate (II)

The modifications with finite G_3 result in the following T- and ρ-dependence of the chiral condensate:

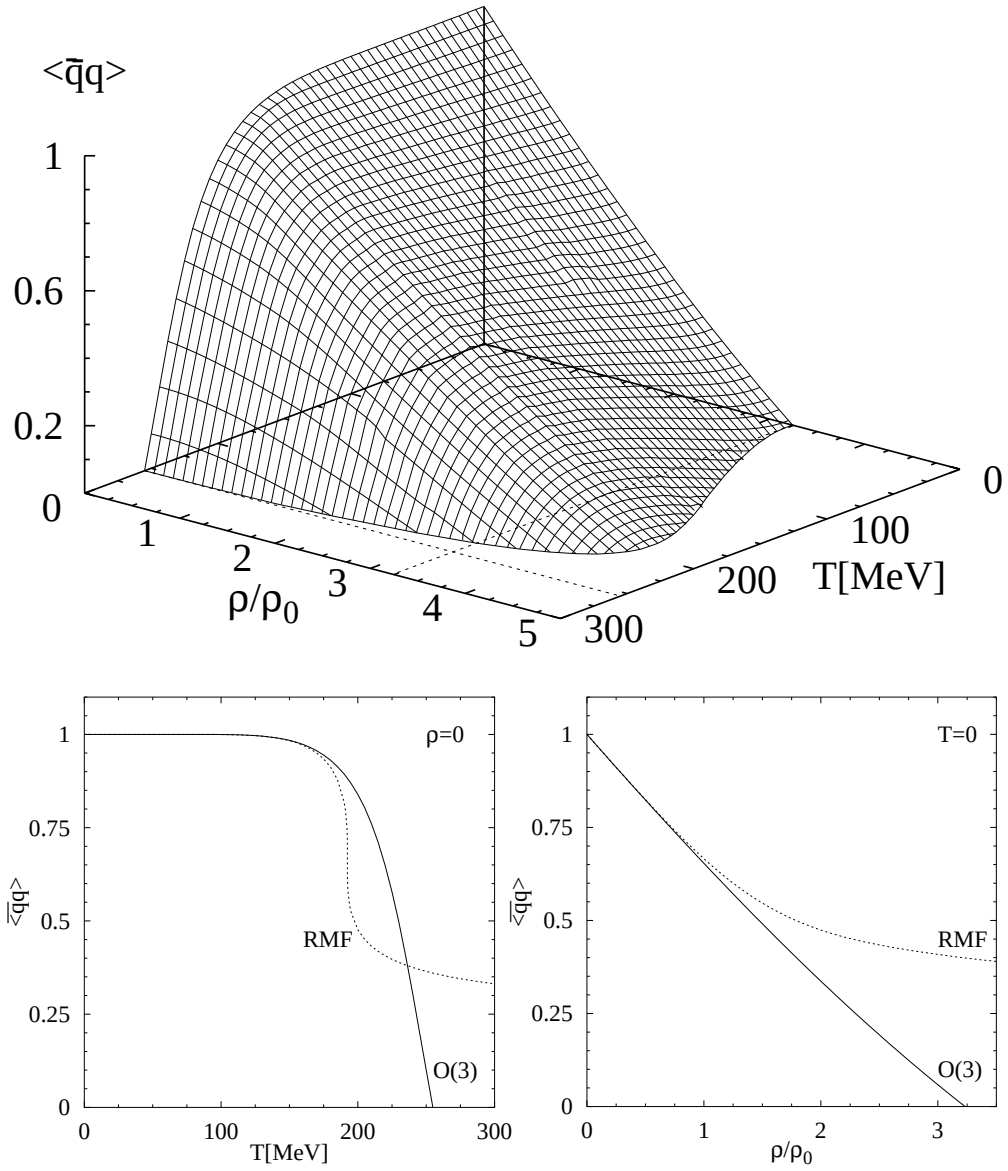

Figure 4.28: $O(3)$-result: the chiral quark condensate $\langle\bar{q}q\rangle \equiv \langle\bar{q}q\rangle(\rho,T)/\langle\bar{q}q\rangle(0,0)$ after fitting the compressibility κ. In the projections $\rho = 0$ and $T = 0$ we plotted the RMF results again (dashed) for comparison.

This corresponds to a situation where the parameters $G_{\rm s}, G_{\rm v}$ and G_3 are adjusted such that they reproduce the empirical values of B, ρ_0 and κ respectively.

The critical temperature at which the phase transition occurs rises from $T_c =$ 192 MeV - which was closer to the $SU(2)_F$-lattice result in (4.1) - to $T_c^{O(3)} =$ 255 MeV. Remember that this number is at most indicative since the model looses its validity near the "real" chiral phase transition.

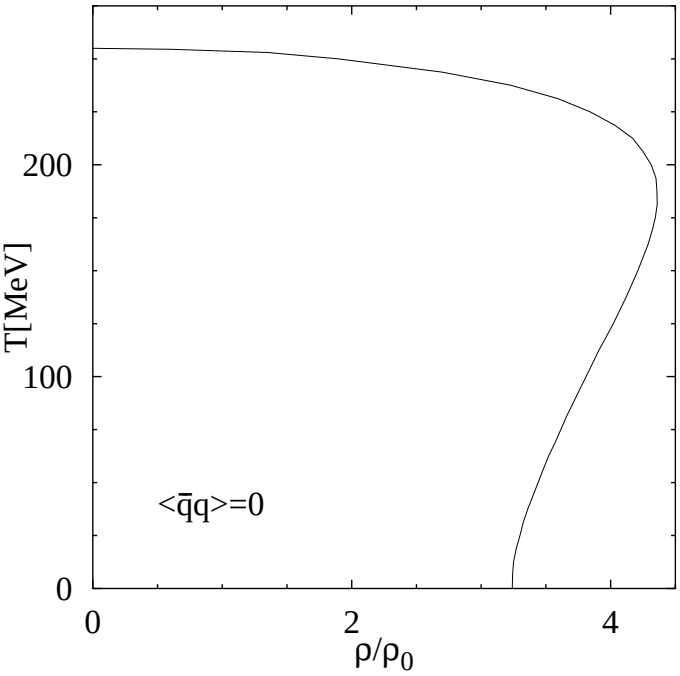

Figure 4.29: Phase diagram in the case $O(3)$.

Facing a situation with vanishing $\langle\bar{q}q\rangle$ one finds the phase diagram shown in Fig. 4.29 which this time is simply the projection of $\langle\bar{q}q\rangle = 0$ taken from Fig. 4.28.

4.4 Pionic Fluctuations

So far we dealt with non-interacting quasi nucleons moving in self-consistently generated scalar and vector mean-fields. These mean-fields could be expressed in terms of the quasi nucleon properties, i.e. rewriting the scalar (vector) mean field in terms of the effective nucleon mass M^* (effective chemical potential μ^*), see eqs. (4.17f).
The nuclear force at a more microscopic level is mediated by exchange of (virtual) mesons. Being the approximate GOLDSTONE bosons of spontaneously

broken chiral symmetry, pions are the lightest mesons with a mass of about $m_\pi = 138\,\mathrm{MeV}$. Therefore pions represent the dominant mesonic contributions at the temperatures we consider. The temperature dependence of $\langle\bar{q}q\rangle(T)$ at low T is determined exclusively by the dynamics of the free and interacting thermal pion gas discussed in section 3.2.2. Heavier mass states are suppressed by their BOLTZMANN factor $\exp(-m_h/T)$.
One can as well argue in favor of implementing pions explicitly into the nuclear matter problem (at $T = 0$) by the comparable scales of the FERMI momentum at saturation density $p_f = (3\pi^2\rho_0/2)^{1/3} = 268\,\mathrm{MeV}$ and the pion mass $p_f \simeq 2m_\pi$.
Unfortunately it is only possible in rare special cases to obtain the partition function of an interacting system in closed form. The field theoretical diagrammatic techniques [26, 27] allow a perturbative calculation of the ground state energy of such a system of interacting fermions. Disconnected closed diagrams (having no external legs) represent contributions to the logarithm of the partition function.
Using such diagrammatic techniques we will add pion contributions to our partition function and thus to the equation of state in this section.
There are two different one-pion exchange contributions: first the so-called HARTREE term

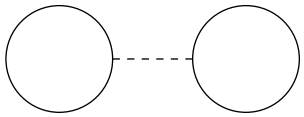

which averages to zero in isospin symmetric matter (since the exchanged 4-momentum is zero ($q^\mu = 0$), this vanishing holds true in general). Secondly there is the FOCK term which remains finite. We will discuss in the next section the influence of this FOCK term on the saturation mechanism and the thermodynamic properties of nuclear matter.

4.4.1 Thermal Pions and Pion Exchange

We just saw that a dynamical description of nuclear matter should incorporate pionic contributions. These will be investigated systematically at finite temperature T and baryon density ρ in this section. Such contributions $P_{\pi,\pi}$ can be seperated into two parts:

$$P_{\pi,\pi}(T,\mu^*,M^*,m_\pi) = P_\pi(T,m_\pi) + P_{1\pi}(T,\mu^*,M^*,m_\pi) + \dots . \tag{4.70}$$

The first part P_π is that of thermal pions discussed in section 3.2.2. It contributes only at finite temperature, it vanishes at $T = 0$. The pion exchange

FOCK term $P_{1\pi}$ also yields a finite contribution at zero temperature. In its complete form it can be found in (C.25). The dots stand for higher order effects such as 2-pion exchange. We will discuss these contributions later in section 4.5.
The field theoretical methods for the evaluation of the partition function can be formulated in terms of EUCLIDean FEYNMAN rules. They can be derived using the standard procedure involving generating functionals from $\mathcal{L}$. They are summarised for our specific case (pseudovector pion-nucleon vertex, see (2.54)) in Appendix A.1.
The detailed evaluation of the 1-pion exchange FOCK diagram (C.1)

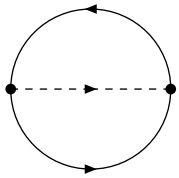

is presented in Appendix C. Each component of such a diagram is replaced by its corresponding term where the lines are assigned EUCLIDean four-momenta which are conserved at each vertex. Integrations over these 4-momenta involve summations over MATSUBARA frequencies ($\rightarrow$ A.5.1). For bosons these frequencies are $2\pi Tn$ (n an integer). For fermions these frequencies are complex $\omega_n = (2n+1)\pi T - i\mu$, with μ the chemical potential. The result of these infinite sums are quadratic polynomials in FERMI-DIRAC distribution functions for nucleons and BOSE-EINSTEIN functions in the case of pions.
Terms which do not contain any distribution functions can be neglected as they represent non-observable shifts of the vacuum energy. Terms involving one single distribution function renormalise the free pion or the free nucleon part. The terms bilinear in distribution functions represent the truly interesting many-body effects from the pion-nucleon interaction. At zero temperature the FERMI distribution function is replaced by a step-function

$$f(E-\mu) \quad \rightarrow \quad \Theta(\mu - E) \tag{4.71}$$

In this limit there are no more effects from thermal anti-nucleons and thermal pions.
We now want to study the consequences of such an additional pion contribution term $P_{\pi,\pi}$ to the partition function, or equivalently our equation of state. Whereas the first term in (4.70) - being only a function of T and m_π - only contributes at finite temperature ($P_\pi(T=0)=0$) to P, the entropy s and the quark condensate $\langle\bar{q}q\rangle$, the second will do so in each step of our "thermodynamics strategy" (most of the time also at $T=0$), see section 4.1.4.

If we extend the equation of state (4.58) again by adding the term $P_{\pi,\pi}$ in (4.70) we end up with

$$\begin{aligned} P(T,\mu^*,\mu,M^*,M,m_\pi) &= P_{\rm FG}(T,\mu^*,M^*) + P_{\pi,\pi}(T,\mu^*,M^*,m_\pi) \\ &+ \frac{(\mu-\mu^*)^2}{2G_{\rm v}} - \frac{(M-M^*)^2}{2G_{\rm s}} - \frac{(M-M^*)^3}{3G_3}. \end{aligned} \tag{4.72}$$

The dynamical situation described by this EOS is such that the quasi nucleons built up by the scalar-vector background fields exchange pions, not the free nucleons. We will implement these pion exchange effects self-consistently, in other words: the resulting mean fields are influenced by the presence of the pion-nucleon interaction.
Since the formulae at zero temperature are much simpler we will display these here. The corresponding finite temperature results are easily assembled by insertion of derivatives of the expressions found in the Appendix at the appropriate places. Therefore we can concentrate on the changes implied by the pion exchange term.
As is usual we will start again with the total pressure from which all other interesting quantities in (4.49) can be derived: our equation of state at $T = 0$ becomes

$$\begin{aligned} P(\mu^*,\mu,M^*) &= P_{\rm FG}(\mu^*,M^*) + P_{1\pi}(\mu^*,M^*) \\ &+ \frac{(\mu-\mu^*)^2}{2G_{\rm v}} - \frac{(M-M^*)^2}{2G_{\rm s}} - \frac{(M-M^*)^3}{3G_3} \end{aligned} \tag{4.73}$$

where $M = 939$ MeV and $m_\pi = 138\,\mathrm{MeV}$ will not be varied. The first two terms in (4.73) are the free FERMI gas term

$$P_{\rm FG}(\mu^*,M^*) = \frac{1}{12\pi^2}\left[\mu^*\left(2\mu^{*2} - 5M^{*2}\right)p_f + 3M^{*4}\ln\frac{\mu^*+p_f}{M^*}\right] \tag{4.74}$$

with

$$p_f = \sqrt{\mu^{*2} - M^{*2}} \tag{4.75}$$

and the 1π-exchange FOCK term (derived in Appendix C.1)

$$\begin{aligned} P_{1\pi}(\mu^*,M^*) &= -\frac{3g_A^2}{32\pi^4 f_\pi^2}\left[\left(\mu^*M^*p_f - M^{*3}\ln\frac{\mu^*+p_f}{M^*}\right)^2\right. \\ &\left. -m_\pi^2 M^{*2}\int_{M^*}^{\mu^*}\mathrm{d}E_1\int_{M^*}^{\mu^*}\mathrm{d}E_2\ln\frac{E_1E_2 - M^{*2} + {m_\pi}^2/2 + \sqrt{(E_1^2-M^{*2})(E_2^2-M^{*2})}}{E_1E_2 - M^{*2} + {m_\pi}^2/2 - \sqrt{(E_1^2-M^{*2})(E_2^2-M^{*2})}}\right]. \end{aligned} \tag{4.76}$$

The first term of $P_{1\pi}$ in (4.76) is the $T = 0$-limit of the P_Δ-term in (C.6). For the reasons given in the Appendix we will neglect it and also all of its derivatives listed below!
The baryon density is defined like $\rho = \partial P/\partial\mu = \partial(P_{\rm FG}+P_{1\pi})/\partial\mu^*$ and becomes

$$\begin{aligned}\rho(\mu^*, M^*) &= \frac{2}{3\pi^2}p_f^3 + \frac{3g_A^2}{8\pi^4 f_\pi^2}M^{*2}\left[\mu^*\left(M^{*2}-\mu^{*2}\right) + M^{*2}p_f \ln\frac{\mu^*+p_f}{M^*}\right] \\ &+\frac{3g_A^2 {m_\pi}^2}{16\pi^4 f_\pi^2}M^{*2}\int_{M^*}^{\mu^*}\mathrm{d}E\,\ln\frac{E\mu^* - M^{*2} + {m_\pi}^2/2 + \sqrt{(E^2-M^{*2})(\mu^{*2}-M^{*2})}}{E\mu^* - M^{*2} + {m_\pi}^2/2 - \sqrt{(E^2-M^{*2})(\mu^{*2}-M^{*2})}}\end{aligned} \tag{4.77}$$

at $T = 0$. The second term is a derivative of P_Δ, therefore it will be neglected too. This decomposition of the density (and other) contribution(s) into a zero range δ-part and a finite range YUKAWA part can be understood by having a look at a pion between two vertices

$$\frac{q^2}{m_\pi^2+q^2} = 1 - \frac{m_\pi^2}{m_\pi^2+q^2} \tag{4.78}$$

which can be split in the same way.
The defining conditions for the self-consistency equations $\partial P/\partial\mu^* = 0$ and $\partial P/\partial M^* = 0$ are unchanged. The latter

$$\frac{\partial P}{\partial M^*} = \frac{\partial}{\partial M^*}(P_{\rm FG}+P_{1\pi}) - \frac{\partial P}{\partial M} = 0 \tag{4.79}$$

leads us to our definition of F:

$$F(\mu^*, M^*) = M - M^* - G_{\rm s}\, n_s + \frac{G_{\rm s}}{G_3}\left(M-M^*\right)^2, \tag{4.80}$$

it can also be used to calculate n_s:

$$n_s = -\frac{\partial P}{\partial M} = \left(M-M^*\right)/G_{\rm s} + \left(M-M^*\right)^2/G_3 = -\frac{\partial}{\partial M^*}\left(P_{\rm FG}+P_{1\pi}\right). \tag{4.81}$$

The contribution that belongs to P_Δ this time is a bit harder to spot. It is the term added to one in the second squared bracket:

$$F(\mu^*, M^*) = M - M^* + \frac{G_\mathrm{s}}{G_3}(M-M^*)^2 + \frac{G_\mathrm{s}}{\pi^2}\left[M^{*3}\ln\frac{\mu^*+p_f}{M^*} - M^*\mu^* p_f\right]$$
$$\cdot\left[1 + \frac{3g_A^2}{16\pi^2 f_\pi^2}\left(\mu^* p_f - 3M^*\ln\frac{\mu^*+p_f}{M^*}\right)\right] + \frac{3g_A^2 m_\pi^2}{16\pi^4 f_\pi^2} G_\mathrm{s} M^* \int_{M^*}^{\mu^*}\mathrm{d}E_1 \int_{M^*}^{\mu^*}\mathrm{d}E_2$$
$$\ln\frac{E_1E_2 - M^{*2} + {m_\pi}^2/2 + \sqrt{(E_1^2-M^{*2})(E_2^2-M^{*2})}}{E_1E_2 - M^{*2} + {m_\pi}^2/2 - \sqrt{(E_1^2-M^{*2})(E_2^2-M^{*2})}} - \frac{3g_A^2 {m_\pi}^2}{16\pi^4 f_\pi^2}\cdot$$
$$\cdot G_\mathrm{s} M^{*3}\int_{M^*}^{\mu^*}\mathrm{d}E_1\int_{M^*}^{\mu^*}\mathrm{d}E_2\left\{\frac{\sqrt{(E_1^2-M^{*2})/(E_2^2-M^{*2})}+1}{E_1E_2-M^{*2}+{m_\pi}^2/2+\sqrt{(E_1^2-M^{*2})(E_2^2-M^{*2})}}\right.$$
$$\left. + \frac{\sqrt{(E_1^2-M^{*2})/(E_2^2-M^{*2})}-1}{E_1E_2 - M^{*2} + {m_\pi}^2/2 - \sqrt{(E_1^2-M^{*2})(E_2^2-M^{*2})}}\right\} \tag{4.82}$$

The zeros $F(\mu^*, M^*) = 0$ of (4.82) are the solutions to the effective mass-SCE. Due to the simple relation between effective chemical potential μ^* and p_f at zero temperature, see (4.75), this function and the whole procedure can as well be formulated in terms of effective mass and FERMI momentum.
Finally the energy density is

$$\epsilon(\mu^*, M^*) \;=\; \mu\rho - P = (\mu^* + G_\mathrm{v}\rho)\rho - P \tag{4.83}$$

and can be used to calculate

$$B = \frac{\epsilon}{\rho} - M = \mu^* - M + G_\mathrm{v}\rho - \frac{P}{\rho}, \tag{4.84}$$

the binding energy per particle. This formula collection should enable the reader to construct the corresponding finite temperature case.

Let us come back to finite T where thermal pions have to be taken care of as well. The changes concerning $P_{1\pi}$ are just the analogue to those just applied. Just the entropy $s \to s + \partial P_\pi/\partial T$, the condensate $\langle\bar{q}q\rangle \to \langle\bar{q}q\rangle + \frac{1}{f_\pi^2}\partial P_\pi/\partial m_\pi^2$ and finally the pressure $P \to P + P_\pi$ now involve a new term due to the consideration of thermal pions. All these changes are straightforward as everything is derived from P in (4.72) in the very general way as before.

4.4.2 The Chiral Condensate (III)

In the previous section we extended our model such that pion contributions can be taken care of. We want to present the changes implied on the quark condensate by the two terms in (4.70) separately. We start with thermal pions,

the resulting changes can be seen in Fig. 4.30:

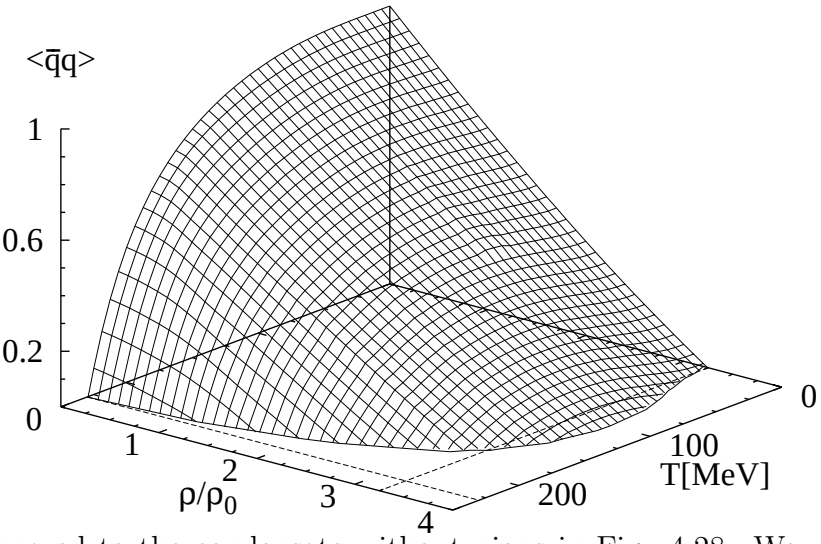

Figure 4.30: Chiral condensate $\langle\bar{q}q\rangle \equiv \langle\bar{q}q\rangle(\rho,T)/\langle\bar{q}q\rangle(0)$ calculated with the additional term O(3) and the contributions of thermal pions P_π from (3.24).

This has to be compared to the condensate without pions in Fig. 4.28. We see that the thermal pions bring the condensate's tail down again making the backbending region less obvious.

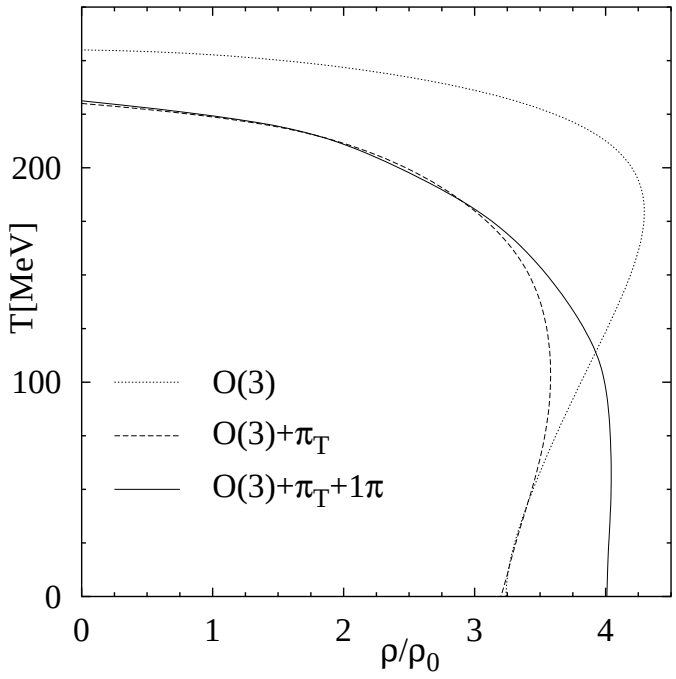

Figure 4.31: The phase diagram for the three different steps in the "evolution" of our model

Remember that we mentioned in section 4.3.4 that the value of $T_c = 192$ MeV in the RMF calculation was obtained in a completely different manner, having the "freedom" to decide on a certain point on the crossover-like curve. Now -

with our condensate going straight to zero - we find a sharp theoretical value for T_c at the point where $\langle \bar{q}q \rangle = 0$.
The results including the 1-pion exchange FOCK term for $\langle \bar{q}q \rangle$ are:

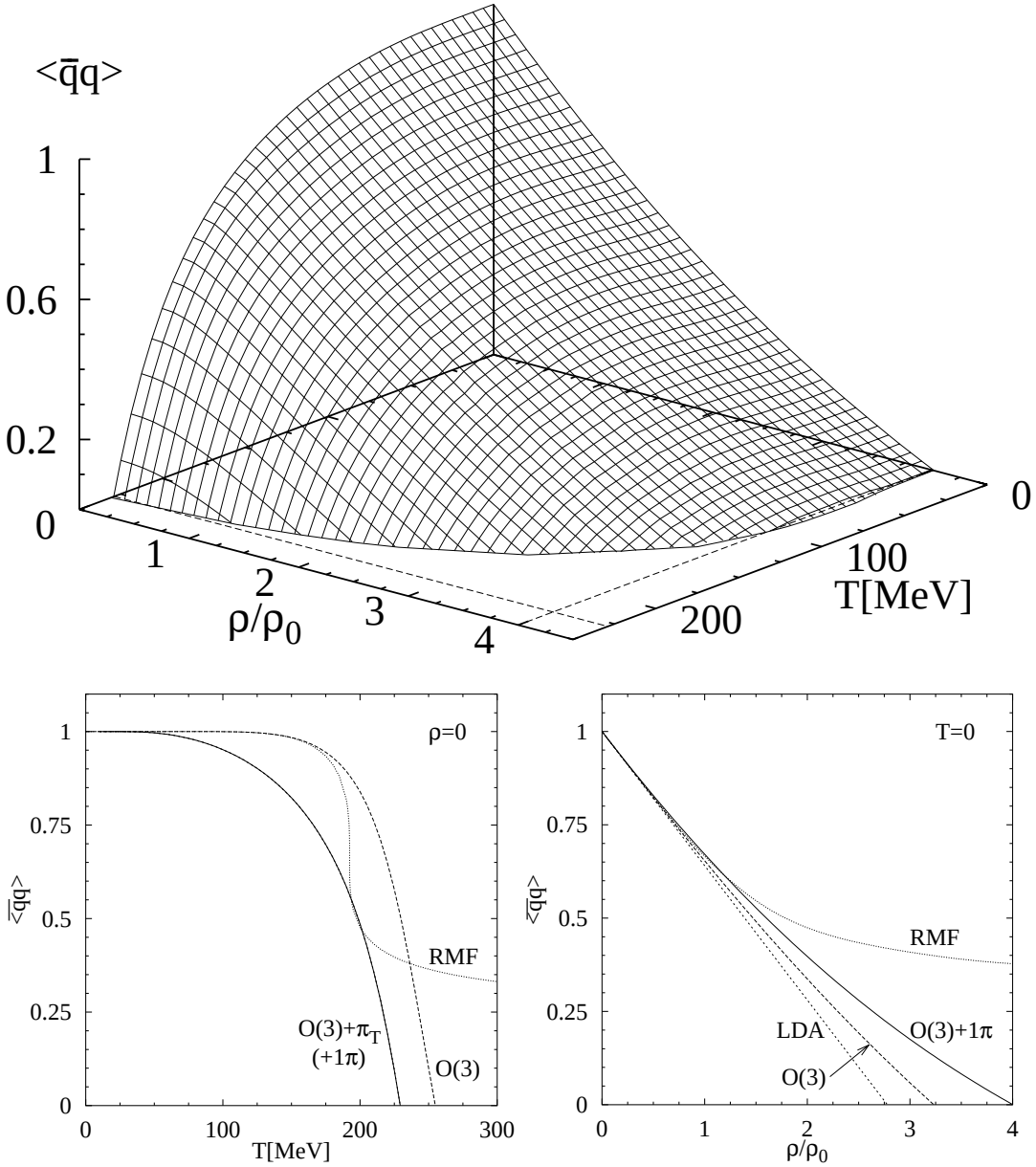

Figure 4.32: The chiral condensate $\langle \bar{q}q \rangle \equiv \langle \bar{q}q \rangle(\rho, T)/\langle \bar{q}q \rangle(0,0)$ calculated both with thermal and exchanged pions and the projections $\rho = 0$ (bottom left) and $T = 0$ (bottom right)

We have decided not to show the whole range of plots for this case again as the changes are rather small and the corresponding figures would just look more or less the same as the ones for the previous case without pions.

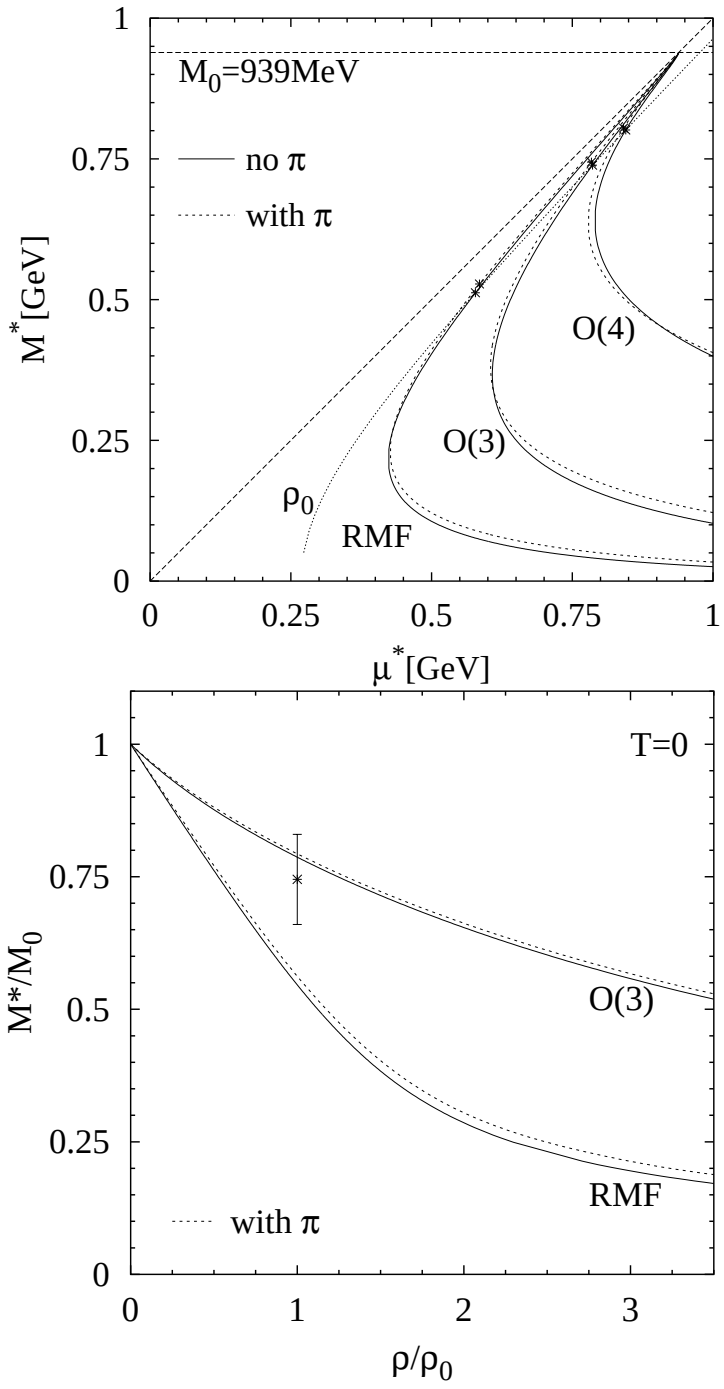

Figure 4.33: Solutions to the mass-SCE equation as a function of μ^* (upper plot) and ρ/ρ_0 (lower plot) for the RMF calculation and the extension with $O(3)$ with and without the contributions due to pion exchange

This is mainly due to the fact that the solutions to the mass-SCE differ only by a few percent. This can be seen by looking at Fig. 4.33 which shows these solutions that correspond to $F = 0$ with (dashed) and without pions (solid), remember that $P_\pi(T = 0) = 0$.
The results presented in the previous section, e.g. the value for $T_c^{\rm LG}$ in (4.69), have large enough error bars to be valid still.
The most drastic changes due to the implementation of pion contributions are visible in the results plotted in Fig. 4.31f. We see that thermal pions are responsible for a decrease in T_c which then has the value listed in Table 4.4.

model	T_c
lattice $[SU(2)_F]$	173 ± 8
RMF	$\sim$192
O(3)	$\sim$255
O(3)+π	$\sim$229

Table 4.4: The values for the critical temperature T_c in the different realisations.

The labels in Fig. 4.32 and 4.33 concerning pions are 'π' which means both, 'π_T' for thermal and '1π' for those from 1-pion exchange.
The projections $\langle\bar{q}q\rangle = 0$ in Fig. 4.31 as well as those with $T = 0$ and $\rho = 0$ in Fig. 4.32 show the chiral quark condensate at each of the steps in our calculation. The first of these clearly shows that the pion contribution concerning their exchange between nucleons has more of an effect on the density side. It is not astonishing - as the name already tells us - that thermal pions do so for varied T. Therefore the contribution of the latter is zero for $T = 0$ whereas that of exchanged pions vanishes for $\rho = 0$, thus the label 1π in brackets.
We want to summarise at this point that with the three parameters $G_{\rm s}, G_{\rm v}$ and G_3 from Table 4.5 we were able to reproduce the following properties of nuclear matter:

$$\begin{aligned} \rho_0 &= 0.17\,\mathrm{fm}^{-3} \\ M^* &\simeq 0.8 \cdot M_0 \\ |E|/A &= 16\,\mathrm{MeV} \\ \kappa &\simeq 240\,\mathrm{MeV} \\ T_c^{(\mathrm{LG})} &\simeq 16.5\,\mathrm{MeV} \end{aligned}$$

Note again that it is possible to adjust G_3 such that it reproduces any value for the compressibility κ in the range 200-600 MeV. The only value which is off is that of the critical temperature T_c of the chiral phase transition, see Table 4.4. However, remember that such a value can at most be indicative since our model looses its validity near the "real" chiral phase transition.

Table 4.5: Parameter sets used to calculate the plots with (bottom three) and without pions, $[G_\mathrm{s},G_\mathrm{v}]$=GeV^{-2}, $[G_n]$=GeV^{n-4}, $[|E|/A,\kappa]$=MeV and $[\rho_0]$=fm^{-3}

set		G_s	G_v	n	G_n^{-1}	$\lvert E\rvert/A$	ρ_0	M^*/M_0	κ
1	RMF	353.277	265.051	–	0	16.0004	0.16974	0.546	557.5
2	O(3)	224.506	105.405	3	0.009	15.9964	0.17027	0.787	243.3
3	O(4)	158.905	60.095	4	0.15	16.0005	0.16965	0.853	251.4
4	RMF+π	339.357	259.942	–	0	15.9965	0.16903	0.562	530.0
5	O(3)+π	212.431	106.502	3	0.009	15.9986	0.17004	0.793	238.5
6	O(4)+π	150.9847	63.3463	4	0.15	15.9989	0.16892	0.856	244.9

4.5 Two-Pion Exchange Terms

We now proceed to the next order in pion exchange contributions. We start with the following diagram

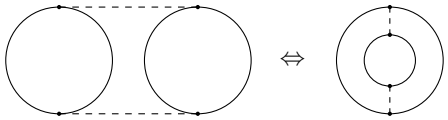

referred to as iterated 1-pion exchange HARTREE term. Non-relativistic calculations [44] indicate that in this order its contribution is rather large. It was found in [44] that this diagram incorporates basically a mechanism for nuclear matter saturation.

Let us briefly sketch the evaluation of this 2-pion exchange diagram when performed in analogy to the 1-pion exchange FOCK diagram presented in the two preceding sections. We label the EUCLIDean four-momenta, where arrows indicate the direction of flow

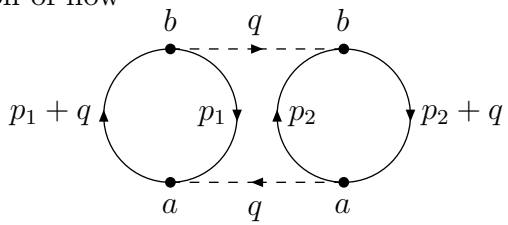

(4.85)

The FEYNMAN rules for the 4 vertices and 6 propagators occuring in this diagram are given in (A.7)-(A.9). The combinatoric factor of this diagram is 1/4 which corresponds to the four possible permutations that map the diagram onto itself. 4-momenta are conserved at each vertex. This time we have two closed fermion loops and therefore no change in sign. We have to perform an isospin and DIRAC trace over each nucleon ring. Summing all possible charge states leads to the isospin factor $\mathbf{tr}\,\tau^a\tau^b\,\mathbf{tr}\,\tau^a\tau^b = 2\delta^{ab}\,2\delta^{ab} = 12$. Furthermore

(A.6) implies 3-dimensional loop integrations over p_1, p_2 and q as well as frequency summations of n_1, n_2 and ν. At this stage the analytic expression for the 2-pion HARTREE diagram reads

$$P_{2\pi} = 3\left(\frac{-ig_A}{2f_\pi}\right)^4 (-4)^2 T^3 \sum_{\nu,n_{1,2}} \int \frac{\mathrm{d}^3p_1 \mathrm{d}^3p_2 \mathrm{d}^3q}{(2\pi)^9} \cdot \\ \cdot \frac{\frac{1}{4}\mathbf{tr}\,\not{q}(-M^* - \not{p}_1 - \not{q})\not{q}(M^* - \not{p}_1)\frac{1}{4}\mathbf{tr}\,\not{q}(-M^* - \not{p}_2 - \not{q})\not{q}(M^* - \not{p}_2)}{(m_\pi^2 + q^2)^2[M^{*2} + p_1^2][M^{*2} + (p_1+q)^2][M^{*2} + p_2^2][M^{*2} + (p_2+q)^2]}. \tag{4.86}$$

A formulation in terms of distribution functions can be found in Appendix C.2. Having a closer look at the ansatz for the 2π-HARTREE diagram in (4.86) we see that a calculation of $P_{2\pi}$ with only the one term corresponding to the diagram above brings about 3 summations and 9 integrations. The 3 summations can be performed analytically resulting in a cubic polynomial in distribution functions. Due to renormalization the terms with no distribution functions will drop out. Single distribution functions renormalise the free nucleon and pion. However, the 9-dimensional momentum space integral still has to be performed. Only a few of these integrations can be performed analytically and we would still end up with at least 4-5 numerical integrations.
The most important thing is that we keep the numerics at a level that still allows playing with the model by hand as the adjustment of parameters to reproduce the properties of nuclear matter needs to be done this way. If such a calculation becomes too time-consuming this becomes unfunctional. Although the parameter tuning is performed at $T = 0$ where calculations are a bit easier and therefore faster, a full calculation like that for (4.85) takes too long to do with the performance of today's ordinary desktop computers. One can imagine that solving the mass self-consistency equation with high precision (we need accuracy at the percent level or better) involves calculation of the corresponding equation of state - or more precisely the function F that is needed in the root finding procedure - a couple of hundred times.
Therefore we decided to use the following approximation (only at $T = 0$): the neglection of thermal pions and of anti-nucleons in higher order. Also the nucleons in this approximation will be treated non-relativistically. In [44] the authors have already calculated the following diagrams

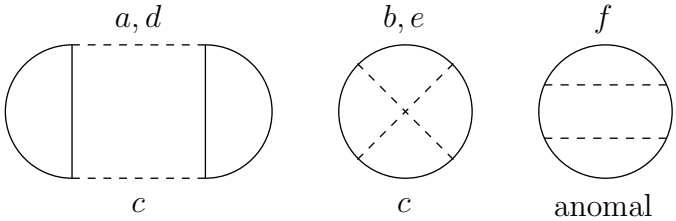

(4.87)

in such a non-relativistic framework. The first of these is identical to (4.85). We will justify using this approximation in section 4.5.2.
The whole 2-pion-exchange term is then assembled from the contributions labelled $a-f$ in (4.87):

$$P_{2\pi}^{(T=0)} = P_{2\pi}^{(a)} + P_{2\pi}^{(b)} + P_{2\pi}^{(c)} + P_{2\pi}^{(d)} + P_{2\pi}^{(e)} + P_{2\pi}^{(f)}. \tag{4.88}$$

In the non-relativistic approximation the contributions $P_{2\pi}^{(i)}(i = a, b, ..., f)$ do not depend upon μ^* and M^* separately but only on the combination in the definition of the FERMI momentum $p_f = \sqrt{\mu^{*2} - M^{*2}}$. It is furthermore advantageous to use the dimensionless variable $u = p_f/m_\pi$.
These contributions can be written as follows:

$$P_{2\pi}^{(a)} = M^* m_\pi^7 \frac{g_A^4}{5(4\pi)^5 f_\pi^4}\Big[-18u^2 + 236u^4 - 4u^3\left(60 + 32u^2\right)\cdot \arctan(2u) + \\ + \left(\frac{9}{2} + 70u^2\right)\ln\left(1+4u^2\right)\Big] \tag{4.89}$$

$$P_{2\pi}^{(b)} = M^* m_\pi^7 \frac{g_A^4}{(2\pi)^5 f_\pi^4}\left\{ -\frac{u^6}{6} + \int_0^u \mathrm{d}x \frac{x(u-x)^2(2u+x)}{2(1+2x^2)}\cdot \right. \tag{4.90}$$
$$\left. \cdot\Big[\left(1+4x^2\right)\arctan(2x) - \left(1+8x^2+8x^4\right)\arctan(x)\Big]\right\}$$

$$P_{2\pi}^{(c)} = \frac{5g_A^4\Lambda}{3(2\pi)^6 f_\pi^4} M^* p_f^6 = M^* m_\pi^6 \frac{5g_A^4\Lambda}{3(2\pi)^6 f_\pi^4} u^6 \tag{4.91}$$

$$P_{2\pi}^{(d)} = M^* m_\pi^7 \frac{3g_A^4}{(2\pi)^6 f_\pi^4}\int_0^u dx\, x^2 \int_{-1}^1 dy \left[2uxy + \left(u^2 - x^2y^2\right)\ln\frac{u+xy}{u-xy}\right]\cdot \\ \cdot\left[\ln(1+s^2) - \frac{2s^2+s^4}{2\,(1+s^2)}\right] \tag{4.92}$$

$$P_{2\pi}^{(e)} = M^* m_\pi^7 \frac{3g_A^4}{(2\pi)^6 f_\pi^4}\int_0^u \mathrm{d}x\Big\{ -\frac{G^2}{16} + \frac{x^2}{8}\int_{-1}^1 \mathrm{d}y \int_{-1}^1 \mathrm{d}z \frac{yz\,\theta(y^2+z^2-1)}{|yz|\sqrt{y^2+z^2-1}}\cdot \\ \cdot\Big[s^2 - \ln\left(1+s^2\right)\Big]\Big[t^2 - \ln\left(1+t^2\right)\Big]\Big\} \tag{4.93}$$

$$P_{2\pi}^{(f)} = M^* m_\pi^7 \frac{g_A^4}{(2\pi)^6 f_\pi^4}\left[\frac{3u^{\frac{1}{2}}}{2}\arctan(2u) - \frac{3}{8u^{\frac{1}{2}}}\ln\left(1+4u^2\right) + u^{\frac{7}{2}} - \frac{3u^{\frac{3}{2}}}{2}\right]^2 \tag{4.94}$$

with the abbreviations $p_f = \sqrt{\mu^{*2} - M^{*2}}$,

$$s = xy + \sqrt{u^2 - x^2 + x^2y^2}\,; \quad t = xz + \sqrt{u^2 - x^2 + x^2z^2}\,; \quad u = \frac{p_f}{m_\pi}$$

$$\text{and } G \;=\; u\left(1+u^2+x^2\right) - \frac{1}{4x}\left[1+(u+x)^2\right]\left[1+(u-x)^2\right]\ln\frac{1+(u+x)^2}{1+(u-x)^2} \tag{4.95}$$

It is important to point out the exceptional position of $P_{2\pi}^{(c)}$ in (4.91) which brings a new parameter Λ into the game. It is a cutoff parameter used to regularise the linear divergence which comes along with the integration over the pion momentum in the inner loop. $P_{2\pi}^{(c)}$ also has a prefactor $\sim M^* m_\pi^6$ whereas all the other terms are $\sim M^* m_\pi^7$.
What we have done so far will rather save us a lot of analytical work. The real gain in time consumption when it comes to the numerical work will be achieved by fitting a polynomial (or several ones) to the whole pressure $P_{2\pi} \equiv P_{2\pi}^{(T=0)}$

$$P_{2\pi}\left(u=\frac{p_f}{m_\pi}\right) \;=\; \sum_{i=a\ldots f} P_{2\pi}^{(i)} = M^* m_\pi^7 \sum_{i=4}^{11} t_i \cdot u^i \tag{4.96}$$

After playing around with several possibilities the choice fell for u to appear in powers of 4...11 which yield the best fit. Clearly for $P_{2\pi}^{(c)}$ depending only upon u^6 the only parameter that will be affected is t_6 making this one special, all other t_i are just numbers but t_6 is a function of Λ and m_π: $t_6 = t_6(\Lambda, m_\pi)$. Of course having a new parameter at hand immediately lets one think about the possibility that it might be used instead of G_3 in order to fix the value for κ. Thus we have set $G_3 = 0$ again and we studied the relation between a value for Λ and the compressibility κ. The result was disillusioning and is shown in Table 4.6:

Λ	G_s	G_v	E/A	ρ_0	κ
300	332	252			
611	333	275	$\sim$16	$\sim$0.17	$\sim$510
900	343	290			

Table 4.6: Relation between the parameter Λ and the compressibility κ, $[G_\mathrm{s}, G_\mathrm{v}]$=GeV^{-2}, $[E/A, \kappa, \Lambda]$=MeV and $[\rho_0]$=fm^{-3}

We see that - no matter what value we pick for Λ - the value for κ stays more or less the same. We have not worked here with the precision we did throughout the last sections as the extra work would only lead to quantitative changes which are not so much of interest. The procedure should be clear by now: before showing or stating any results the properties of nuclear matter have to be adjusted, for the choice of G_s and G_v see Fig. 4.2.
If we look at the value of G_v we see that it does not change much. This we can easily understand: it is possible to keep G_v fixed and to use G_s and κ to shift the binding energy minimum to the appropriate position. Therefore G_v

and κ seem to function the same way! This is due to the fact that the two terms they belong to have the same structure $\sim p_f^6$:

$$P_{2\pi}^{(c)} = \frac{5g_A^4}{3(2\pi)^6 f_\pi^4} M^* \Lambda p_f^6 \tag{4.97}$$

$$P_{\mathrm{v}} = \frac{(\mu-\mu^*)^2}{2G_{\mathrm{v}}} = \frac{1}{2} G_{\mathrm{v}} \rho^2 = \frac{2}{9\pi^4} G_{\mathrm{v}} p_f^6 \tag{4.98}$$

where the first term is taken from (4.91) and P_{v} is the first term of the total pressure as given e.g. in (4.72). Because of their different pre-factors with M^* appearing in $P_{2\pi}^{(c)}$ they end up at different positions: the latter makes its way into the mass-SCE whereas P_{v} does not. But overall there is nothing much new to learn from this new parameter Λ. We will set $\Lambda = 611\,\mathrm{MeV}$.
In order to achieve the precision we wanted we fitted polynomials to the pressure for different regions of u as shown in Table 4.7 below.

u	t_4	t_5	t_6'	t_7
$0 \le u \le 0.97$	$9.335{\cdot}10^{-4}$	-0.0149	-2.4052	-0.3058
$0.97 < u \le 4$	0.1462	-0.3241	-2.4950	0.4848
$4 < u \le 8$	1.2468	-2.5312	-0.6168	-0.3968
u	t_8	t_9	t_{10}	t_{11}
$0 \le u \le 0.97$	0.5138	-0.1075	-0.1846	0.08629
$0.97 < u \le 4$	-0.2684	0.04278	$-3.7805{\cdot}10^{-3}$	$1.405{\cdot}10^{-4}$
$4 < u \le 8$	-0.0222	$2.036{\cdot}10^{-3}$	$-1.049{\cdot}10^{-4}$	2.3305

in any case: $t_6 = t_6' + 0.9667 \cdot \Lambda/m_\pi \equiv t_6(\Lambda, m_\pi)$

Table 4.7: The parameters used to calculate the approximative polynomial in (4.96). We used double precision in our calculation, the values listed are rounded.

The polynomial fit to the 2-pion exchange pressure contribution in (4.96) can be written as a function of Fermi momentum or effective chemical potential

$$P_{2\pi}(M^*, m_\pi, u) = M^* \sum_{i=4}^{11} t_i p_f^i m_\pi^{7-i} = P_{2\pi}(M^*, \mu^*, m_\pi) \tag{4.99}$$

due to the fact that

$$u = \frac{p_f}{m_\pi} = \sqrt{\mu^{*2} - M^{*2}}/m_\pi = u(M^*, \mu^*, m_\pi). \tag{4.100}$$

Apart from being evaluated much faster it has the further advantage of being more easily differentiated. With the help of

$$\frac{\partial u}{\partial M^*} = \frac{\partial}{\partial M^*}\frac{p_f}{m_\pi} = m_\pi^{-1}\frac{\partial}{\partial M^*}\left(\mu^{*2} - M^{*2}\right)^{1/2} = \frac{-M^*}{m_\pi p_f} = \frac{-M^*}{m_\pi^2 u} \quad (4.101)$$

$$\frac{\partial}{\partial \mu^*}u^i = \frac{iu^{i-2}\mu^*}{m_\pi^2} \quad (4.102)$$

we get for the contribution necessary to adapt the mass-SCE to the new situation

$$\begin{aligned}\frac{\partial P_{2\pi}}{\partial M^*} &= \frac{P_{2\pi}}{M^*} + \left(M^* m_\pi^7 \sum_{i=4}^{11} t_i \cdot iu^{i-1}\frac{\partial u}{\partial M^*}\right) \overset{(4.101)}{=} \frac{P_{2\pi}}{M^*} - M^{*2} m_\pi^5 \sum_{i=4}^{11} it_i u^{i-2} \\ &= m_\pi^7 \sum_{i=4}^{11} t_i \cdot u^i - M^{*2} m_\pi^5 \sum_{i=4}^{11} it_i u^{i-2} = m_\pi^5 \sum_{i=4}^{11} t_i \left(m_\pi^2 u^i - M^{*2} iu^{i-2}\right)\end{aligned} \quad (4.103)$$

This will give us a contribution to the scalar density because $P_{2\pi}$ is part of $P_{\pi,\pi}$ as in (4.70). Remember that the scalar density can be calculated from $n_s = -\partial P/\partial M = -\partial/\partial M^*(P_{FG} + P_{\pi,\pi})$.
The contribution to the baryon density can be handled analogously:

$$\frac{\partial P_{2\pi}}{\partial \mu^*} = M^* m_\pi^7 \sum_{i=4}^{11} t_i \cdot \frac{\partial}{\partial \mu^*} u(M^*, \mu^*, m_\pi)^i \overset{(4.102)}{=} M^* m_\pi^5 \sum_{i=4}^{11} it_i u^{i-2}\mu^*. \quad (4.104)$$

Last but not least we will come to the contribution to the chiral quark condensate $\langle\bar{q}q\rangle$ in the form of $\partial P_{2\pi}/\partial m_\pi^2$. In this case we have to pay special attention because of $t_6 = t_6(m_\pi)$

$$\begin{aligned}\frac{\partial P_{2\pi}}{\partial m_\pi^2} &= \frac{\partial}{\partial m_\pi^2}\left[M^* \sum_{i=4}^{11} t_i p_f^i (m_\pi^2)^{(7-i)/2}\right] = \\ &= M^* m_\pi^5 \sum_{i=4}^{11} \frac{7-i}{2} t_i u^i + M^* m_\pi^7 u^6 \frac{\partial t_6}{\partial m_\pi^2}\end{aligned}$$

These formulae enable us to extend the zero temperature formula collection in section 4.4.1 once more. We will present the results in the next section.

4.5.1 The Chiral Condensate (IV)

We proceed to present the results of such a calculation. Note that now we add the changes due to 2-pion exchange to the results in 4.4.2 where we had a finite value for G_3 and the 1-pion exchange was taken care off in the form presented in Appendix C.1.

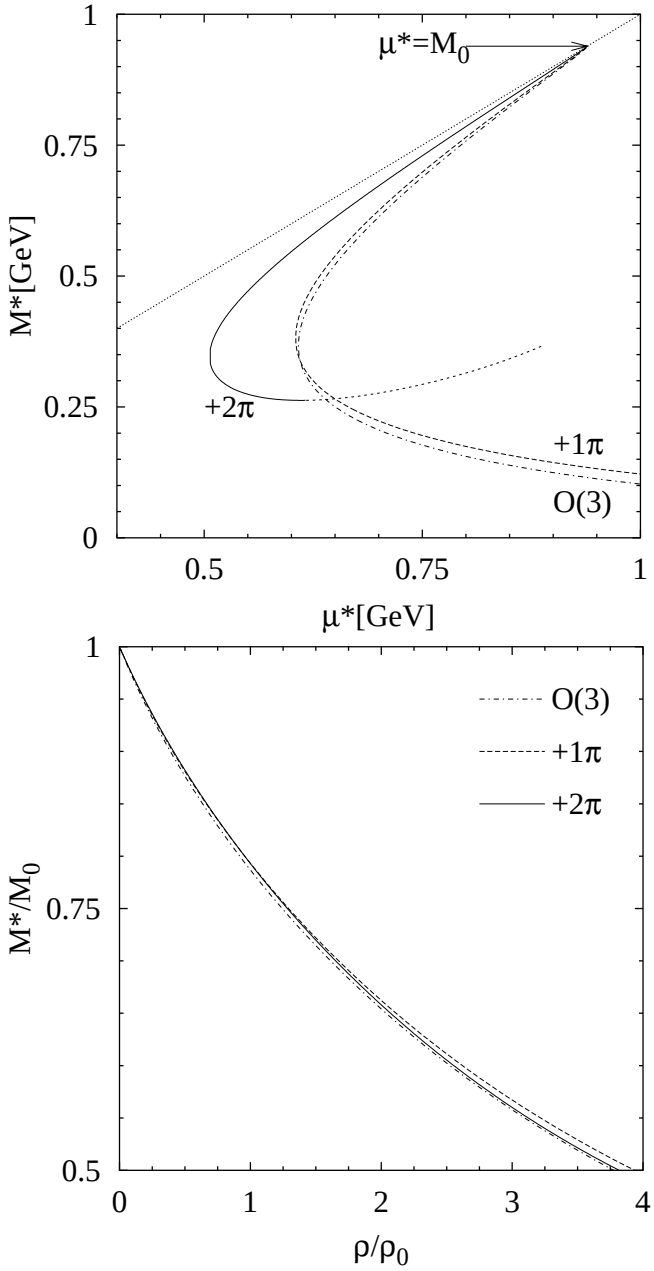

Figure 4.34: Solutions to the mass-SCE equation as a function of μ^* (upper plot) and ρ/ρ_0 (lower plot) for the calculation including 2-pion exchange.

We see in Fig. 4.34 that the solutions to the mass-SCE in the case including 2-pion exchange differ a lot when plotted as a function of effective chemical potential μ^* (upper plot). For very high densities $\rho \gg 10\rho_0$ the effective nucleon mass starts to rise again for the approximation we use. However, we are not bothered with such high densities. As soon as we study these effective mass values as a function of baryon density again the results differ very little in the density region interesting to us (lower plot).
The parameter set used in the calculation of the figures in this section is the bottom one in Table 4.8 with a new value $G_3 = 117.647\,\mathrm{GeV}^{-1}$ which shifts the value for the compressibility back into the correct range, see (4.52). That new value is then $\kappa = 250.7\,\mathrm{MeV}$.

Table 4.8: Parameter sets used to calculate the figures including 2-pion exchange [G_s,G_v]=GeV^{-2}, [G_3]=GeV^{-1}, [$\Lambda, E/A, \kappa$]=MeV and [ρ_0]=fm^{-3}

G_s	G_v	Λ	G_3^{-1}	E/A	ρ_0	M^*/M_0	κ
206.447	121.455	611	0.009	16.0028	0.17032	0.795	233.7
206.194	122.766	611	0.0085	15.9951	0.17034	0.793	250.7

The changes in the chiral condensate are:

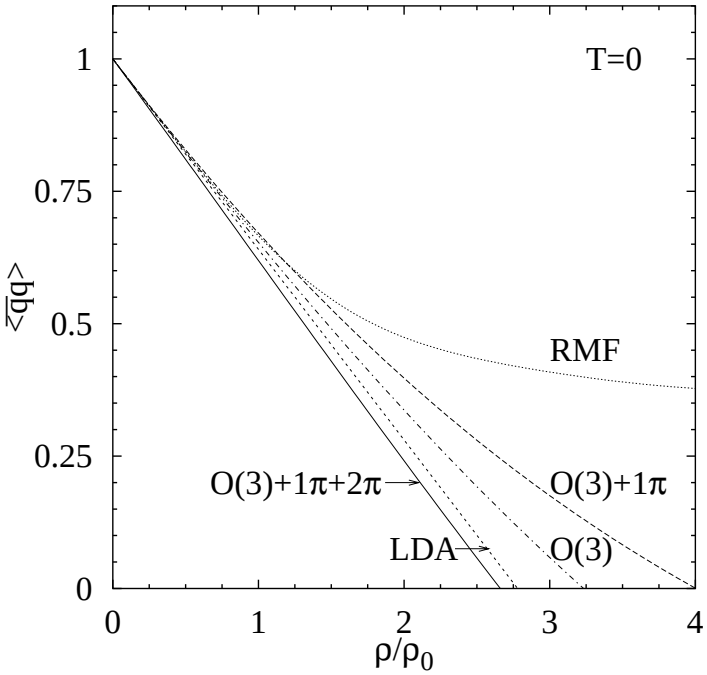

Figure 4.35: Density dependence of the chiral quark condensate at $T = 0$ for various cases

We have plotted all cases again to allow comparisons. The new result including the approximative 2π-exchange as described in this section now drops even

faster than the linear density approximation (LDA), see section 3.2.3 - especially (3.31). We have also shown the relativistic mean field (RMF) calculation from the WALECKA model as well as all the different stages of our model.

In all three figures the $O(3)$-case is dash-dotted, the case including the (full) 1π-exchange FOCK term in addition (labelled '$+1\pi$') is dashed and the case with both pion exchange distributions (sometimes just labelled '$+2\pi$') is drawn with a solid line.

4.5.2 Justification to Use the Approximation

The validity of the approximation used in the previous section can be examined by comparing its result of the 1π-exchange FOCK term to the full calculation as discussed in 4.4.2. The corresponding calculation in the non-relativistic framework is presented in the previous section. Such a term is a function of

$$P'_{1\pi} = P'_{1\pi}(T=0,u) = P'_{1\pi}(p_f, m_\pi) = P'_{1\pi}(\mu^*, M^*, m_\pi), \tag{4.105}$$

see (4.100). It has the following form in the framework mentioned

$$\begin{aligned} P'_{1\pi} &= m_\pi^6 \left(\frac{g_A}{4\pi^2 f_\pi}\right)^2 \left[-\frac{2}{3}u^6 - \frac{u^2}{4} + \frac{3u^4}{2} - 2u^3 \arctan(2u) + \right. \\ &\qquad \left. + \left(\frac{3u^2}{4} + \frac{1}{16}\right) \ln\left(1+4u^2\right)\right] \end{aligned} \tag{4.106}$$

where the first term in brackets $-2u^6/3$ is the equivalent of the P_Δ-term in (C.6) of our full calculation, therefore this term will be neglected.
The usual derivatives of $P'_{1\pi}$ in (4.106) that allow correct treatment of this approximation are

$$\frac{\partial P'_{1\pi}}{\partial M^*}, \quad \frac{\partial P'_{1\pi}}{\partial \mu^*} \quad \text{and} \quad \frac{\partial P'_{1\pi}}{\partial m_\pi^2}. \tag{4.107}$$

The form of the mass-SCE does not differ from that in (4.62):

$$F(M^*) = M - M^* - G_\mathrm{s}\, n_s + \frac{G_\mathrm{s}}{G_3}(M-M^*)^2 = 0. \tag{4.108}$$

It contains the scalar density which has to be modified just the way we did when we used the full 1-pion exchange FOCK term. This time we only have to replace $P_{1\pi}$ by $P'_{1\pi}$. Then

$$n_\mathrm{s} = -\frac{\partial P_{FG}}{\partial M^*} \quad \rightarrow \quad n_\mathrm{s} - \frac{\partial P'_{1\pi}}{\partial M^*} \tag{4.109}$$

with

$$\frac{\partial P'_{1\pi}}{\partial M^*} = -\frac{3g_A^2 M^* m_\pi^2}{32\pi^4 f_\pi^2}\left[m_\pi^2 \ln\frac{m_\pi^2+4p_f^2}{m_\pi^2} - 4m_\pi p_f \arctan\left(\frac{2p_f}{m_\pi}\right) + 4p_f^2\right]. \quad (4.110)$$

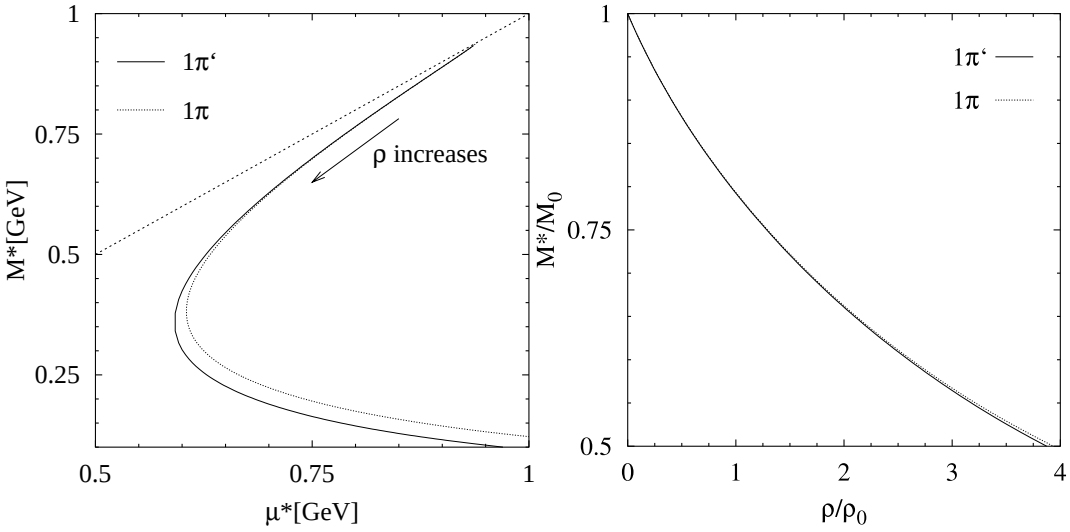

Figure 4.36: Solutions to the mass self-consistency equation in both cases including 1-pion exchange. The full treatment 1π is dotted, the approximation $1\pi'$ plotted with a solid line. Remember that going along the curve in the left plot (M^* as a function of effective chemical potential) in direction of the arrow starting from $\rho = 0$ at $M^* = \mu^* = M_0$ is going to $\rho \to \infty$. In the right plot (M^* as a function of baryon density) we see that for small baryon density the approximation is excellent.

The modifications in the baryon density applied in the calculation of the right plot in Fig. 4.36 have similar shape as those for n_s

$$\begin{aligned}\rho &\to \rho + \frac{\partial P'_{1\pi}}{\partial \mu^*} \\ \frac{\partial P'_{1\pi}}{\partial \mu^*} &= \frac{3g_A^2 \mu^* m_\pi^2}{32\pi^4 f_\pi^2}\left[m_\pi^2 \ln\frac{m_\pi^2+4p_f^2}{m_\pi^2} - 4m_\pi p_f \arctan\left(\frac{2p_f}{m_\pi}\right) + 4p_f^2\right]. \quad (4.111)\end{aligned}$$

The changes in the chiral quark condensate $\langle\bar{q}q\rangle$ defined in (3.20) are two-fold. First there is the change due to the scalar density as in (4.109f) and secondly there appears an additional term due to the m_π-dependence of $P'_{1\pi}$ itself:

$$\langle\bar{q}q\rangle \to \langle\bar{q}q\rangle + \frac{1}{f_\pi^2}\frac{\partial P'_{1\pi}}{\partial m_\pi^2} = \langle\bar{q}q\rangle + \frac{1}{2m_\pi f_\pi^2}\frac{\partial P'_{1\pi}}{\partial m_\pi}. \quad (4.112)$$

We have reduced the derivative with respect to m_π^2 to one with respect to m_π by use of $\partial m_\pi^2 = 2m_\pi \partial m_\pi$. This derivative is

$$\frac{\partial P'_{1\pi}}{\partial m_\pi} = \frac{6P'_{1\pi}}{m_\pi} + m_\pi^3 \left(\frac{g_A}{4\pi^2 f_\pi}\right)^2 \left[\frac{1}{2}p_f^2 - \frac{6p_f^4}{m_\pi^2} + \frac{6p_f^3}{m_\pi}\arctan(2u) + \frac{4p_f^4}{m_\pi^2(1+4u^2)} - \frac{3p_f^2}{2}\ln\left(1+4u^2\right) - \frac{8p_f^2\,(3u^2/4+1/16)}{1+4u^2}\right]. \quad (4.113)$$

The actual calculation has been performed using the very same parameters as in the corresponding calculation labelled $O(3)+\pi$ in Table 4.5. These parameters are:

$$G_{\rm s} = 212.431\,{\rm GeV}^{-2}, \quad G_{\rm v} = 106.502\,{\rm GeV}^{-2}, \quad G_3^{-1} = 0.009\,{\rm GeV},$$
$$g_A = 1.267, \quad m_\pi = 138\,{\rm MeV}, \quad f_\pi = 92.4\,{\rm MeV}. \quad (4.114)$$

They lead to the results shown in Fig. 4.37:

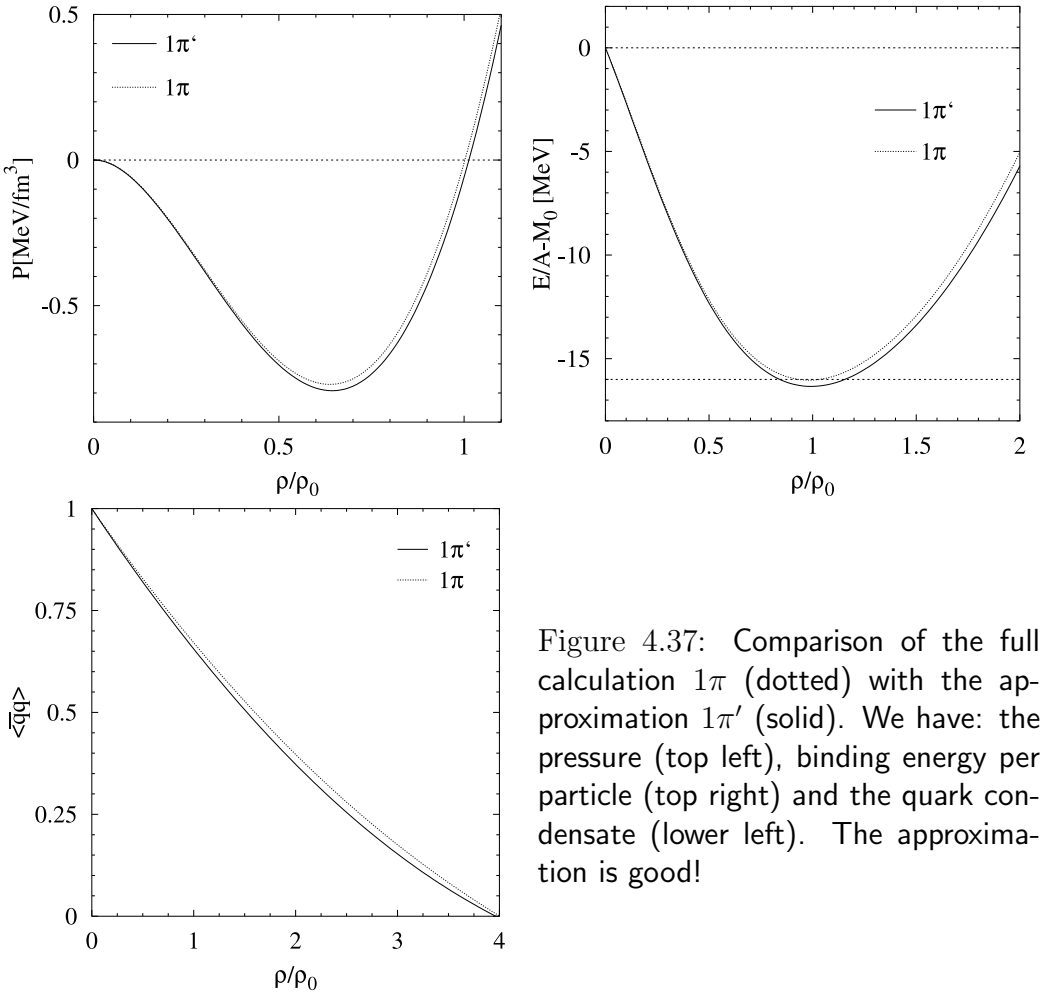

Figure 4.37: Comparison of the full calculation 1π (dotted) with the approximation $1\pi'$ (solid). We have: the pressure (top left), binding energy per particle (top right) and the quark condensate (lower left). The approximation is good!

Note that the results presented for the approximation this time are **not** optimised by adjustment of the parameters. They would improve if we did!

Chapter 5

Summary and Conclusions

The main interest in this work was to study the thermodynamics of the chiral quark condensate $\langle\bar{q}q\rangle$.
After recalling basic symmetries and symmetry breaking patterns of Quantum Chromodynamics (QCD) in chapter 2 we constructed the chiral effective Lagrangian to leading order. Low-energy QCD is realised as an effective field theory of weakly interacting GOLDSTONE bosons coupled to heavy nucleons. The interactions between these particles are ruled by chiral symmetry.
In chapter 3 we gave an outline of field theoretical concepts at finite temperature and density. We formulated the thermodynamics in the grand canonical ensemble. The latter is the appropriate framework when dealing with relativistic many-particle systems. Our focus was again on the temperature and density dependence of the chiral condensate. In this context we also rediscovered the low density theorem which states that to leading order in density the chiral condensate drops linearly with a slope determined by σ_N. The so-called pion-nucleon sigma term $\sigma_N = m_q \cdot \partial M/\partial m_q \simeq 45\,\mathrm{MeV}$ gives the portion of the nucleon mass coming from the finite quark mass. The temperature dependence of $\langle\bar{q}q\rangle(T)$ at low T is determined exclusively by the dynamics of the free and interacting thermal pion gas for which we stated a formula that allows to study the quantitative influence of the 1- and 2-loop contributions of the thermal pion gas on the condensate.
However, this is not the only reason to include pions as explicit degrees of freedom. Pions also represent the dominant meson exchange contributions at the temperatures we consider here. Furthermore at the nuclear matter saturation density $\rho_0 \simeq 0.17\,\mathrm{fm}^{-3} = 2p_f^3/(3\pi^2)$ the FERMI momentum $p_f = 268\,\mathrm{MeV}$ and the pion mass $m_\pi = 138\,\mathrm{MeV}$ are comparable scales $p_f \simeq 2m_\pi$.
We finally reached the main part of the present work in chapter 4 where we first confirmed that working with the 2-parameter WALECKA model is equiva-

lent to performing the calculations using a Lagrangian with scalar and vector four-nucleon contact interactions as long as both are treated in mean field approximation. We constructed an equation of state whose parameters were adjusted such that they reproduce the known properties of nuclear matter. Apart from the saturation density ρ_0 already mentioned these are the binding energy per nucleon of about $B = 16\,\mathrm{MeV}$ and the nuclear matter (in-)compressibility $\kappa = (250 \pm 10)\,\mathrm{MeV}$.
In the relativistic 2-parameter mean field model, namely the Walecka model, the well-known problems reappeared: only two of the nuclear matter properties can be fit in this restrictive approach, the compressibility $\kappa = 558\,\mathrm{MeV}$ came out more than a factor "2" too large. On the other handside the effective nucleon mass $M^* \simeq 0.54M$ was too small.
Therefore we extended this model by adding a higher order term in the scalar mean field. It turned out that using a quartic term instead of a cubic one results in an effective nucleon mass being too large. Therefore the additional term $G_3(M - M^*)^3/3$ was preferred. The mean scalar and vector fields could be expressed in terms of the effective nucleon mass and chemical potential. The adjustment of this single new parameter G_3 fixed both problems: not only did we shift the value of κ into the correct range, at the same time the effective nucleon mass increased to a more realistic - but not too large - value of $M^*(\rho_0) \simeq 0.8M$. Simultaneously it lowered the critical temperature T_c^{LG} of the liquid-gas phase transition, a further welcome effect. The value predicted by our calculation $T_c^{\mathrm{LG}} = (16.5 \pm 0.5)\,\mathrm{MeV}$ was found to be in perfect agreement with a recent analysis of limiting temperatures in heavy ion collisions [3].
The only value we failed to reproduce was that of the critical temperature $T_c = (173 \pm 8)\,\mathrm{MeV}$ of the chiral phase transition known from [35]. This is not astonishing as it represents the temperature at which nucleons dissolve, they are no longer the correct degrees of freedom. The value found in our calculation can at most be indicative since our model looses its validity near the "real" chiral phase transition.
In the next step we went beyond the mean-field description. We included the one-pion exchange Fock diagram into the partition function fully relativistically. In this form we automatically accounted for various scattering processes of thermal pions (and thermal antinucleons) with nucleons.
The 1π-exchange corrections were also included in the self-consistent determination of the effective nucleon mass and chemical potential, or equivalently the scalar and vector mean-fields. Its contribution led to an upward shift in the density dependence of $\langle\bar{q}q\rangle$. This trend is easily understood keeping in mind that the 1π-exchange Fock term is repulsive.

A non-relativistic approximation, in which effects from thermal pions and antinucleons were neglected, turned out to work well in the temperature and density regime of interest. This opened the possibility to treat (the attractive) 2π-exchange corrections in the same approximation reliably. By 2π-exchange we mean iterated 1π-exchange HARTREE and FOCK contribitions where PAULI blocking is automatically taken care of.
A cutoff parameter Λ was needed to regularise the linear divergence of the pion loop integral. It turned out that its effect could be absorbed by readjustment of the parameter G_{v} used to fix the value of the saturation density ρ_0.
Having at hand a dynamical description of nuclear matter which at the same time includes systematically pion exchange contributions and fulfills the empirical constraints at the saturation point we could focus on the temperature and density dependence of $\langle\bar{q}q\rangle$. This was done using a "master formula" which required taking the pressure's derivative with respect to the pion mass.

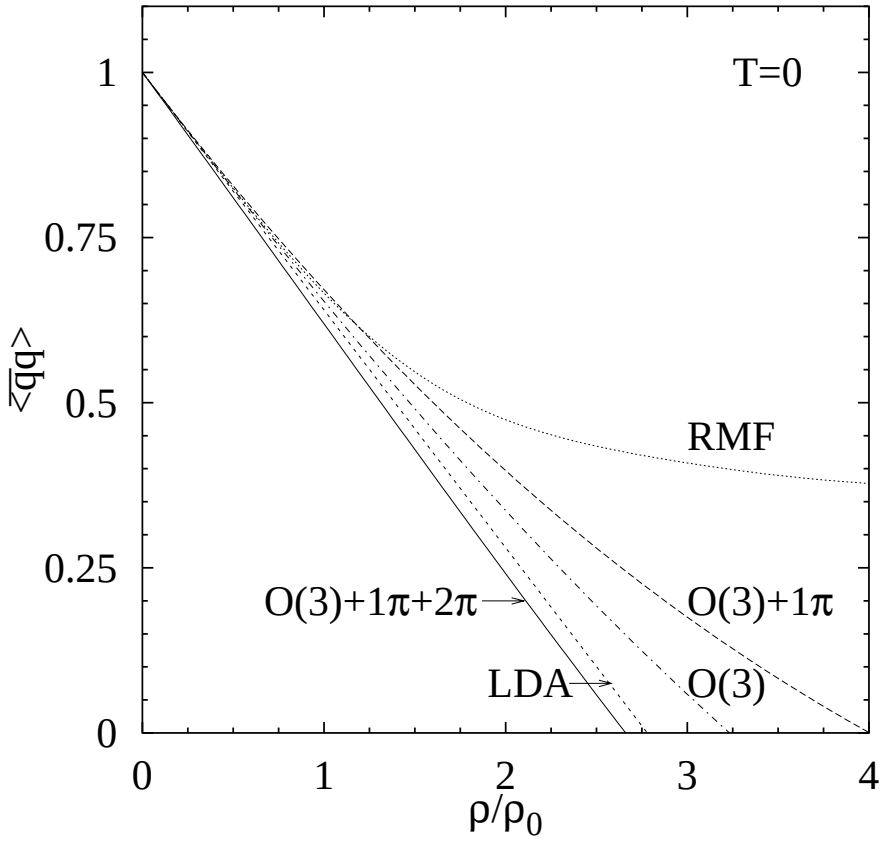

The resulting deviations from the linear decrease of $\langle\bar{q}q\rangle$ (low density theorem) were found to be astonishingly small. This result is in contrast to the work of [43]. There a chiral approach to nuclear matter has been utilised in order to

quantify the deviations from the low density theorem. In that calculation the dropping of $\langle\bar{q}q\rangle$ is reduced by only $\sim 25\%$ at normal nuclear matter density. This effect comes mainly from a diagram where an attractive nucleon-nucleon contact interaction is iterated with 1π-exchange. The dynamical origin of the associated contact coupling and possible implicit quark dependences are not discussed in [43].
Furthermore it has been demonstrated in [62] that the same iterative diagram leads to very unrealistic single particle properties. Therefore the results of [43] for $\langle\bar{q}q\rangle(\rho)$ need not be taken too seriously.

Our free parameters $G_\mathrm{s}, G_\mathrm{v}$ and G_3 were used to adjust the values of the following nuclear matter properties (in this order):

$$\begin{aligned} |E|/A &= 16\,\mathrm{MeV} \\ \rho_0 &= 0.17\,\mathrm{fm}^{-3} \\ \kappa &= 250\,\mathrm{MeV} \end{aligned}$$

From this we predict the values of the effective nucleon mass at saturation density and the liquid-gas phase transition temperature:

$$\begin{aligned} M^*(\rho_0) &= 0.8 \cdot M \\ T_c^{(\mathrm{LG})} &= 16.5\,\mathrm{MeV} \end{aligned}$$

As mentioned before both these values are in the range they should be in. Therefore our nuclear matter equation of state seems to be realistic. The calculation in this more realistic mean field model with finite G_3 shifted the quark condensate $\langle\bar{q}q\rangle$ towards the linear density approximation result. This is mainly due to the fact that the effective nucleon mass is higher, rising from 54% in the WALECKA model to $M^*(\rho_0) \simeq 0.8M$. The scalar and baryon density differ less in the case with an increased value of M^*.
The perturbatively added pion exchange contributions resulted in a shift away from the linear density result of the condensate $\langle\bar{q}q\rangle$ in the case of the repulsive 1-pion exchange FOCK term. In contrast the attractive 2-pion exchange contributions resulted in a shift of $\langle\bar{q}q\rangle$ towards and even slightly below the linear density line. The two are of the same order of magnitude, the 2-pion exchange effects being around twice as large as those from the 1-pion exchange FOCK term.
We finally conclude that the linear density approximation can be trusted at small densities up to about two times normal nuclear matter density $\sim 2\rho_0$ keeping in mind its inherent $\pm 20\%$ inaccuracy originating from the pion nucleon sigma term σ_N.

Appendix A

Mathematical Details

A.1 Feynman Rules

Besides his ambitions as a hobby painter Feynman invented the "theoretical physicist's favorite drawings" in his noble prize winning work [8, 26, 27, 63, 64, 65, 66, 67, 68, 69]. In this section we will give a brief summary on how to calculate Feynman diagrams. Their components are mainly lines (of all kinds) and dots where these intersect. Each piece of such a diagram is replaced by one of the mathematical expressions in the next section, the lines describing particle propagation. The dots represent points where three or more particles run together, they are called vertices. Their terms contain the structure and strength of the coupling.

Turning a diagram into the corresponding path integral is achieved via the following step-by-step procedure:

- replace each component by its corresponding term (A.1)
- add the symmetry factor of the diagram (A.2)
- every line is addressed a momentum p (A.3)
- ensure 4-momentum conservation at each vertex (A.4)
- each closed fermion loop implies performing the trace (see section A.1.2) and adds a factor of -1 (A.5)
- for every propagator integrate over all momenta and sum all Matsubara frequencies $\Leftrightarrow T\sum_n \int \frac{\mathrm{d}^3 p}{(2\pi)^3}$ (A.6)

Examples are calculated in Appendix C.

A.1.1 Vertex and Propagators

• Pion-nucleon vertex:

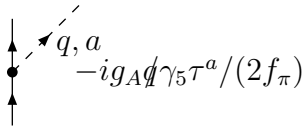

$$-ig_A \not{q}\gamma_5\tau^a/(2f_\pi) \tag{A.7}$$

• Thermal nucleon propagator:

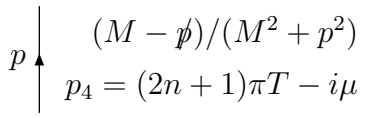

$$\frac{M-\not{p}}{M^2+\vec{p}^2+[(2n+1)\pi T - i\mu]^2} \tag{A.8}$$

• Thermal pion propagator:

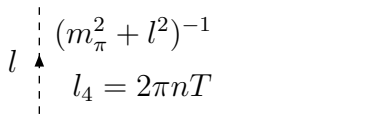

$$\frac{1}{m_\pi^2+\vec{l}^2+(2\pi n T)^2} \tag{A.9}$$

A.1.2 Traces

The trace over an odd number of momenta vanishes [70] whereas we will use the following identities in performing the trace over an even number of momenta

$$\frac{1}{4}\mathbf{tr}\,\not{p}_1\not{p}_2 \;=\; -p_1\cdot p_2 \tag{A.10}$$

$$\frac{1}{4}\mathbf{tr}\,\not{p}_1\not{p}_2\not{p}_3\not{p}_4 \;=\; (p_1\cdot p_2)(p_3\cdot p_4) - (p_1\cdot p_3)(p_2\cdot p_4) + (p_1\cdot p_4)(p_2\cdot p_3) \tag{A.11}$$

where we used the FEYNMAN dagger defined like $\not{p}_i = \gamma_\mu p_i^\mu$. Obviously we use EINSTEIN's summation convention which implies a sum whenever indices appear twice. The scalar product is defined in (A.25), the γ-matrices can be found in section A.3.1.

A.2 SU(N)

The generators of the group $SU(N), N = 2, 3, ...$ are $G^a, a = 1, ..., N^2 - 1$. They satisfy the commutation relations

$$\left[G^a, G^b\right] = if^{abc}G^c \tag{A.12}$$

where the f^{abc} are the group structure constants [71, 72].
The two most interesting examples for us are $SU(N = 2, 3)$. We will discuss their most commonly used representations in the following section.

A.2.1 Pauli Matrices

The Pauli spin matrices form a basis of the $SU(2)$ group and are defined as

$$\vec{\tau} = (\tau_1, \tau_2, \tau_3) \tag{A.13}$$

where

$$\tau_1 = \begin{pmatrix} 0 & 1 \\ 1 & 0 \end{pmatrix}, \quad \tau_2 = \begin{pmatrix} 0 & -i \\ i & 0 \end{pmatrix}, \quad \tau_3 = \begin{pmatrix} 1 & 0 \\ 0 & -1 \end{pmatrix}. \tag{A.14}$$

The product of two such matrices can be written as

$$\tau_i\tau_j = \delta_{ij} + i\epsilon_{ijk}\tau_k. \tag{A.15}$$

They obey the following (anti)commutator relations

$$\begin{aligned} \left[\frac{\tau_i}{2}, \frac{\tau_j}{2}\right] &= i\,\epsilon_{ijk}\frac{\tau_k}{2}, \\ \left\{\frac{\tau_i}{2}, \frac{\tau_j}{2}\right\} &= \frac{\delta_{ij}}{2}, \end{aligned} \tag{A.16}$$

where ϵ_{ijk} is the totally antisymmetric tensor of third degree.
Apart from its use in spin notation the τ-matrices are used in the description of isospin. E.g. up $|u\rangle$ and down quark $|d\rangle$ form an isospin $SU(2)$ doublet:

$$|u\rangle = \begin{pmatrix} 1 \\ 0 \end{pmatrix}, \quad |d\rangle = \begin{pmatrix} 0 \\ 1 \end{pmatrix} \tag{A.17}$$

with $\tau_\pm = (\tau_1 \pm i\tau_2)/2$ we have

$$\tau_3|u\rangle = |u\rangle, \quad \tau_3|d\rangle = -|d\rangle, \quad \tau_-|u\rangle = |d\rangle, \quad \tau_+|d\rangle = |u\rangle \tag{A.18}$$

The electric charge of the quarks is

$$Q = \frac{1}{2}(B + \tau_3) \tag{A.19}$$

with the baryon number $B = 1/3$. The same relations hold for the nucleon doublet of proton and neutron with $B = 1$.

A.2.2 Gell-Mann Matrices

The Gell-Mann matrices $\lambda_a, a = 1, ..., 8$ form a basis of the $SU(3)$ group thus being the three-dimensinal analogon to the Pauli matrices:

$$\lambda_1 = \begin{pmatrix} 0 & 1 & 0 \\ 1 & 0 & 0 \\ 0 & 0 & 0 \end{pmatrix}, \quad \lambda_2 = \begin{pmatrix} 0 & -i & 0 \\ i & 0 & 0 \\ 0 & 0 & 0 \end{pmatrix}, \quad \lambda_3 = \begin{pmatrix} 1 & 0 & 0 \\ 0 & -1 & 0 \\ 0 & 0 & 0 \end{pmatrix},$$
$$\lambda_4 = \begin{pmatrix} 0 & 0 & 1 \\ 0 & 0 & 0 \\ 1 & 0 & 0 \end{pmatrix}, \quad \lambda_5 = \begin{pmatrix} 0 & 0 & -i \\ 0 & 0 & 0 \\ i & 0 & 0 \end{pmatrix}, \quad \lambda_6 = \begin{pmatrix} 0 & 0 & 0 \\ 0 & 0 & 1 \\ 0 & 1 & 0 \end{pmatrix},$$
$$\lambda_7 = \begin{pmatrix} 0 & 0 & 0 \\ 0 & 0 & -i \\ 0 & i & 0 \end{pmatrix}, \quad \lambda_8 = \frac{1}{\sqrt{3}} \begin{pmatrix} 1 & 0 & 0 \\ 0 & 1 & 0 \\ 0 & 0 & -2 \end{pmatrix}. \tag{A.20}$$

They are hermitian, their trace vanishes and they are normalised such that $\mathrm{Tr}(\lambda_\mathrm{a}\lambda_\mathrm{b}) = 2\delta_\mathrm{ab}$. Their (anti)commutator relations take on the form

$$\begin{aligned} \left[\frac{\lambda_a}{2}, \frac{\lambda_b}{2}\right] &= i f_{abc} \frac{\lambda_c}{2}, \\ \left\{\frac{\lambda_a}{2}, \frac{\lambda_b}{2}\right\} &= \frac{1}{3}\,\delta_{ab} + i\, d_{abc} \frac{\lambda_c}{2}, \end{aligned} \tag{A.21}$$

where the structure functions f_{abc} are totally antisymmetric whereas the d_{abc} are totally symmetric. The matrices $\lambda_1, \lambda_2, \lambda_3$ form a basis of the $SU(2)$ subalgebra.

A.3 Conventions

As is common in particle physics we will use simple units: setting the speed of light $c = 1$ gives the same dimension to length and time

$$[x] = [t] = \mathrm{fm} = 10^{-15}\,\mathrm{m} \to \mathrm{GeV}^{-1} \tag{A.22}$$

Also setting the unit of action $\hbar = 1$ and using the well-known and easy to remember identity for the Planck constant $197\,\mathrm{Mev\,fm}^{-1} = \hbar c = 1$ yields

$$[E] = [p] = [M] = \mathrm{fm}^{-1} = 0.197\,\mathrm{GeV} \tag{A.23}$$

and simplifies the relation between energy and momentum $E^2 = p^2 + M^2$. An *electron volt* is the energy accumulated by a particle with charge $q = 1e$ after running through a potential difference of 1 V:

$$1\,\mathrm{eV} = 1.602 \cdot 10^{-19}\,\mathrm{J}. \tag{A.24}$$

Our calculations are performed in EUCLIDean space, therefore the scalar product of two 4-vectors takes on the form

$$p \cdot q = p_\mu q^\mu = \vec{p} \cdot \vec{q} + p_4 q_4. \tag{A.25}$$

We will try throughout this work to stick with the following agreement concerning indices: greek indices label 4-vectors and run from 0 to 3 (MINKOWSKI space) or 1 to 4 (EUCLIDean space): $x^\mu = (x^0, \vec{x}) \equiv (t, \vec{x})$ or $x^\mu = (\vec{x}, x^4) \equiv (\vec{x}, \tau) = (\vec{x}, it)$ respectively. Latin letters $a, b, c, ... = 1, ..., 8$ label color indices and finally $i, j, k, ... = 1, ..., 3$ label the components of 3-vectors.

A.3.1 γ-Matrices

DIRAC linearised the relativistic energy momentum relation in his study of the electron. A consequence of this linearisation process were solutions with negative energy which DIRAC addressed to antiparticles first, see e.g. [8, 70, 73]. In order to succeed he defined $\vec{\alpha}$ and β with the properties

$$\left.\begin{array}{c} \alpha_i^2 = \beta^2 = 1 \\ \{\alpha_i, \alpha_j\} = 0\,; \quad i \neq j \end{array}\right\} \{\alpha_i, \alpha_j\} \;=\; 2\,\delta_{ij},$$
$$\text{as well as } \{\alpha_i, \beta\} \;=\; 0 \tag{A.26}$$

which ensured cancellation of the mixed terms. As they didn't commute α_i and β couldn't be scalar numbers but had to be $(n \times n)$ matrices. The lowest possible dimension in which the requirements (A.26) are fullfilled is four. These (4×4) matrices are not unique. In the most commonly used DIRAC-PAULI representation they have the form

$$\vec{\alpha} = \begin{pmatrix} 0 & \vec{\tau} \\ \vec{\tau} & 0 \end{pmatrix}, \quad \beta = \begin{pmatrix} \mathbf{1_2} & 0 \\ 0 & -\mathbf{1_2} \end{pmatrix}, \tag{A.27}$$

$\vec{\tau}$ being the PAULI matrices in (A.14) and $\mathbf{1_2}$ the (2×2) unit matrix. The definition of the γ-matrices like

$$\gamma^0 := \beta; \quad \vec{\gamma} := \beta\vec{\alpha} = \begin{pmatrix} 0 & \vec{\tau} \\ -\vec{\tau} & 0 \end{pmatrix} \quad \Leftrightarrow \quad \gamma^\mu = (\gamma^0, \vec{\gamma}) \tag{A.28}$$

leads to the elegant reformulation of the anticommutator relations $\{\gamma_\mu, \gamma_\nu\} = \gamma_\mu\gamma_\nu + \gamma_\nu\gamma_\mu = -2\delta_{\mu\nu}$ as compared to (A.26).

A.4 Distribution functions

From the spin-statistics theorem we know that bosons, carrying integer spin $n = 0, 1, 2, ...$, are to be described by Bose-Einstein whereas fermions with their spin $(2n + 1)/2$ by Fermi-Dirac distribution functions. We will show quick derivations of the two by introducing creation and annihilation operators[1] $a^\dagger$ and a as well as abstract state vectors $|n\rangle$ of the system with properties

$$\langle n|n'\rangle = \delta_{nn'} \quad \text{orthogonality} \tag{A.29}$$

$$\sum_{n=0}^{\infty} |n\rangle\langle n| = 1 \quad \text{completeness.} \tag{A.30}$$

They form a complete set with the bras $\langle n|$ and kets $|n\rangle$ as row and column vectors in infinite-dimensional vector space.

A.4.1 Bose-Einstein Distribution Function

Let us first consider a non-interacting time-independent single-particle quantum mechanical state occupied by bosons with energy E each. There may be any number of bosons in that state[2]. Acting on a number eigenstate $a^\dagger$ creates a boson (thus all states $|n\rangle$ can be built from the vacuum $|0\rangle$)

$$a^\dagger|n\rangle = (n+1)^{1/2}|n+1\rangle, \qquad |n\rangle = (n!)^{-1/2}(a^\dagger)^n|0\rangle, \tag{A.31}$$

a annihilates one (or the vacuum)

$$a|n\rangle = n^{1/2}|n-1\rangle, \quad a|0\rangle = 0. \tag{A.32}$$

The coefficients follow from the requirement that a and $a^\dagger$ be Hermitian conjugates and that $a^\dagger a$ be the number operator

$$N|n\rangle = a^\dagger a|n\rangle = n|n\rangle. \tag{A.33}$$

The following commutator relation holds for bosons

$$\left[a, a^\dagger\right]_- = aa^\dagger - a^\dagger a = 1 \tag{A.34}$$

Up to an additive constant the Hamiltonian must be $E \cdot N$:

$$H = \frac{E}{2}\left(aa^\dagger + a^\dagger a\right) = E\left(a^\dagger a + \frac{1}{2}\right) = E(N + \frac{1}{2}) \tag{A.35}$$

[1] *the tools commonly known from second quantization [74]*

[2] *This system may be thought of as a quantized simple harmonic oscillator.*

with the zero point energy $E/2$ which can usually be ignored.
As the $|n\rangle$ are number *and* energy eigenstates we can assign a chemical potential to the particles. The partition function is

$$\begin{aligned} \mathcal{Z} &= \mathbf{Tr}\, \exp(-\beta(H-\mu N)) = \sum_{n=0}^{\infty} \langle n|e^{-\beta(E-\mu)N}|n\rangle = \\ &= \sum_{n=0}^{\infty} e^{-\beta(E-\mu)n} = \left[1-e^{-\beta(E-\mu)}\right]^{-1} \end{aligned} \tag{A.36}$$

from which we can derive the mean number of bosons

$$N = T\frac{\partial \ln \mathcal{Z}}{\partial \mu} = -T\frac{\partial}{\partial \mu}\ln\left[1-e^{-\beta(E-\mu)}\right] = \frac{1}{e^{\beta(E-\mu)}-1} = b(E-\mu) \tag{A.37}$$

where we used the definition of the Bose function

$$b(x) = \frac{1}{e^{x/T}-1} \tag{A.38}$$

and summarise some relations of it

$$b(sE) = \frac{s-1}{2} + sb(E),\ s = \pm 1 \tag{A.39}$$

$$b(-x) = -b(x) - 1 \tag{A.40}$$

which will be helpful throughout our calculations.

A.4.2 Fermi-Dirac Distribution Function

The same problem will now be handled with a fermionic degree of freedom. The Pauli exclusion principle forbids occupation of a single-particle state with more than one fermion. The only two states in the system are $|0\rangle$ and $|1\rangle$:

$$\alpha^\dagger|0\rangle = |1\rangle, \quad \alpha|1\rangle = |0\rangle, \quad \alpha^\dagger|1\rangle = |0\rangle, \quad \alpha|0\rangle = 0. \tag{A.41}$$

The fermion creation and annihilation operators have the property that their square is zero $\alpha\alpha = \alpha^\dagger\alpha^\dagger = 0$. They are Hermitian conjugates with $N = \alpha^\dagger\alpha$

$$N|0\rangle = \alpha^\dagger\alpha|0\rangle = 0, \qquad N|1\rangle = \alpha^\dagger\alpha|1\rangle = |1\rangle. \tag{A.42}$$

They satisfy the anti-commutation relation

$$\left\{\alpha, \alpha^\dagger\right\}_+ = \alpha\alpha^\dagger + \alpha^\dagger\alpha = 1 \tag{A.43}$$

The Hamiltonian is

$$H = \frac{1}{2}E\left(\alpha^\dagger\alpha - \alpha\alpha^\dagger\right) = E\left(N - \frac{1}{2}\right) \tag{A.44}$$

This time the zero-point energy is equal in magnitude but opposite in sign. It can be dropped again. As in (A.36) we calculate the partition function but now the sum terminates at $n = 1$

$$\mathcal{Z} = \mathbf{Tr}\, e^{-\beta(H-\mu N)} = \sum_{n=0}^{1}\langle n|e^{-\beta(E-\mu)N}|n\rangle = 1 + e^{-\beta(E-\mu)} \tag{A.45}$$

The mean number of fermions is N ranging from 0 to 1, the mean energy is EN with

$$N = \frac{1}{e^{\beta(E-\mu)}+1} = f(E-\mu) \tag{A.46}$$

where we used the definition of f for the FERMI function

$$f(x) \;=\; \frac{1}{e^{x/T}+1} \tag{A.47}$$

As for b in (A.38f) we state some relations and introduce the abbreviations

$$f_E^\pm = f(E \pm \mu^*); \quad f_i^\pm = f(E_i \pm \mu^*); \quad f_{s_i}^\pm = f(s_i E_i \pm \mu^*) \tag{A.48}$$

$$f(sE+\mu^*) \;=\; \frac{1-s}{2} + sf(E+s\mu^*),\; s = \pm 1 \tag{A.49}$$

$$f(-x) \;=\; 1 - f(x). \tag{A.50}$$

The FERMI function f as well as b are both periodoc

$$\begin{aligned} f(x + 2\pi i T n) &= f(x) \\ b(x + 2\pi i T n) &= b(x) \end{aligned} \tag{A.51}$$

which is a direct yield of the properties of the imaginary exponential function. Another useful relation

$$b(x + i\pi T) = -f(x) \tag{A.52}$$

allows replacement of f with b and vice versa.

A.5 Formula Collection and MATSUBARA frequencies

Decomposition into partial fractions and other helpful relations [75, 76, 77]:

$$\frac{1}{u^2+v^2} = \sum_{s=\pm 1} \frac{s}{2v} \cdot \frac{1}{iu+sv} \tag{A.53}$$

$$\frac{1}{a \cdot b} = \frac{1}{b-a}\left(\frac{1}{a}-\frac{1}{b}\right) \tag{A.54}$$

$$\frac{1}{x+1}\left(1+\frac{1}{y-1}\right) = \frac{1}{x/y+1}\left(\frac{1}{x+1}+\frac{1}{y-1}\right) \tag{A.55}$$

$$\ln\left(x^2+a^2\right) = \int_1^{a^2} \frac{\mathrm{d}\Theta^2}{\Theta^2+x^2} + \ln\left(1+x^2\right) \tag{A.56}$$

$$\sum_{n=-\infty}^{\infty} \frac{1}{(2n+1)^2\pi^2+\Theta^2} = \frac{1}{\Theta}\left(\frac{1}{2}-\frac{1}{\exp(\Theta)+1}\right). \tag{A.57}$$

Taking Derivatives

For the case of differentiating with respect to a variable that appears as the boundary condition of an integral

$$\frac{\mathrm{d}}{\mathrm{d}x}\int_{u(x)}^{v(x)} f(x,t)\mathrm{d}t = v'(x)f(x,v(x)) - u'(x)f(x,u(x)) + \int_{u(x)}^{v(x)} \frac{\partial}{\partial x} f(x,t)\mathrm{d}t \tag{A.58}$$

is a helpful formula.

A.5.1 Direct Summation Of MATSUBARA Frequencies

According to the FEYNMAN rules in thermal field theory the thermal propagators, see (A.8) and (A.9), contain the MATSUBARA frequencies ($n\epsilon\mathbb{Z}$)

$$E_f = (2n+1)\pi T \qquad \text{(fermions)} \tag{A.59}$$

$$E_b = 2n\pi T \qquad \text{(bosons)} \tag{A.60}$$

which have to be summed. These summations of MATSUBARA frequencies can be reformulated such that they resemble the TAYLOR expansion of well-known analytic functions. Their relation to bosons with b from (A.38) is

$$T\sum_{n\epsilon\mathbb{Z}} \frac{1}{2\pi i T n + x} = b(x) + \frac{1}{2} \tag{A.61}$$

$$T\sum_{n\epsilon\mathbb{Z}}\frac{1}{(2\pi iTn+x)(2\pi iTn+y)} = \frac{b(x)-b(y)}{y-x} \quad (A.62)$$

$$T\sum_{n\epsilon\mathbb{Z}}\frac{1}{(2\pi nT-i\mu)^2+E^2} = \frac{1+b(E+\mu)+b(E-\mu)}{2E}. \quad (A.63)$$

For fermions we have

$$T\sum_{n\epsilon\mathbb{Z}}\frac{1}{[(2n+1)i\pi T+x][(2n+1)i\pi T+y]} = \frac{f(x)-f(y)}{x-y} \quad (A.64)$$

$$T\sum_{n\epsilon\mathbb{Z}}\frac{1}{[(2n+1)\pi T-i\mu]^2+E^2} = \frac{-1+f_E^+ + f_E^-}{2E} \quad (A.65)$$

with f from (A.47) and $f_E^\pm$ as in (A.48).

A.6 Contact Interaction Lagrangian

A contact interaction Lagrangian of the form as in (4.28) with an additional term corresponding to $n = 3$ would be

$$\mathcal{L}_3^{ci} = \mathcal{L}_{Dirac}^{\mu} + \frac{G_{\rm v}}{2}\left(\bar\psi\gamma_\mu\psi\right)^2 - \frac{G_{\rm s}}{2}\left(\bar\psi\psi\right)^2 + \frac{G_3'}{3}\left(\bar\psi\psi\right)^3 \quad (A.66)$$

where $\mathcal{L}_{Dirac}^{\mu} = \bar\psi[i\gamma_\mu\partial^\mu - M + \mu\gamma_0]\psi$. (A.66) behaves under the transformation in (4.29) like

$$\begin{aligned}\mathcal{L}_3^{ci} = \mathcal{L}_{Dirac}^{\mu} &+ \frac{G_{\rm v}}{2}\left[\left(\bar\psi\gamma_\mu\psi\right)^2 - 2\bar\psi\gamma_\mu\psi\langle\psi^\dagger\psi\rangle\delta_{\mu 0} + \langle\psi^\dagger\psi\rangle^2\right]\\ &- \frac{G_{\rm s}}{2}\left[\left(\bar\psi\psi\right)^2 - 2\bar\psi\psi\langle\bar\psi\psi\rangle + \langle\bar\psi\psi\rangle^2\right]\\ &+ \frac{G_3'}{3}\left[\left(\bar\psi\psi\right)^3 - 3\left(\bar\psi\psi\right)^2\langle\bar\psi\psi\rangle + 3\left(\bar\psi\psi\right)\langle\bar\psi\psi\rangle^2 - \langle\bar\psi\psi\rangle^3\right].\end{aligned}$$

Neglecting quadratic and higher fluctuations and using (4.31f) this can be written like

$$\begin{aligned}\mathcal{L}_3^{ci} &= \bar\psi\left[i\partial\!\!\!/ - \left(M - G_{\rm s}n_{\rm s} - G_3'n_{\rm s}^2\right) + \left(\mu - G_{\rm v}\rho\right)\gamma_0\right]\psi\\ &\quad + \frac{1}{2}G_{\rm v}\rho^2 - \frac{1}{2}G_{\rm s}n_{\rm s}^2 - \frac{1}{3}G_3'n_{\rm s}^3\end{aligned} \quad (A.67)$$

Reading off again the effective mass M^* from this Lagrangian allows reformulation of the corresponding mass self-consistency equation in the form

$$M - M^* = G_{\rm s}n_{\rm s} + G_3'n_{\rm s}^2 \quad (A.68)$$

which we compare to our improved calculation of the relativistic mean field ansatz with the new term added as in (4.58) with $n = 3$ where the corresponding equation reads

$$M - M^* = G_{\rm s} n_{\rm s} - \frac{G_{\rm s}}{G_3}(M - M^*)^2. \tag{A.69}$$

These two equations are not identical, but in both cases the relation between $(M - M^*)$ and $n_{\rm s}$ is complicated, $M - M^* = G_{\rm s} n_{\rm s}$ as in the relativistic mean field calculation does **not** hold any more!
However, the mean field $\bar{\sigma}$ is still generated from the shift in (quasi) nucleon mass $\bar{\sigma} = (M - M^*)/g_\sigma$. Therefore the equation of state in (4.58) can be derived from a Lagrangian of the form

$$\mathcal{L}_n = \mathcal{L}_W - \frac{1}{3}\lambda_3 \bar{\sigma}^3 \tag{A.70}$$

which is constructed by adding a term $-\lambda_n \bar{\sigma}^n/n$ as that in (4.27) with $n = 3$ to the Walecka Lagrangian $\mathcal{L}_W$ in (4.12). The new term is of the same type as $\mathcal{L}(\bar{\sigma}, \bar{\omega}_0)$, independent of ψ and $\bar{\psi}$, and therefore - as was shown in (4.14) - directly ends up in the pressure $P = P_{\rm FG} + \frac{1}{2} m_\omega^2 \bar{\omega}^2 - \frac{1}{2} m_\sigma^2 \bar{\sigma}^2 - \frac{1}{3}\lambda_3 \bar{\sigma}^3$. Insertion of $\bar{\sigma}$ into our new term allows to recover

$$-\frac{1}{3}\lambda_3 \bar{\sigma}^3 = -\frac{1}{3}\lambda_3 \frac{(M - M^*)^3}{g_\sigma^3} = -\frac{1}{3G_3}(M - M^*)^3 \tag{A.71}$$

the form of the new term as in (4.58) with $G_3 = g_\sigma^3/\lambda_3$.

Appendix B

The Ideal Gas Pressure

The grand canonical partition function $\mathcal{Z}$, see (3.2), represents the most direct access for a statistical treatment of ideal quantum gases.

B.1 Derivation of P_{FG}

In this appendix we will derive the expression for the pressure P_{FG}, see (3.2), of a non-interacting FERMI gas with mass M from the DIRAC Lagrangian

$$\mathcal{L}_{Dirac} \;=\; \bar{\psi}\,(i\not{\partial} - M)\,\psi = \psi^\dagger\gamma^0\left(i\gamma^0\frac{\partial}{\partial t} + i\vec{\gamma}\vec{\nabla} - M\right)\psi \tag{B.1}$$

where $\bar{\psi} = \psi^\dagger\gamma^0$ and

$$i\not{\partial} = i\gamma_\mu\partial^\mu = i\gamma_0\frac{\partial}{\partial t} + i\vec{\gamma}\vec{\nabla} = -\gamma_0\frac{\partial}{\partial \tau} + i\vec{\gamma}\vec{\nabla} \tag{B.2}$$

where in the last step we used $\tau = it \;\Leftrightarrow\; \mathrm{d}t = -i\mathrm{d}\tau$. This will be of use later. The conjugate field to the ordinary field ψ is

$$\Pi \;=\; \frac{\partial\mathcal{L}}{\partial(\partial\psi/\partial t)} = \frac{\partial}{\partial(\partial\psi/\partial t)}\left[i\psi^\dagger\underbrace{\gamma^0\gamma^0}_{=1}\frac{\partial\psi}{\partial t}\right] = i\psi^\dagger \tag{B.3}$$

The standard procedure leads us to the corresponding HAMILTON density

$$\mathcal{H} = \Pi\frac{\partial\psi}{\partial t} - \mathcal{L} = \psi^\dagger\left(i\frac{\partial}{\partial t}\right)\psi - \mathcal{L} = \bar{\psi}(-i\vec{\gamma}\vec{\nabla} + M)\psi. \tag{B.4}$$

If we permit conserved charges then we go over to

$$\mathcal{H}(\Pi,\psi) \to \mathcal{K}(\Pi,\psi) = \mathcal{H}(\Pi,\psi) - \mu N, \tag{B.5}$$

in that case the DIRAC Lagrangian (B.1) can be written as

$$\mathcal{L}_{Dirac} \to \mathcal{L}^{\mu}_{Dirac} = \bar{\psi}\left(i\partial\!\!\!/ - M + \mu\gamma_0\right)\psi \tag{B.6}$$

and the partition function becomes

$$\mathcal{Z}_{FG} = \mathbf{Tr}\, e^{-\beta K} = \mathbf{Tr}\, e^{-\beta(H-\mu N)} = \int \mathrm{d}\psi_\alpha \langle\psi_\alpha| \exp(-\beta(H-\mu N))|\psi_\alpha\rangle. \tag{B.7}$$

In order to be able to calculate the integral appearing here, we will first calculate $\langle\psi_\alpha| \exp(-\beta H)|\psi_\alpha\rangle$ and then perform (B.5). The transition amplitude in going from state ψ_α to state ψ_β after time t_f is $A_{\beta\alpha} = \langle\psi_\beta| \exp -iHt_f|\psi_\alpha\rangle$. In statistical physics we are interested in the case where a system goes back to, or sits in, its original state after time t_f. We will now calculate the corresponding amplitude. Therefore we split the time interval t_f into N time steps $\Delta t = t_f/N$.

$$\begin{aligned} A_{\alpha\alpha} &= \langle\psi_\alpha| \exp(-iHt_f)|\psi_\alpha\rangle = \langle\psi_\alpha| \exp(-iHN\Delta t)|\psi_\alpha\rangle = \\ &= \langle\psi_\alpha| \underbrace{\exp(-iH\Delta t)\ldots\exp(-iH\Delta t)}_{N \text{ times}} |\psi_\alpha\rangle \end{aligned} \tag{B.8}$$

We now insert complete sets of states $\int \mathrm{d}\psi_i|\psi_i\rangle\langle\psi_i| = \mathbf{1}$ at each time interval

$$\begin{aligned} A_{\alpha\alpha} &= \int \langle\psi_\alpha|e^{-iH\Delta t}|\psi_N\rangle\langle\psi_N|e^{-iH\Delta t}|\psi_{N-1}\rangle\langle\psi_{N-1}|e^{-iH\Delta t}|\psi_{N-2}\rangle\cdots \\ &\cdots \langle\psi_2|e^{-iH\Delta t}|\psi_1\rangle\langle\psi_1|\psi_\alpha\rangle\, \mathrm{d}\psi_1\mathrm{d}\psi_2\cdots\mathrm{d}\psi_N \end{aligned} \tag{B.9}$$

as well as for the conjugate states $\int \mathrm{d}\Pi_i/2\pi|\Pi_i\rangle\langle\Pi_i| = \mathbf{1}$ which leads to

$$\begin{aligned} A_{\alpha\alpha} &= \int \prod_{i=1}^{N} \mathrm{d}\psi_i\, \langle\psi_\alpha|\Pi_N\rangle\langle\Pi_N|e^{-iH\Delta t}|\psi_N\rangle\langle\psi_N|\Pi_{N-1}\rangle\cdot \\ &\cdot \langle\Pi_{N-1}|e^{-iH\Delta t}|\psi_{N-1}\rangle\langle\psi_{N-1}|\Pi_{N-2}\rangle\langle\Pi_{N-2}|e^{-iH\Delta t}|\psi_{N-2}\rangle\cdots \\ &\cdots \langle\psi_2|\Pi_1\rangle\langle\Pi_1|e^{-iH\Delta t}|\psi_1\rangle\langle\psi_1|\psi_\alpha\rangle \frac{\mathrm{d}\Pi_1}{2\pi}\frac{\mathrm{d}\Pi_2}{2\pi}\cdots\frac{\mathrm{d}\Pi_N}{2\pi} = \\ &= \int \prod_{i=1}^{N} \frac{\mathrm{d}\psi_i\mathrm{d}\Pi_i}{2\pi} \exp\left(i\int \mathrm{d}^3x\, \Pi_N\psi_{N+1}\right) \exp\left(-i\int \mathrm{d}^3x\, \Pi_N\psi_N\right)\cdot \\ &\cdot \exp\left(-i\Delta t\int \mathrm{d}^3x\, \mathcal{H}(\Pi_N,\psi_N)\right)\cdots\delta(\psi_1-\psi_\alpha). \end{aligned} \tag{B.10}$$

where we have used

$$\langle\psi_{N+1}|\Pi_N\rangle = \exp\left(i\int \mathrm{d}^3x\, \Pi_N(\vec{x})\psi_{N+1}(\vec{x})\right) \tag{B.11}$$

$$\langle\Pi_N|e^{-iH_N\Delta t}|\psi_N\rangle = \langle\Pi_N|\psi_N\rangle e^{-iH_N\Delta t} = \exp\left(-i\int \mathrm{d}^3x\, \Pi_N\psi_N\right) e^{-iH_N\Delta t} \tag{B.12}$$

$$\langle\psi_1|\psi_\alpha\rangle = \delta(\psi_1-\psi_\alpha) \tag{B.13}$$

as well as

$$H_N = \int \mathrm{d}^3x\, \mathcal{H}(\Pi_N, \psi_N) \tag{B.14}$$

and $\psi_{N+1} = \psi_\alpha$. Let us now consider $N \to \infty$:

$$\begin{aligned} A_{\alpha\alpha} &= \langle\psi_\alpha|\exp(-iHt_f)|\psi_\alpha\rangle = \lim_{N\to\infty}\int\prod_{i=1}^{N}\frac{\mathrm{d}\psi_i\mathrm{d}\Pi_i}{2\pi}\delta(\psi_1-\psi_\alpha)\cdot \\ &\quad \cdot\exp\left\{-i\Delta t\sum_{j=1}^{N}\int\mathrm{d}^3x\,\left[\mathcal{H}(\Pi_j,\psi_j)-\Pi_j\frac{\psi_{j+1}-\psi_j}{\Delta t}\right]\right\} = \\ &= \int[\mathrm{d}\Pi]\int_{\psi(\vec{x},0)}^{\psi(\vec{x},t_f)}[\mathrm{d}\psi]\exp\left[i\int_0^{t_f}\mathrm{d}t\int\mathrm{d}^3x\,\left(\Pi\frac{\partial\psi}{\partial t}-\mathcal{H}\right)\right] = \\ &= \int[\mathrm{d}\Pi]\int_{periodic}[\mathrm{d}\psi]\exp\left[\int_0^{\beta}\mathrm{d}\tau\int\mathrm{d}^3x\,\left(i\Pi\frac{\partial\psi}{\partial\tau}-\mathcal{H}\right)\right]. \end{aligned}$$

where we switched to imaginary time $\tau = it$ in the last step. The expression "periodic" on the second integral simply means $\psi_\alpha(\vec{x}) = \psi_\alpha(\vec{x},0) = \psi_\alpha(\vec{x},\beta)$. We can now identify

$$\langle\psi_\alpha|\exp(-\beta H)|\psi_\alpha\rangle = \int[\mathrm{d}\Pi]\int_{per.}[\mathrm{d}\psi]\exp\left[\int_0^{\beta}\mathrm{d}\tau\int\mathrm{d}^3x\left(i\Pi\frac{\partial\psi}{\partial\tau}-\mathcal{H}\right)\right] \tag{B.15}$$

which, after using (B.5), we will insert back into (B.7) to obtain

$$\mathcal{Z}_{FG} = \int[\mathrm{d}\Pi]\int_{per.}[\mathrm{d}\psi]\exp\left[\int_0^{\beta}\mathrm{d}\tau\int\mathrm{d}^3x\left(i\Pi\frac{\partial\psi}{\partial\tau}-\mathcal{H}+\mu N\right)\right]. \tag{B.16}$$

Insertion of $\Pi = i\psi^\dagger$ from (B.3), $\mathcal{H}$ from (B.4) and $N = \psi^\dagger\psi = \bar{\psi}\gamma_0\psi$ yields for the exponent

$$\begin{aligned} &\int_0^{\beta}\mathrm{d}\tau\int\mathrm{d}^3x\left(i^2\psi^\dagger\frac{\partial\psi}{\partial\tau}+\bar{\psi}(i\vec{\gamma}\vec{\nabla}-M+\mu\gamma_0)\psi\right) = \\ &\overset{(B.2)}{=}\int_0^{\beta}\mathrm{d}\tau\int\mathrm{d}^3x\,\bar{\psi}\left(i\not{\partial}-M+\mu\gamma_0\right)\psi. \end{aligned} \tag{B.17}$$

Inserting (B.17) back into (B.16) allows writing

$$\mathcal{Z}_{FG} = \int\left[\mathrm{i}\mathrm{d}\psi^\dagger\right][\mathrm{d}\psi]\exp\left\{\int_0^{\beta}\mathrm{d}\tau\int\mathrm{d}^3x\,\bar{\psi}\left(i\not{\partial}-M+\mu\gamma_0\right)\psi\right\}. \tag{B.18}$$

This path integral will be FOURIER transformed by setting

$$\begin{aligned}
\int \left[\mathrm{i d}\psi^\dagger\right] \int_{per.} [\mathrm{d}\psi] &\rightarrow \prod_n \prod_{\vec{p}} \prod_\alpha \int i\mathrm{d}\tilde{\psi}^\dagger_{\alpha;n}(\vec{p})\psi^\dagger_{\alpha;n}(\vec{p}) \\
\int_0^\beta \mathrm{d}\tau \int \mathrm{d}^3x &\rightarrow \beta \sum_{n,\vec{p}} \\
i\vec{\nabla} &\rightarrow -\vec{p} \\
\frac{\partial}{\partial\tau} &\rightarrow i\omega_f
\end{aligned} \tag{B.19}$$

as well as

$$\psi_\alpha(\vec{x},\tau) = (1/V^{\frac{1}{2}}) \sum_n \sum_{\vec{p}} e^{i(\vec{p}\vec{x}+\omega_f\tau)} \tilde{\psi}_{\alpha;n}(\vec{p}). \tag{B.20}$$

to receive

$$\begin{aligned}
\mathcal{Z}_{FG} &= \prod_n \prod_{\vec{p}} \prod_\alpha \int i\mathrm{d}\tilde{\psi}^\dagger_{\alpha;n}(\vec{p})\psi^\dagger_{\alpha;n}(\vec{p}) \exp\left\{\beta \sum_{n,\vec{p}} e^{-i(\vec{p}\vec{x}+\omega_f\tau)} \tilde{\psi}^\dagger_{\alpha;n}(\vec{p})\gamma_0 \cdot \right. \\
&\cdot \left. \left(-\gamma_0 i\omega_f + \vec{\gamma}\,(-\vec{p}) - M + \mu\gamma_0\right) e^{i(\vec{p}\vec{x}+\omega_f\tau)} \psi_{\alpha;n}(\vec{p})\right\} \\
&= \prod_{n,\vec{p},\alpha} \int i\mathrm{d}\tilde{\psi}^\dagger_{\alpha;n}(\vec{p})\psi^\dagger_{\alpha;n}(\vec{p}) \exp\left\{\sum_{n,\vec{p}} i\tilde{\psi}^\dagger_{\alpha;n}(\vec{p}) \cdot \mathbf{D} \cdot \psi_{\alpha;n}(\vec{p})\right\}
\end{aligned} \tag{B.21}$$

where

$$\mathbf{D} = \left[-i\beta\left((-i\omega_f + \mu) - \gamma_0\vec{\gamma}\vec{p} - M\gamma_0\right)\right]. \tag{B.22}$$

Integrals over (anticommuting) GRASSMANN variables[1] were introduced to be able to deal with path integrals over fermionic coordinates. The integral for our purposes is

$$\int \mathrm{d}\eta_1^\dagger \mathrm{d}\eta_1 \cdots \mathrm{d}\eta_N^\dagger \mathrm{d}\eta_N \exp(\eta^\dagger D\eta) = \mathbf{det}\,\mathbf{D}, \tag{B.23}$$

which simplifies our partition function further

$$\mathcal{Z}_{FG} = \mathbf{det}\,\mathbf{D} \tag{B.24}$$

where $\mathbf{D}$ is a 4×4 matrix

[1] *they're connected to* PAULI*'s exclusion principle and the spin-statistics theorem, see A.4.2*

of the form

$$\begin{aligned}\mathcal{Z}_{FG} &= \mathbf{det}\,\beta\cdot \\ &\cdot\begin{pmatrix} -\omega_f - i\mu + iM & 0 & ip_z & ip_x - p_y \\ 0 & -\omega_f - i\mu + iM & ip_x + p_y & -ip_z \\ ip_z & ip_x - p_y & -\omega_f - i\mu - iM & 0 \\ ip_x + p_y & -ip_z & 0 & -\omega_f - i\mu - iM \end{pmatrix} = \\ &= \prod_n \prod_{\vec{p}} \beta^4 \left(M^2 + \vec{p}^{\,2} - \mu^2 + 2i\omega_f\mu + \omega_f^2\right)^2 \end{aligned} \tag{B.25}$$

In addition to the DIRAC indices (4×4) we also have to take into account the momentum and frequency space. The matrix $\mathbf{D}$ is quasi ∞-dimensional and diagonal in these spaces. This leads to the products over n and $\vec{p}$ in (B.25). Let us take the logarithm of this expression

$$\begin{aligned}\ln \mathcal{Z}_{FG} &= \ln \prod_{n,\vec{p}} \beta^4 \left(M^2 + \vec{p}^{\,2} - \mu^2 + 2i\omega_f\mu + \omega_f^2\right)^2 = \\ &= 2\sum_{n,\vec{p}} \ln \beta^2 \left(M^2 + \vec{p}^{\,2} - \mu^2 + 2i\omega_f\mu + \omega_f^2\right) = \\ &= 2\sum_{n,\vec{p}} \ln \left\{\beta^2 \left[(\omega_f + i\mu)^2 + E^2\right]\right\} = \qquad \left| E = \sqrt{M^2 + \vec{p}^{\,2}} \right. \\ &= \sum_{n,\vec{p}} \ln \left\{\beta^2 \left[(\omega_f + i\mu)^2 + E^2\right]\right\}^2 = \\ &= \sum_{n,\vec{p}} \ln \left\{\beta^4 \left[(\omega_f + i\mu)^2 + E^2\right] \left[(\omega_f + i\mu)^2 + E^2\right]^*\right\} = \\ &= \sum_{n,\vec{p}} \ln \left\{\beta^4 \left[(\omega_f + i\mu)^2 + E^2\right] \left[(\omega_f - i\mu)^2 + E^2\right]\right\} = \\ &= \sum_{n,\vec{p}} \ln \Big\{ \beta^4 \left[(\omega_f + i(\mu + E))(\omega_f - i(\mu + E)) \cdot \right. \\ &\qquad \left. \cdot\, (\omega_f - i(\mu - E))(\omega_f + i(\mu - E))\right] \Big\} = \\ &= \sum_{n,\vec{p}} \left\{\ln \left[\beta^2 \left(\omega_f^2 + (E - \mu)^2\right)\right] + \ln \left[\beta^2 \left(\omega_f^2 + (E + \mu)^2\right)\right]\right\}. \end{aligned} \tag{B.26}$$

In the following we will insert ω_f from (A.59) which causes the antiperiodicity of the fermion fields in imaginary time. We will also make use of the equations (A.56) and (A.57) to rewrite (B.26) in the following form:

$$\begin{aligned}
&\sum_{n,\vec{p}} \ln\left[\beta^2\left(\omega_f^2+(E\pm\mu)^2\right)\right] = \sum_{n,\vec{p}} \ln\left[(2n+1)^2\pi^2+\beta^2\left(E\pm\mu\right)^2\right] = \\
= &\sum_{\vec{p}} \int_1^{\beta^2(E\pm\mu)^2} \sum_{n=-\infty}^{\infty} \frac{1}{(2n+1)^2\pi^2+\Theta^2} \mathrm{d}\Theta^2 + \ln\left[1+(2n+1)^2\pi^2\right] = \\
= &\sum_{\vec{p}} \int_1^{\beta^2(E\pm\mu)^2} \frac{1}{\Theta}\left(\frac{1}{2}-\frac{1}{e^{\Theta}+1}\right)\mathrm{d}\Theta^2 = \\
= &\sum_{\vec{p}} \int_1^{\sqrt{\beta^2(E\pm\mu)^2}} \frac{1}{\Theta}\left(\frac{1}{2}-\frac{1}{e^{\Theta}+1}\right)2\Theta\mathrm{d}\Theta = \\
= &\sum_{\vec{p}} \int_1^{\pm\beta(E\pm\mu)} 1-\frac{2}{e^{\Theta}+1}\mathrm{d}\Theta = \left[x-2\ln\left(e^x+1\right)\right]_1^{\pm\beta(E\pm\mu)} \qquad \text{(B.27)}
\end{aligned}$$

where we have dropped the term independent of β and μ in the second step because the partition function is only defined up to an arbirtary constant. Thermodynamical quantities are independent of the choice of this constant. If we drop more such terms in the following we will do so without further notice!

$$\begin{aligned}
\ln \mathcal{Z}_{FG} &= \sum_{\vec{p}} -2\beta E + 2\ln\left(e^{\beta(E+\mu)}+1\right) + 2\ln\left(e^{\beta(E-\mu)}+1\right) = \\
&= 2V\int \frac{\mathrm{d}^3p}{(2\pi)^3}\,\beta E + \ln\left(1+e^{-\beta(E-\mu)}\right) + \ln\left(1+e^{-\beta(E+\mu)}\right) \qquad \text{(B.28)}
\end{aligned}$$

allows reading off directly the pressure $P_{FG} = N_f T/V \cdot \ln \mathcal{Z}_{FG}$ we wanted which can be written as

$$P_{FG} = 4T\int \frac{\mathrm{d}^3p}{(2\pi)^3}\,\ln\left(1+e^{-\beta(E-\mu)}\right) + \ln\left(1+e^{-\beta(E+\mu)}\right) \qquad \text{(B.29)}$$

where the number of flavors $N_f = 2$ is taken into account explicitly. Using partial integration $\int u'v = [uv] - \int uv'$ we find

$$\frac{2T}{\pi^2}\int \mathrm{d}p\, \underbrace{p^2}_{=u'} \underbrace{\ln\left(1+e^{-\beta(\sqrt{p^2+M^2}\pm\mu)}\right)}_{=v} = 2T\left[\frac{1}{3}p^3\cdot v\right]_0^{\infty} - 2T\int \frac{\mathrm{d}p}{\pi^2}\frac{1}{3}p^3\frac{-\beta p}{E}f_E^{\pm}$$

It is easily checked that the first term on the righthand side vanishes.
After changing the integration variable from p to E in (B.29) P_{FG} can be written in the following compact way

$$P_{FG} = \frac{2}{3\pi^2}\int_M^{\infty} \mathrm{d}E\left(E^2-M^2\right)^{3/2}\left[f_E^- + f_E^+\right]. \qquad \text{(B.30)}$$

In the next section we will take the derivatives of this term.

B.2 Derivatives of P_{FG}

In this section we will replace the baryon mass M and chemical potential μ in (B.29) and (B.30) with the corresponding quantities of a quasi nucleon M^*, μ^*.

$$\begin{aligned} P_{FG} &= 4T \int \frac{\mathrm{d}^3 p}{(2\pi)^3} \ln\left(1 + e^{-\beta(\sqrt{p^2+M^{*2}}-\mu^*)}\right) + \ln\left(1 + e^{-\beta(\sqrt{p^2+M^{*2}}+\mu^*)}\right) \\ &= \frac{2}{3\pi^2} \int_{M^*}^{\infty} \mathrm{d}E \left(E^2 - M^{*2}\right)^{3/2} \left[f_E^- + f_E^+\right] \end{aligned} \tag{B.31}$$

with $f_E^{\pm}$ this time from (A.48).
In order to be able to calculate the scalar and baryon densities (4.41) and (4.42) in the various stages of our model we need to take the derivatives of P_{FG} with respect to M^* and μ^*, that is $n_\mathrm{s} = -\partial P_{FG}/\partial M^*$ and $\rho = \partial P_{FG}/\partial \mu^*$. Taking these derivatives - which is more easily performed using the first term in (B.31) - yields

$$n_\mathrm{s} = 4 \int \frac{\mathrm{d}^3 p}{(2\pi)^3} \frac{M^*}{E} \left[f_E^- + f_E^+\right] \tag{B.32}$$

$$\rho = 4 \int \frac{\mathrm{d}^3 p}{(2\pi)^3} \left[f_E^- - f_E^+\right] \tag{B.33}$$

for the densities.

Appendix C

Pion Exchange Diagrams

In this appendix we present the detailed calculation of the FEYNMAN diagrams appearing throughout this work. The first part C.1 will be concerned with the 1π-exchange FOCK term. It will be organised such that its first subsection contains the actual derivation of the pressure contribution of the diagram whereas the second subsection contains a summary of the various derivatives taken. The latter being important in calculating the corresponding contributions to the related thermodynamical quantities, see section 3.1. The second part C.2 only represents a derivation of the ansatz for the leading 2π-exchange diagram.

The reader only interested in the final results can skip most of the text and proceed to (C.25) and (4.88) for the 1- and 2-pion exchange pressure contributions respectively.

C.1 The 1π-exchange Fock Term

In this section we will perform the detailed calculation of the pressure term $P_{1\pi}$ of the following 1-pion exchange diagram

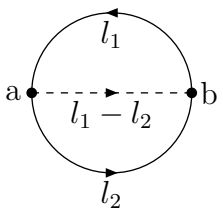

(C.1)

in EUCLIDean space using the Feynman rules summarised in Appendix A.1.

C.1.1 Calculation of $P_{1\pi}$

Starting with the vertex labelled a and going around anti-clockwise[1] we pick up these terms ($\not{q} = \not{l}_1 - \not{l}_2$)

$$\begin{aligned}
&\frac{-ig_A \not{q}\gamma_5\tau^a}{2f_\pi}\frac{M-\not{l}_2}{M^2+l_2^2}\frac{-ig_A(-\not{q})\gamma_5\tau^b}{2f_\pi}\frac{M-\not{l}_1}{M^2+l_1^2}\frac{1}{{m_\pi}^2+q^2} = \\
&\qquad\qquad (M+\not{l}_2)\overbrace{\gamma_5\gamma_5}^{=1}(\not{l}_1-\not{l}_2) \\
= \quad &\frac{-g_A^2}{4f_\pi^2}\tau^a\tau^b\frac{(\not{l}_1-\not{l}_2)\overbrace{\gamma_5(M-\not{l}_2)(\not{l}_2-\not{l}_1)\gamma_5}(M-\not{l}_1)}{[M^2+l_2^2][M^2+l_1^2][{m_\pi}^2+(l_1-l_2)^2]}
\end{aligned} \tag{C.2}$$

As mentioned in (A.5) we also have to consider the closed fermion loop with its minus sign and trace as well as the summations and integrations in (A.6). The pion at a must be the same as the one at b thus we add a δ_{ab}. Using (A.15) to perform the isospin trace and adding the symmetry factor (A.2) - which is 1/2 - the ansatz for the **full** pressure contribution of the diagram in (C.1) can be written as

$$\begin{aligned}
P_{1\pi}^{\mathbf{f}} \quad = \quad &\frac{g_A^2}{8f_\pi^2}\underbrace{\overset{\text{Isospin}}{\mathbf{tr}\tau^a\tau^b\delta^{ab}}}_{=6}T^2\sum_{n_1,n_2}\int\frac{\mathrm{d}^3l_1}{(2\pi)^3}\int\frac{\mathrm{d}^3l_2}{(2\pi)^3} \\
&\frac{\mathbf{tr}(\not{l}_1-\not{l}_2)(M^*+\not{l}_2)(\not{l}_1-\not{l}_2)(M^*-\not{l}_1)}{[{M^*}^2+l_1^2][{M^*}^2+l_2^2][{m_\pi}^2+(l_1-l_2)^2]}
\end{aligned} \tag{C.3}$$

Using (A.10) and (A.11) we will first calculate the trace of the numerator in the integrand where every second term vanishes due to the fact that the trace over an odd number of momenta is zero

$$\begin{aligned}
&\frac{1}{4}\mathbf{tr}(\not{l}_1-\not{l}_2)(M^*+\not{l}_2)(\not{l}_1-\not{l}_2)(M^*-\not{l}_1) = \\
= \quad &-M^*\left(l_1^2+l_2^2-l_1l_2\left(l_1^2+l_2^2\right)\right)-{M^*}^2(l_1-l_2)^2 = \\
= \quad &-\left({M^*}^2-l_1l_2\right)(l_1-l_2)^2 = \\
= \quad &\left({M^*}^2+l_1^2\right)l_2\,(l_2-l_1)+\left({M^*}^2+l_2^2\right)l_1\,(l_1-l_2)+ \\
&\qquad +2{M^*}^2\left[{m_\pi}^2-\left({m_\pi}^2+(l_1-l_2)^2\right)\right]
\end{aligned} \tag{C.4}$$

On first sight the expansion in the last line might cause astonishment but considering this to be an integrand proves worth writing it in this form. Because

[1] *the order of γ matrices does matter*

then the first two terms are linear in $(l_1 - l_2)$. Thus they integrate to zero leaving us with

$$P_{1\pi}^{\mathrm{f}} = \frac{3T^2 g_A^2}{f_\pi^2} \sum_{n_1,n_2} \int \frac{\mathrm{d}^3 l_1 \mathrm{d}^3 l_2 \quad 2M^{*2}\left[{m_\pi}^2 - ({m_\pi}^2 + (l_1 - l_2)^2)\right]}{(2\pi)^6 \underbrace{[M^{*2} + l_1^2][M^{*2} + l_2^2][{m_\pi}^2 + (l_1 - l_2)^2]}} \\ \frac{2M^{*2}{m_\pi}^2}{[M^{*2} + l_1^2][M^{*2} + l_2^2][{m_\pi}^2 + (l_1 - l_2)^2]} - \frac{2M^{*2}}{[M^{*2} + l_1^2][M^{*2} + l_2^2]}$$

(C.5)

Let us write this in the form

$$P_{1\pi}^{\mathrm{f}} = 6\frac{g_A^2 M^{*2}}{f_\pi^2}\left[{m_\pi}^2 A(m_\pi) - \Delta_N^2\right] =: P_{1\pi} + P_\Delta \tag{C.6}$$

with

$$\begin{aligned} A(m_\pi) &= \sum_{n_1,n_2} \int \frac{\mathrm{d}^3 l_1 \mathrm{d}^3 l_2}{(2\pi)^6} \frac{T^2}{[M^{*2} + l_1^2][M^{*2} + l_2^2][{m_\pi}^2 + (l_1 - l_2)^2]} \\ \Delta_N^2 &= \sum_{n_1,n_2} \int \frac{\mathrm{d}^3 l_1 \mathrm{d}^3 l_2}{(2\pi)^6} \frac{T^2}{[M^{*2} + l_1^2][M^{*2} + l_2^2]} \end{aligned} \tag{C.7}$$

and let us investigate them one after the other starting with the second and simpler one. It is obviously of the contact interaction type as the terms introduced in section 4.1.3. Its effects can thus be absorbed into readjustment of the parameters $G_{\mathrm{s,v}}$. Nevertheless we will have a closer look at it. The first thing one recognises is the fact that it is not necessary to integrate and sum twice as it will have the same effect to work with

$$\Delta_N^2 = T^2 \sum_{n\epsilon\mathbb{Z}} \int \frac{\mathrm{d}^3 l}{(2\pi)^3} \frac{1}{\left(M^2 + l^2\right)^2} \Leftrightarrow \Delta_N = T \sum_{n\epsilon\mathbb{Z}} \int \frac{\mathrm{d}^3 l}{(2\pi)^3} \frac{1}{M^2 + l^2} \tag{C.8}$$

The order of summation and integration should not bother us. Remembering the form of the nucleon propagator, the corresponding Matsubara function in (A.8) and using $E^2 = M^{*2} + \vec{l}^2$ we can write

$$\begin{aligned}
\Delta_N &= T\int\frac{\mathrm{d}^3l}{(2\pi)^3}\sum_{n\epsilon\mathbb{Z}}\frac{1}{E^2+[\pi T(2n+1)-i\mu]^2} \\
&\overset{(A.53)}{=} T\int\frac{\mathrm{d}^3l}{(2\pi)^3}\sum_{n}\sum_{s=\pm1}\frac{s}{2E}\frac{1}{i\pi T(2n+1)+\mu+sE} \\
&\overset{(A.61)}{=} \int\frac{\mathrm{d}^3l}{(2\pi)^3}\frac{1}{2E}\left[b(i\pi T+\mu^*+E)-b(i\pi T+\mu^*-E)\right] \\
&= \int_0^\infty\frac{\mathrm{d}p\,p^2}{2\pi^2}\frac{1}{2E}\left[f(\mu^*-E)-f(\mu^*+E)\right] \\
&\overset{(A.50)}{=} \frac{1}{4\pi^2}\int_{M^*}^\infty\mathrm{d}E\sqrt{E^2-M^{*2}}\left[1-f(E-\mu^*)-f(E+\mu^*)\right] \\
&\to \frac{1}{4\pi^2}\int_{M^*}^\infty\mathrm{d}E\sqrt{E^2-M^{*2}}\left[f(E-\mu^*)-f(E+\mu^*)\right]. \qquad \text{(C.9)}
\end{aligned}$$

The factor of one in the last step vanishes due to nucleon mass renormalisation. The corresponding renormalised pressure contribution then takes on the form

$$P_\Delta^{\mathrm{ren}} = -6g_{\pi N}^2\Delta_N^2 = -\frac{g_{\pi N}^2}{8\pi^4}\left\{\int_{M^*}^\infty\mathrm{d}E\sqrt{E^2-M^{*2}}\left[f_E^- - f_E^+\right]\right\} \qquad \text{(C.10)}$$

where we use the abbreviation for the Fermi function stated in (A.48). The pion nucleon coupling constant $g_{\pi N} = 12.9$ is given in (2.63). The step from solutions of the self-consistent mass equation to values of the baryon density is highly non-trivial. Explicitly taking the contribution P_Δ^{ren} into account leads to negative values of the baryon density and makes physical discussion impossible. Therefore we neglect this term.
Let us now have a look at the first term $P_{1\pi} = 6g_A^2M^{*2}{m_\pi}^2A(m_\pi)/f_\pi^2$ where we start again using (A.8) and (A.9) respectively on $A(m_\pi)$ from (C.7):

$$\begin{aligned}
A(m_\pi) &= T\sum_{n_1\epsilon\mathbb{Z}}T\sum_{n_2\epsilon\mathbb{Z}}\iint\frac{\mathrm{d}^3l_1}{(2\pi)^3}\frac{\mathrm{d}^3l_2}{(2\pi)^3}\left\{\left[E_1^2+(\pi T(2n_1+1)-i\mu^*)^2\right]\cdot\right. \\
&\quad\left.\cdot\left[E_2^2+(\pi T(2n_2+1)-i\mu^*)^2\right]\cdot\left[E_3^2+(2\pi T(n_1-n_2))^2\right]\right\}^{-1}
\end{aligned} \qquad \text{(C.11)}$$

with the energies $E_i = \sqrt{M^{*2}+\vec{l}_i^{\,2}}, \quad i=1,2$ and

$$E_3 = \sqrt{{m_\pi}^2+\vec{l}_3^{\,2}}; \quad \vec{l}_3 = \vec{l}_1 - \vec{l}_2. \qquad \text{(C.12)}$$

Comparing with the vector identity of the scalar product

$$\vec{l}_1 \cdot \vec{l}_2 = |\vec{l}_1||\vec{l}_2|x$$

where $x = \cos\angle(\vec{l}_1, \vec{l}_2)$ which we use evaluating E_3^2

$$\begin{aligned} E_3^2 &= {m_\pi}^2 + (\vec{l}_1 - \vec{l}_2)^2 = {m_\pi}^2 + E_1^2 + E_2^2 - 2M^{*2} - 2x|\vec{l}_1||\vec{l}_2| \\ E_3 \mathrm{d}E_3 &= -|\vec{l}_1||\vec{l}_2|\mathrm{d}x; \qquad E_i \mathrm{d}E_i = |\vec{l}_i|\mathrm{d}l_i = l_i \mathrm{d}l_i, \quad i = 1,2 \end{aligned} \tag{C.13}$$

we can understand how one can directly perform two of the l_1-integrations but only one of the l_2-integrations as they are not independent

$$\begin{aligned} \int_0^\infty \frac{\mathrm{d}^3 l_1 \mathrm{d}^3 l_2}{(2\pi)^6} &= \frac{1}{(2\pi)^6} \int_0^\infty \mathrm{d}l_1 \, |\vec{l}_1| 4\pi \int_0^\infty \mathrm{d}l_2 \, |\vec{l}_2| 2\pi \int_{-1}^{+1} \mathrm{d}x |\vec{l}_1||\vec{l}_2| \\ &\overset{(C.13)}{=} \frac{1}{8\pi^4} \int_{M^*}^\infty \mathrm{d}E_1 \, E_1 \int_{M^*}^\infty \mathrm{d}E_2 \, E_2 \int_{E_3^-}^{E_3^+} \mathrm{d}E_3 \, E_3 \end{aligned} \tag{C.14}$$

where $E_3^\pm = \sqrt{{m_\pi}^2 + \left(\sqrt{E_1^2 - M^{*2}} \pm \sqrt{E_2^2 - M^{*2}}\right)^2} = E_3(x = \mp 1)$. Note the sign in the last step! Let us now replace the integrations

$$A(m_\pi) = \frac{1}{8\pi^4} \int_{M^*}^\infty \mathrm{d}E_1 \int_{M^*}^\infty \mathrm{d}E_2 \int_{E_3^-}^{E_3^+} \mathrm{d}E_3 \, \mathcal{S} \tag{C.15}$$

where $S = S(E_1, E_2, E_3)$ takes on the form

$$\begin{aligned} \mathcal{S} &= T \sum_{n_1 \epsilon \mathbb{Z}} T \sum_{n_2 \epsilon \mathbb{Z}} \frac{E_1}{E_1^2 + (\pi T(2n_1+1) - i\mu^*)^2} \\ &\quad \cdot \frac{E_2}{E_2^2 + (\pi T(2n_2+1) - i\mu^*)^2} \cdot \frac{E_3}{E_3^2 + (2\pi T(n_1 - n_2))^2} \overset{(A.53)}{=} \\ &= T^2 \sum_{n_1, n_2} \sum_{s_1 = \pm 1} \frac{s_1}{2E_1} \frac{E_1}{i(\pi T(2n_1+1) - i\mu^*) + s_1 E_1} \sum_{s_2 = \pm 1} \frac{s_2}{2E_2} \cdot \\ &\quad \cdot \frac{E_2}{i(\pi T(2n_2+1) - i\mu^*) + s_2 E_2} \sum_{s_3 = \pm 1} \frac{s_3}{2E_3} \frac{E_3}{i(2\pi T(n_1 - n_2)) + s_3 E_3} = \\ &= \left(\frac{1}{2}\right)^3 \sum_{s_1, s_2, s_3} T \sum_{n_1} \frac{s_1}{h_1 + \mu^* + s_1 E_1}; \quad h_i = i\pi T(2n_i + 1) \\ &\quad T \sum_{n_2} \frac{s_2}{h_2 + \mu^* + s_2 E_3} \cdot \frac{-s_3}{2\pi i T n_2 - 2\pi i T n_1 - s_3 E_3} \end{aligned}$$

This can be simplified further

$$\begin{aligned}\mathcal{S} &\overset{(A.54)}{=} \frac{1}{8}\sum_{s_1,s_2,s_3} T\sum_{n_1}\frac{s_1}{h_1+\mu^*+s_1E_1}\frac{s_2s_3}{h1+\mu^*+s_2E_2+s_3E_3} \\ &\quad \underbrace{\left(T\sum_{n_2}\frac{1}{h_2+\mu^*+s_2E_2}\right.}_{\overset{(A.61)}{=} b(\mu^*+s_2E_2+i\pi T)+\frac{1}{2}} \underbrace{\left.-T\sum_{n_2}\frac{1}{2\pi iTn_2-2\pi iTn_1-s_3E_3}\right)}_{\overset{(A.61,A.40,A.51)}{=} b(s_3E_3)+1-\frac{1}{2}} \\ &\overset{(A.52)}{=} -f(\mu^*+s_2E_2)+\frac{1}{2}\end{aligned} \tag{C.16}$$

Using (A.54) again on the summation over n_1 above and performing the same tricks we can tranform the first part of (C.16) into

$$\begin{aligned}&T\sum_{n_1}\frac{s_1}{h_1+\mu^*+s_1E_1}\frac{s_2s_3}{h1+\mu^*+s_2E_2+s_3E_3} = \\ &\frac{s_1s_2s_3}{s_2E_2+s_3E_3-s_1E_1}\Big(f(\mu^*+s_2E_2+s_3E_3)-f(\mu^*+s_1E_1)\Big)\end{aligned}$$

therefore $\mathcal{S}$ becomes

$$\begin{aligned}\mathcal{S} &= \frac{1}{8}\sum_{s_1,s_2,s_3}\frac{s_1s_2s_3}{s_2E_2+s_3E_3-s_1E_1}\Big(b(-s_3E_3)+f(\mu^*+s_2E_2)\Big)\cdot \\ &\quad \cdot\Big(f(\mu^*+s_1E_1)-f(\mu^*+s_2E_2+s_3E_3)\Big)\end{aligned} \tag{C.17}$$

It does not make sense to mix nucleon and pion energies. Thus it is preferable to only have single energies as arguments in the various distribution functions. Insertion of $x=\exp[(s_2E_2+\mu^*)/T]$ and $y=(-s_3E_3/T)$ into (A.55) proves the identity

$$\begin{aligned}&f(\mu^*+s_2E_2+s_3E_3)[f(s_2E_2+\mu^*)+b(-s_3E_3)] = \\ &= f(s_2E_2+\mu^*)[1+b(-s_3E_3)]\end{aligned}$$

This together with (C.17) inserted into (C.15) yields

$$\begin{aligned}A(m_\pi) &= \frac{1}{64\pi^4}\int_{M^*}^{\infty}\mathrm{d}E_1\int_{M^*}^{\infty}\mathrm{d}E_2\int_{E_3^-}^{E_3^+}\mathrm{d}E_3\sum_{s_1,s_2,s_3}\frac{s_1s_2s_3}{s_1E_1-s_2E_2+s_3E_3}\cdot \\ &\quad \cdot\Big[f^+_{s_1}f^+_{s_2}+f^+_{s_1}b(s_3E_3)+f^+_{s_2}b(-s_3E_3)\Big]\end{aligned} \tag{C.18}$$

where we have used the fact that it does not make a difference to the sum if we replace $s_3 \to -s_3$ with the abbreviation (A.48). It is now time to collect terms

$$\sum_{s_1,s_2,s_3} \frac{s_1 s_2 s_3}{s_1 E_1 - s_2 E_2 + s_3 E_3} \Big[f_{s_1}^+ f_{s_2}^+ + f_{s_1}^+ b(s_3 E_3) + f_{s_2}^+ b(-s_3 E_3) \Big] =$$
$$= \frac{h^{++}}{E_1+E_2+E_3} + \frac{h^{+-}}{E_1-E_2+E_3} + \frac{h^{-+}}{-E_1+E_2+E_3} + \frac{h^{--}}{-E_1-E_2+E_3} \tag{C.19}$$

where the $h^{s_1 s_2}$ contain the distribution functions

$$\begin{aligned} h^{++} &= -(1-f_1^-)f_2^+ - (1-f_1^-)(-1-b(E_3)) - f_2^+ b(E_3) \\ &\quad -f_1^+(1-f_2^-) - f_1^+ b(E_3) - (1-f_2^-)(-1-b(E_3)) \\ &= f_1^+ f_2^- + f_1^- f_2^+ - [f_1^+ + f_1^- + f_2^+ + f_2^-] b(E_3) \\ &\quad + \underbrace{2}_{\text{vacuum}} + \underbrace{2b(E_3)}_{\text{pion}} - \underbrace{[f_1^+ + f_1^- + f_2^+ + f_2^-]}_{\text{nucleon}} \end{aligned}$$

and some vacuum as well as pion and nucleon mass renormalisation terms. In very compact form the $h^{s_1 s_2}$ can be written as

$$\begin{aligned} h^{++} &= f_1^+ f_2^- + f_1^- f_2^+ - [f_1^+ + f_1^- + f_2^+ + f_2^-] b(E_3) + ... \\ h^{+-} &= f_1^+ f_2^+ + f_1^- f_2^- + [f_1^+ + f_1^- - f_2^+ - f_2^-] b(E_3) - f_1^+ - f_2^- \\ h^{-+} &= f_1^+ f_2^+ + f_1^- f_2^- + [f_2^+ + f_2^- - f_1^+ - f_1^-] b(E_3) - f_1^+ - f_1^- \\ h^{--} &= f_1^+ f_2^- + f_1^- f_2^+ + [f_1^+ + f_1^- - f_2^+ + f_2^-] b(E_3) - 2b(E_3) \end{aligned}$$

where the last terms can be ommitted - due to renormalisation - as mentioned above. Collecting like terms again, e.g. the ones containing $f_1^+ f_2^- + f_1^- f_2^+$ which appear in h^{++} and h^{--} lead to

$$\frac{1}{E_1+E_2+E_3} + \frac{1}{-E_1-E_2+E_3} = \frac{2E_3^2}{E_3^2-(E_1+E_2)^2} \tag{C.20}$$

and allow us to write after analogous treatment of the other terms

$$P_{1\pi} = \overbrace{\frac{3 g_A^2 {m_\pi}^2}{(2\pi)^4 f_\pi^2}}^{=:\,\xi} M^{*2} \int_{M^*}^{\infty} \mathrm{d}E_1 \int_{M^*}^{\infty} \mathrm{d}E_2 \int_{E_3^-}^{E_3^+} \mathrm{d}E_3 \cdot$$
$$\cdot \Bigg\{ \frac{E_3}{E_3^2-(E_1+E_2)^2} \Big[f_1^+ f_2^- + f_1^- f_2^+ \Big] + \frac{E_3}{E_3^2-(E_1-E_2)^2} \Big[f_1^+ f_2^+ + f_1^- f_2^- \Big]$$
$$+ \frac{(E_1+E_2) b(E_3)}{E_3^2-(E_1+E_2)^2} \Big[f_1^+ + f_1^- + f_2^+ + f_2^- \Big] + \frac{(E_2-E_1) b(E_3)}{E_3^2-(E_1-E_2)^2} \Big[f_1^+ + f_1^- - f_2^+ - f_2^- \Big] \Bigg\} \tag{C.21}$$

where the factors of 2 have been absorbed in the prefactor and $E_3^{\pm}$ as defined above after (C.14). We can still use the (anti)symmetric character of these terms to simplify

$$\begin{aligned} P_{1\pi} &= \xi M^{*2} \int_{M^*}^{\infty} \mathrm{d}E_1 \int_{M^*}^{\infty} \mathrm{d}E_2 \int_{E_3^-}^{E_3^+} \mathrm{d}E_3 \\ &\Bigg\{ \frac{E_3}{E_3^2-(E_1+E_2)^2} 2 f_1^+ f_2^- + \frac{E_3}{E_3^2-(E_1-E_2)^2}\Big[f_1^+ f_2^+ + f_1^- f_2^-\Big] \\ &+ \left[\frac{(E_1+E_2)}{E_3^2-(E_1+E_2)^2} + \frac{(E_2-E_1)}{E_3^2-(E_1-E_2)^2}\right] 2b(E_3)\Big[f_1^+ + f_1^-\Big]\Bigg\} \end{aligned} \tag{C.22}$$

where we can see that the E_3-integration is possible analytically for the first two integrations but becomes complicated in the last term due to the E_3-dependence of the appearing Bose distribution function. Instead we will perform the E_2-integration in the latter case thus rewriting

$$\begin{aligned} P_{1\pi} &= \xi M^{*2} \Bigg\{ \int_{M^*}^{\infty} \mathrm{d}E_1 \int_{M^*}^{\infty} \mathrm{d}E_2\, 2\Big[f_1^+ f_2^-\Big] \int_{E_3^-}^{E_3^+} \mathrm{d}E_3 \frac{E_3}{E_3^2-(E_1+E_2)^2} \\ &+ \int_{M^*}^{\infty} \mathrm{d}E_1 \int_{M^*}^{\infty} \mathrm{d}E_2 \Big[f_1^+ f_2^+ + f_1^- f_2^-\Big] \int_{E_3^-}^{E_3^+} \mathrm{d}E_3 \frac{E_3}{E_3^2-(E_1-E_2)^2} \\ &+ \int_{M^*}^{\infty} \mathrm{d}E_1 \int_{m_\pi}^{\infty} \mathrm{d}E_3\, 2b(E_3)\Big[f_1^+ + f_1^-\Big] \int_{E_2^-}^{E_2^+} \mathrm{d}E_2 \\ &\quad \left[\frac{(E_1+E_2)}{E_3^2-(E_1+E_2)^2} + \frac{(E_2-E_1)}{E_3^2-(E_1-E_2)^2}\right]\Bigg\} \end{aligned} \tag{C.23}$$

with $E_2^{\pm} = \sqrt{M^{*2} + \left(\sqrt{E_1^2 - M^{*2}} \pm \sqrt{E_3^2 - {m_\pi}^2}\right)^2}$. Performing these integrations analytically $\left(\vec{l}_{1,2} = \sqrt{E_{1,2}^2 - M^{*2}};\quad \vec{l}_3 = \sqrt{E_3^2 - {m_\pi}^2}\right)$

$$\int_{E_3^-}^{E_3^+} \mathrm{d}E_3 \frac{E_3}{E_3^2-(E_1 \mp E_2)^2} = \frac{1}{2}\ln\frac{{m_\pi}^2/2 - M^{*2} + \vec{l}_1\vec{l}_2 \pm E_1E_2}{{m_\pi}^2/2 - M^{*2} - \vec{l}_1\vec{l}_2 \pm E_1E_2} =: \frac{1}{2}\ln L_1^{\pm}$$

$$\begin{aligned} &\int_{E_2^-}^{E_2^+} \mathrm{d}E_2 \frac{(E_1+E_2)}{E_3^2-(E_1+E_2)^2} + \frac{(E_2-E_1)}{E_3^2-(E_1-E_2)^2} = \\ &= \frac{1}{2}\ln\frac{{m_\pi}^2(M^{*2} - E_1^2 + {m_\pi}^4/4 + \vec{l}_1\vec{l}_3) - M^{*2}E_3^2}{{m_\pi}^2(M^{*2} - E_1^2 + {m_\pi}^4/4 - \vec{l}_1\vec{l}_3) - M^{*2}E_3^2} =: \frac{1}{2}\ln L_2 \end{aligned} \tag{C.24}$$

and inserting them back into (C.23) we finally end up with

$$P_{1\pi} = \xi M^{*2} \int_{M^*}^{\infty} \mathrm{d}E_1 \left\{ \int_{M^*}^{\infty} \mathrm{d}E_2 \, \left(\left[f_1^+ f_2^- \right] \ln(L_1^-) + \right. \right.$$
$$\left. \left. + \left[f_1^+ f_2^+ + f_1^- f_2^- \right] \frac{1}{2} \ln(L_1^+) \right) + \left[f_1^+ + f_1^- \right] \int_{m_\pi}^{\infty} \mathrm{d}E_3 \, b(E_3) \ln(L_2) \right\} \tag{C.25}$$

This is the pressure contribution of the 1-pion-exchange Fock term where ξ is defined in (C.21), the $L_i^{(\pm)}$ in (C.25), $f_i^{\pm}$ in (A.48) und b in (A.38).

C.2 Two Pion Exchange

In this section we want to rewrite the ansatz for the 2-pion exchange diagram in (4.85) in terms of distribution functions. Our starting point will be the ansatz in (4.86):

$$P_{2\pi} \;=\; 3\left(\frac{-ig_A}{2f_\pi}\right)^4 (-4)^2 T^3 \sum_{\nu,n_{1,2}} \int \frac{\mathrm{d}^3p_1 \mathrm{d}^3p_2 \mathrm{d}^3q}{(2\pi)^9} \cdot$$
$$\cdot \frac{\frac{1}{4}\mathbf{tr}\,\not{q}(-M^*-\not{p}_1-\not{q})\not{q}(M^*-\not{p}_1)\frac{1}{4}\mathbf{tr}\,\not{q}(-M^*-\not{p}_2-\not{q})\not{q}(M^*-\not{p}_2)}{(m_\pi^2+q^2)^2[M^{*2}+p_1^2][M^{*2}+(p_1+q)^2][M^{*2}+p_2^2][M^{*2}+(p_2+q)^2]} \tag{C.26}$$

With the help of (A.10f) and some analysis the traces in our ansatz (4.86) can be evaluated therefore the numerator takes on the form

$$\begin{aligned}
&\frac{1}{4}\mathbf{tr}\,\not{q}(M^*+\not{p}_1+\not{q})\not{q}(M^*-\not{p}_1)\frac{1}{4}\mathbf{tr}\,\not{q}(M^*+\not{p}_2+\not{q})\not{q}(M^*-\not{p}_2) = \\
&= \left(M^{*2}q^2+q^2p_1^2+q^3p_1\right)\cdot\left(M^{*2}q^2+q^2p_2^2+q^3p_2\right) = \\
&= \left(p_1q\left[M^{*2}+(p_1+q)^2\right]-q(p_1+q)\left[M^{*2}+p_1^2\right]+2M^{*2}q^2\right)\cdot \\
&\cdot\ \left(p_2q\left[M^{*2}+(p_2+q)^2\right]-q(p_2+q)\left[M^{*2}+p_2^2\right]+2M^{*2}q^2\right) = \\
&= \left(p_1qE_3^2-q(p_1+q)E_1^2+2M^{*2}q^2\right)\left(p_2qE_4^2-q(p_2+q)E_2^2+2M^{*2}q^2\right)
\end{aligned}$$

with the replacements

$$E_{1,2}^2 = M^{*2}+p_{1,2}^2;\; E_{3,4}^2 = M^{*2}+(p_{1,2}+q)^2;\; E_5^2 = {m_\pi}^2+q^2 \tag{C.27}$$

The usefulness of the expansion towards the lengthly expression in the last step becomes obvious as soon as we bring the denominator - which becomes $E_5^4E_1^2E_3^2E_2^2E_4^2$ - back into the game. The integrand in (4.86) can now be written in the following form

$$\frac{1}{E_5^4}\left[\frac{p_1qp_2q}{E_1^2E_2^2}-\overbrace{\frac{p_1qq(p_1+q)}{E_1^2E_4^2}}^{p_2\to p_2-q,E_4\to E_2}-\overbrace{\frac{q(p_1+q)p_2q}{E_2^2E_3^2}}^{p_2\to p_2+q,E_2\to E_4}+\frac{q(p_1+q)q(p_2+q)}{E_3^2E_4^2}\right.$$
$$\left.+2M^{*2}q^2\left(\frac{p_1q}{E_1^2E_2^2E_4^2}-\underbrace{\frac{q(p_1+q)}{E_2^2E_3^2E_4^2}}_{p_1\to p_1-q,E_3\to E_1}+\frac{p_2q}{E_1^2E_2^2E_3^2}-\underbrace{\frac{q(p_2+q)}{E_1^2E_3^2E_4^2}}_{p_2\to p_2-q,E_4\to E_2}\right)+\frac{4M^{*4}q^4}{E_1^2E_2^2E_3^2E_4^2}\right]$$

Only the last term survives

$$
\begin{aligned}
P_{2\pi} &= 3\frac{g_A^4}{f_\pi^4}T^3\sum_{\nu,n_{1,2}}\int\frac{\mathrm{d}^3p_1\mathrm{d}^3p_2\mathrm{d}^3q}{(2\pi)^9}\frac{4M^{*4}q^4}{E_1^2E_2^2E_3^2E_4^2E_5^4} \\
&\overset{(2.63)}{=} 12g_{\pi N}^4T^3\sum_{\nu,n_{1,2}}\int\frac{\mathrm{d}^3p_1\mathrm{d}^3p_2\mathrm{d}^3q}{(2\pi)^9}\left[\underbrace{\frac{q^4}{\left(m_\pi^2+q^2\right)^2}}\right]E_1^{-2}E_2^{-2}E_3^{-2}E_4^{-2} \\
&= 1-\frac{2m_\pi^2}{m_\pi^2+q^2}+\frac{m_\pi^4}{(m_\pi^2+q^2)^2} \qquad \text{(C.28)}
\end{aligned}
$$

where we have used the GOLDBERGER-TREIMAN relation from section 2.9. Considering the limit $m_\pi^2\to\infty$ and taking the derivative with respect to m_π^2 of the second term

$$
\begin{aligned}
\lim_{m_\pi^2\to\infty}\frac{m_\pi^2}{m_\pi^2+q^2} &= 1 \qquad \text{(C.29)} \\
-\frac{\partial}{\partial m_\pi^2}\frac{1}{m_\pi^2+q^2} &= \frac{1}{\left(m_\pi^2+q^2\right)^2} \qquad \text{(C.30)}
\end{aligned}
$$

shows us that it is sufficient to explore an even simpler term

$$
\begin{aligned}
\tilde{P}_{2\pi} &= 12g_{\pi N}^4T^3\sum_{\nu,n_{1,2}}\int\frac{\mathrm{d}^3p_1\mathrm{d}^3p_2\mathrm{d}^3q}{(2\pi)^9}\left[\frac{1}{m_\pi^2+q^2}\right]E_1^{-2}E_2^{-2}E_3^{-2}E_4^{-2} \\
&= 12g_{\pi N}^4T^3\sum_{\nu,n_{1,2}}\int\frac{\mathrm{d}^3p_1\mathrm{d}^3p_2\mathrm{d}^3q}{(2\pi)^9}\,G \qquad \text{(C.31)}
\end{aligned}
$$

where

$$
\begin{aligned}
G &= \left[(m_\pi^2+q^2)(M^{*2}+p_1^2)(M^{*2}+p_2^2)(M^{*2}+(p_1+q)^2)(M^{*2}+(p_2+q)^2)\right]^{-1}= \\
&= \sum_{s_{1,2,3,4,5}}\frac{s_1s_2s_3s_4s_5}{32E_1E_2E_3E_4E_5}\cdot \\
&\quad\cdot\left\{\frac{2\left[f(s_2E_2+\mu)-f(s_4E_4+\mu)\right]f(-s_1E_1-\mu)f(s_3E_3+\mu)}{\left(s_3E_3-s_1E_1-s_5E_5\right)\left(s_3E_3-s_1E_1+s_2E_2-s_4E_4\right)}\right. \\
&\quad\left.+\frac{\left[f(s_1E_1+\mu)-f(s_3E_3+\mu)\right]\left[f(s_2E_2+\mu)-f(s_4E_4+\mu)\right]b(s_5E_5)}{\left(s_5E_5-s_3E_3+s_1E_1\right)\left(s_5E_5-s_4E_4+s_2E_2\right)}\right\} \qquad \text{(C.32)}
\end{aligned}
$$

represents the formulation in terms of distribution functions we were interested in.

Bibliography

[1] D.J. Gross and F. Wilczek, Phys. Rev. Lett. **30** (1973) 1343

[2] H.D. Politzer, Phys. Rev. Lett. **30** (1973) 1346

[3] J.B. Natowitz, K. Hagel, Y. Ma, M. Murray, L. Qin, R. Wada and J. Wang, Phys. Rev. Lett. **89** (2002) 212701-1

[4] T.-P. Cheng, L.-F. Li, *Gauge theory of elementary particle physics*, Oxford Science Publications, Clarendon Press

[5] C.N. Yang and R. Mills, Phys. Rev. **96** (1954) 191

[6] T. Muta, *Foundations of Quantum Chromodynamics*, World Scientific, Singapore, 1998

[7] A.W. Thomas, W. Weise *The Structure of the Nucleon*, Wiley-VCH Verlag Berlin GmbH, 2001

[8] M.E. Peskin, D.V. Schroeder, *An Introduction to Quantum Field Theory*, Addison-Wesley, New York, 1995

[9] M. Gell-Mann, Phys. Lett. **8** (1964) 214

[10] G. Zweig, CERN-Report **TH-401** (1964)

[11] H. Fritzsch and M. Gell-Mann, Proceedings of the XVI International Conference on High Energy Physics, Volume 2, p. 135, Chicago, 1972

[12] H. Fritzsch, M. Gell-Mann and H. Leutwyler, Phys. Lett. **B47** (1973) 365

[13] Particle Data Group, *Particle Physics Booklet* or *http://pdg.lbl.gov/*, K. Hagiwara et al., Phys. Rev. **D66** (2002) 010001

[14] E. Noether, Nachr. Ges. Wiss. Göttingen **171** (1918) 235

[15] G. 't Hooft, *Recent developments in gauge theories*,
Plenum, New York, 1980

[16] S. Coleman, *Secret Symmetry: An Introduction to Spontaneous Symmetry Breakdown and Gauge Fields*
in A.Zachichi, *Laws of Hadronic Matter (Part A)*, Academic Press, 1973

[17] J. Goldstone, Nuovo Cimento **19** (1961) 152

[18] M. Gell-Mann, R. Oakes and B. Renner, Phys. Rev. **175** (1968) 2195

[19] G. Colangelo, J. Gasser and H. Leutwyler,
Phys. Rev. Lett. **86** (2001) 5008-5010

[20] R. Koch, Z. Phys. **C15** (1982) 161
R. Koch and E. Pietarinen, Nucl. Phys. **A336** (1980) 331

[21] J. Gasser, H. Leutwyler and M. Sainio, Phys. Lett. **B253** (1991) 252,260

[22] J. Stahov, hep-ph/0206041

[23] M.M. Pavan, R.A. Arndt, I.I. Strakovsky and R.L. Workman,
PiN Newslett. **16** (2002) 110-115, hep-ph/0111066

[24] M.L. Goldberger and S. Treiman, Phys. Rev. **111** (1966) 354

[25] R.A. Arndt, R.L. Workman and M.M. Pavan,
Phys. Rev. **C49** (1994) 272

[26] J.I. Kapusta, *Finite-temperature field theory*,
Cambridge Monographs on Mathematical Physics, 1989

[27] M. Le Bellac, *Thermal field theory*, Cambridge University Press, 1996

[28] H. Hellmann, *Einführung in die Quantenchemie*,
Deuticke Verlag, Leipzig, 1937

[29] R.P. Feynman, Phys. Rev. **56** (1939) 340

[30] J. Gasser and H. Leutwyler, Phys. Lett. **B184** (1987) 83

[31] P. Gerber and H. Leutwyler, Nucl. Phys. **B321** (1989) 387

[32] D. Toublan, Phys. Rev. **D56** (1997) 5629

[33] N. Kaiser, Phys. Rev. **C59** (1999) 2945

[34] W. Weise, *Quarks, hadrons and dense nuclear matter*, Les Houches, Session LXVI: Trends in Nuclear Physics, Elsevier, 1998

[35] F. Karsch, E. Laermann, A. Peikert, Nucl. Phys. **B605** (2001) 579-599

[36] C.F. von Weizsäcker, Z. Phys. **96** (1935) 431

[37] H.A. Bethe, Rev. Mod. Phys. **8** (1936) 139

[38] E. Segrè, *Nuclei and Particles*, Benjamin, New York, 1977

[39] B. Povh, K. Rith, C. Scholz, F. Zetsche, *Teilchen und Kerne*, Springer Lehrbuch, 1994

[40] J.P. Blaizot, Phys. Rep. **64** (1980) 171

[41] D. Vretenar, G.A. Lalazissis, R. Behnsch, W. Pöschl and P. Ring, Nucl. Phys. **A621** (1997) 853

[42] A. Akmal, V.R. Pandharipande, D.G. Ravenhall, Phys. Rev. **C58** (1998) 1804

[43] M. Lutz, B. Friman and Ch. Appel, Phys. Lett. **B474** (2000) 7

[44] N. Kaiser, S. Fritsch and W. Weise, Nucl. Phys. **A697** (2002) 255-276 [nucl-th/0105057]

[45] J.D. Walecka, Ann. Phys. **83** (1974) 491

[46] P. Ring, Prog. Part. Nucl. Phys. **37** (1996) 193 and refs. therein

[47] M. Bender, P.-H. Heenen and P.-G. Reinhard, *Self-Consistent Mean-Field Models for Nuclear Structure*, to appear in Rev. Mod. Phys. (2003)

[48] B.D. Serot and J.D. Walecka, *The relativistic nuclear many-body problem*, Adv. Nucl. Phys. **16** (1986) 1

[49] B.D. Serot and J.D. Walecka, Int. J. Mod. Phys. **E6** (1997) 515

[50] M. Flaskamp, *Chirales Kondensat und thermische Feldtheorie bei endlicher Baryonendichte*, diploma thesis, TU-München, 1.12.1999

[51] T.M. Schwarz, *Studium der thermodynamischen Eigenschaften im Nambu-Jona-Lasinio-Modell bei endlicher Temperatur und Dichte*, diploma thesis, Uni Heidelberg, 1.2.1999

[52] T.M. Schwarz, S.P. Klevansky, G. Papp, Phys. Rev. **C60** (1999) 055205

[53] Y. Nambu, G. Jona-Lasinio, Phys. Rev. **122** (1961) 345,
Phys. Rev. **124** (1961) 246

[54] U. Vogl and W. Weise, Prog. Part. Nucl. Phys. **27** (1991) 195

[55] S.P. Klevansky, Rev. Mod. Phys. **64** (1992) 649 and refs. therein

[56] M. Alford, K. Rajagopal und F. Wilczek, Phys. Lett. **B422** (1998) 247-256

[57] J. Berges, K. Rajagopal, Nucl. Phys. **B538** (1999) 215-232

[58] B. ter Haar, R. Malfliet, Phys. Rep. **149** (1987) 207

[59] C.H. Johnson, D.J. Horen and C. Mahaux, Phys. Rev. **C36** (1987) 2252

[60] M. Jaminon, C. Mahaux, Phys. Rev. **C40** (1989) 354

[61] M. Brack, C. Guet, H.B. Hakansson, Phys. Rep. **123** (1985) 275

[62] S. Fritsch and N. Kaiser, nucl-th/0207057

[63] R.P. Feynman, A.R. Hibbs, *Quantum Mechanics and Path Integrals*,
McGraw Hill, 1965

[64] R.P. Feynman, *Quantum Elektrodynamics*,
New York, W.A.Benjamin Inc., 1962

[65] I. Bender, *Pfadintegrale in der Quantenmechanik*,
Skript zur gleichnamigen Vorlesung in HD, WS 97/98

[66] F. Halzen, A.D. Martin, *Quarks and Leptons: An Introductory Course in Modern Particle Physics*, John Wiley & Sons, 1983

[67] U. Mosel, *Fields, symmetries and quarks*, McGraw Hill, 1989

[68] M. Kaku, *Quantum field theory: a modern introduction*,
Oxford University Press, Oxford 1993

[69] R.D. Mattuck, *A guide to Feynman diagrams in the many-body problem*,
McGraw Hill, 1976

[70] C. Itzykson, J.-B. Zuber, *Quantum Field Theory*,
McGraw Hill International Editions

[71] M. Hamermesh, *Group Theory and its Applications to Physical Problems*, Dover Publications, 1990

[72] J.P. Elliott, P.G. Dawber, *Symmetry in physics, volume 1+2*, Oxford University Press, 1979

[73] J.D. Bjorken, S.D. Drell, *Relativistische Quantenmechanik* und *Relativistische Quantenfeldtheorie*, BI Hochschultaschenbücher

[74] A.L. Fetter, J.D. Walecka, *Quantum Theory of Many-particle Physics*, McGraw Hill, 1971

[75] M.L. Boas, *Mathematical methods in the physical sciences*, John Wiley and Sons, 1983

[76] I.N. Bronstein, K.A. Semendjajew *Taschenbuch der Mathematik*, Verlag Nauka, Moskau, 1991

[77] M. Abramowitz, I.A. Stegun, *Handbook of mathematical functions with formulas, graphs and mathematical tables*, Dover Publications, 1965

Acknowledgements - Danksagung

An erster Stelle möchte ich mich natürlich bei Herrn Univ.-Prof. Dr. Wolfram Weise für die Aufnahme an seinem Lehrstuhl und die Vergabe dieser interessanten Doktorarbeit bedanken. Ausserdem danke ich ihm für seine Geduld bei den teils länger andauernden Schwierigkeiten in der Bewältigung der nicht wenig anspruchsvollen Numerik sowie bei der Fertigstellung dieses Dokuments.

An zweiter Stelle geht mein Dank in nicht minderem Umfang an Herrn Dr. habil. Norbert Kaiser für seine intensive, kompetente Betreuung und seine stets offene Tür.

Desweiteren gilt mein Dank der gesamten Arbeitsgruppe. Ich hätte es selbst nie für möglich gehalten, einen kompletten Lehrstuhl mit durchweg "normal gebliebenen" theoretischen Physikern erleben zu dürfen. Für die vielen, meist äusserst interessanten Seminare, sowie das Arbeitsklima, in dem ich mich immer wohl fühlte, möchte ich mich an dieser Stelle bedanken.
Zusätzlich möchte ich mich bei Roland Schneider, Stefan Fritsch, Thorsten Renk, Stefan Wetzel, Eugenio Marco und Niklas Beisert für die unterhaltende Gestaltung so mancher Nachmittags-Session, Abende (nicht nur bei Konferenzen) und sonstiger Freizeitgestaltung neben den fachlichen Hilfestellungen und Diskussionen bedanken.

Ich möchte auch ausdrücklich meinen Freunden ausserhalb der Physik danken, die fast durchweg Verständnis dafür hatten, dass ich für sie in den letzten Wochen und Monaten leider nicht in dem Umfang Zeit aufwenden konnte, wie wir uns das alle gewünscht hätten.

Last but not least danke ich meiner Familie, auf deren Unterstützung ich glücklicherweise immer zählen konnte und kann. Explizit erwähnen möchte ich hier meine Eltern sowie meine Partnerin Nicole, die meine Launen während der Fertigstellung dieser Dissertation erdulden musste, und unsere Tochter Lisa Sophie, die am 6.4.02 das Licht der Welt erblickte. Insbesondere ihr beiden habt mir die Kraft verliehen, diese Arbeit fertigzustellen.
Für Euren immens wichtigen Rückhalt danke ich Euch!